DISPERSION OF FULLERENES IN NATURAL WATER AND THEIR BEHAVIOR IN WATER TREATMENT PROCESS

A Thesis
Presented to
The Academic Faculty

by

Hoon Hyung

In Partial Fulfillment
of the Requirements for the Degree
Doctor of Philosophy in the
School of Civil and Environmental Engineering

Georgia Institute of Technology
August 2008

DISPERSION OF FULLERENES IN NATURAL WATER AND THEIR BEHAVIOR IN WATER TREATMENT PROCESS

Approved by:

Dr. Jae-Hong Kim, Advisor
School of Civil and Environmental Engineering
Georgia Institute of Technology

Dr. Seung Soon, Jang
School of Material Science and Engineering
Georgia Institute of Technology

Dr. Joseph B. Hughes
School of Civil and Environmental Engineering
Georgia Institute of Technology

Dr. Vernon L. Snoeyink
School of Civil and Environmental Engineering
University of Illinois

Dr. Michael H. Bergin
School of Civil and Environmental Engineering
Georgia Institute of Technology

Date Approved: June 11, 2008

[To Se-Eun and Juhee]

ACKNOWLEDGEMENTS

Firstly, I would like to thank my advisor, Dr. Jae-Hong Kim. He not only provided me a chance to become a piece of this great legacy of Georgia Tech., but also showed me the example of a great advisor with extensive knowledge, creative mind, and friendliness.

I acknowledge my thesis committee, Dr. Joseph Hughes, Dr. Vernon Snoeyink, Dr. Michael Bergin, and Dr. Seung Soon Jang for agreeing to be my committee and providing invaluable comments and advices on my research.

All the members of Dr. Kim and Dr. Huang's groups and Korean graduate students in the environmental engineering program are greatly appreciated. It was very nice to share friendship with them in and out of the campus and discussions and advices from them brought me valuable idea on my research.

My heartful gratitude should go to all my family. Especially, I greatly appreciate my wife, Juhee, and my daughter, Se-Eun, for all their sacrifice and endurance during my study.

Finally, I would like to acknowledge Bureau of Reclamation, US Department of Interior and US Environmental Protection Agency (USEPA) for their generous funding support.

TABLE OF CONTENTS

LIST OF TABLES

LIST OF FIGURES

SUMMARY

With expected mass production of fullerenes due to their special properties and various applications, understanding the fate of fullerenes in natural and engineered water environments is imperative for the proper assessment of ecotoxicity and potential human health effects of these carbon based nanomaterials.

This research address the outstanding questions closely related to the fate of fullerenes in natural and engineered water environments. Specifically, this research is focused on investigating 1) the stability of fullerenes in the natural water, 2) interaction between fullerenes and natural organic matter (NOM) and 3) behavior of fullerenes in the conventional water treatment system.

The experimental results show that multi-walled nanotubes (MWNT) were readily dispersed as an aqueous suspension in both model NOM (Suwannee River NOM (SRNOM)) solutions and natural surface water (actual Suwannee River water with unaltered NOM background) and MWNT remained stable for over one month. Microscopy analyses suggested that the suspension consisted primarily of individually dispersed MWNT. The concentration of MWNT in NOM background solution could be successfully measured by thermal optical transmittance (TOT) analysis. For the same initial MWNT concentrations, the concentrations of suspended MWNT in SRNOM solutions and Suwannee River water were considerably higher than that in a solution of

1 % sodium dodecyl sulfate, a commonly used surfactant to stabilize carbon nanotubes (CNT) in the aqueous phase.

The effect of NOM characteristics and water quality parameters on NOM adsorption to MWNT was investigated with isotherm experiment. The experimental results fitted well with a modified Freundlich isotherm model that took into account of the heterogeneous nature of NOM. Experiments performed with various NOM samples suggested that the degree of NOM adsorption was proportional to the aromatic carbon content of NOM. The NOM adsorption to MWNT was also dependent on water quality parameters: adsorption increased as pH decreased and ionic strength increased. As a result of NOM adsorption to MWNT, a fraction of MWNT formed a stable suspension in water, the concentration of which depended on the amount of NOM adsorbed per unit mass of MWNT. The amount of MWNT suspended in water was also affected by ionic strength and pH.

Dispersion of representative fullerenes such as C_{60}, single-walled carbon nanotube (SWNT), and multi-walled carbon nanotube (MWNT) in the aqueous phase containing SRNOM was investigated. Four dispersion methods were tested (*i.e.*, mechanical mixing or sonication after either adding solid phase fullerenes into the aqueous phase or contacting organic phase containing fullerenes with the aqueous phase) to simulate possible spillage scenarios to the aqueous environment. The experimental results showed that MWNT formed water stable suspensions by the mechanical mixing and sonication and SWNT by the sonication, only when they were added as solids directly to water

containing NOM. C_{60} formed water stable colloidal suspensions in all cases except when solids were added to water and ultrasound was applied. In most cases, the presence of NOM facilitated the fullerene dispersion in the aqueous phase.

The removal of representative fullerenes in conventional water treatment process was investigated. Jar tests were performed with MWNT, C_{60}, and fullerol suspended in the aqueous phase. Effect of the presence of NOM and water quality parameters such as pH and alkalinity were also assessed. The experimental result suggested that in the scenario of the fullerene spillage in water environments, the fullerenes would be generally well removed by the conventional water treatment process. The removal of the carbon nanomaterials was hindered by the presence of NOM and water quality parameters such as pH and alkalinity were also important factors for the removal of fullerenes.

CHAPTER 1

INTRODUCTION

Fullerenes are the third allotropes of carbon, which have the structure similar to a graphene but contain pentagon rings as well as hexagon rings to produce three dimensional structures such as spheres (*e.g.*, C_{60} and C_{70}) and tubes (*e.g.*, single walled carbon nanotubes (SWNT) and multi-walled carbon nanotubes (MWNT)). Sphere shaped fullerenes, commonly called buckyballs, have nano-sized cage-like structure and are composed of combinations of pentagons and hexagons [1]. Carbon nanotubes (CNT) consist of the sheets of covalently bonded carbon atoms in hexagonal arrays that are seamlessly rolled into a hollow cylindrical shape with at least one side capped with a hemisphere of the buckyball structure [2]. CNT have extremely high aspect ratio with diameters ranging from 1 to 200 nm and length from 10 to100 micrometers. CNT are categorized into two main species; single-walled nanotube (SWNT) and multi-walled nanotube (MWNT). The latter results from co-axial assembly of multiple SWNTs. Fullerenes are being considered for extensive range of applications due to their exceptional physical, chemical and electro-optical properties [3] and demands and productions of the fullerenes are expected to rapidly grow during the next decade [4].

However, concerns have raised due to the recent findings that fullerenes can interact with living organisms and cause toxic effects that are unique to this class of materials. For instance, SWNT showed higher pulmonary toxicity than quartz, a well

known industrial hazards [5] and C_{60} showed cytotoxicity inhibiting cell growth [6]. Such findings carry an additional significance as fullerenes have been found in particulate matter emitted from coal-fueled power plants [7], common fuel-gas combustion source [8], and even in nature [9], although sporadically in small masses.

Despite the possible toxicological and environmental effects of the fullerenes, limited research has been performed on the fate and the transport of the fullerenes in aquatic environments, mainly due to their extremely hydropphobic nature. However, recent studies show that C_{60} can exist as nano-scale aggregates in aqueous phase [6] and facile dispersion of CNT in aqueous phase can be achieved by the addition of surfactants and polymers such as sodium dodecyl sulfate (SDS) [10], sodium dodecylbenzene sulfonate (NaDDBS) [11], and polyvinyl pyrrolidone (PVP) [12]. These results suggested the possibility that these carbon based nanomaterials, which were not generally considered as a potential contaminant, can be dispersed in aquatic environments with unexpected level by the interaction with organic materials existing in the natural system. Therefore, understanding the behavior of fullerenes in natural and engineered aquatic environments is imperative for accurate assessment of ecotoxicity and ultimate human health effect of these carbon based nanomaterials.

This research addresses several outstanding questions on the fate and the transport of fullerenes in natural and engineered environments such as whether fullerenes can form stable dispersion in the aqueous phase, how the concentration of fullerenes in the natural

water can be measured, what type of interaction would occur between NOM and fullerenes, and what is the behavior of fullerenes in conventional water treatment system.

The first objective of this study was to verify MWNT stabilization, as an aqueous suspension, in both synthetic solutions containing model NOM (Suwannee River natural organic matter (SRNOM)) and natural surface water with high NOM background (Suwannee River), and to develop a method to quantify MWNT suspended in NOM solutions based on thermal optical analysis (Chapter 2).

The second objective of this study is evaluating the dispersion of the fullerenes under different spillage scenarios to water body, (*i.e*. the spillage of solid phase fullerenes or fullerenes dissolved in common organic solvents) and understanding the role of NOM on fullerene dispersion under these scenarios. For the purpose, a systematic, comparative investigation on the dispersion of representative fullerenes, C_{60}, SWNT and MWNT, in model natural waters was performed. Different spillage scenarios were simulated by 1) applying either mechanical mixing or sonication after directly adding solid phase fullerenes into the aqueous phase and 2) applying either mechanical mixing or sonication after contacting organic solvent containing fullerenes with the aqueous phase. SRNOM was used as a model NOM and sodium dodecylsulfate (SDS), an anionic surfactant commonly used for the fullerene dispersion, was used for a comparison purpose (Chapter 3).

The third objective of this study was to investigate the effect of NOM characteristics and water quality parameters on adsorptive interaction between MWNT

and NOM in water. Specifically, the characteristics of NOM adsorption to MWNT was studied from batch isotherm experiments, which were performed with various NOM samples under different pH and ionic strength conditions. The experimental result was analyzed using Freundlich isotherm model and critically compared to the adsorption of activated carbon. Finally, the amount of stable MWNT suspension formed in water as a result of NOM adsorption under varying conditions was quantitatively analyzed (Chapter 4).

Finally, jar tests were performed using C_{60} and multi-walled carbon nanotubes (MWNT) as model fullerene compounds to investigate the behavior of water-stable fullerene suspensions in the drinking water treatment process. The effect of the existence of natural organic matter (NOM) and water quality parameters such as pH and the alkalinity on the removal of these novel carbon nanomaterials was also investigated (Chapter 5).

Literature Cited

1. Kroto, H. W.; Heath, J. R.; Obrien, S. C.; Curl, R. F.; Smalley, R. E., C-60 - Buckminsterfullerene. *Nature* **1985,** *318*, (6042), 162-163.
2. Iijima, S., Helical Microtubules of Graphitic Carbon. *Nature* **1991,** *354*, (6348), 56-58.
3. Colvin, V. L., The potential environmental impact of engineered nanomaterials *Nature Biotechnology* **2004,** *22*, (6), 760-760.
4. Tremblay, J. F., Mitsubishi chemical aims at breakthrough. *Chemical & Engineering News* **2002,** *80*, (49), 16-17.
5. Lam, C. W.; James, J. T.; McCluskey, R.; Hunter, R. L., Pulmonary toxicity of single-wall carbon nanotubes in mice 7 and 90 days after intratracheal instillation. *Toxicological Sciences* **2004,** *77*, (1), 126-134.
6. Fortner, J. D.; Lyon, D. Y.; Sayes, C. M.; Boyd, A. M.; Falkner, J. C.; Hotze, E. M.; Alemany, L. B.; Tao, Y. J.; Guo, W.; Ausman, K. D.; Colvin, V. L.; Hughes, J. B., C-60 in water: Nanocrystal formation and microbial response. *Environmental Science & Technology* **2005,** *39*, (11), 4307-4316.
7. Utsunomiya, S.; Jensen, K. A.; Keeler, G. J.; Ewing, R. C., Uraninite and Fullerene in Atmospheric Particles. *Environmental Science and Technology* **2002,** *36*, (2), 4943-4947.
8. Murr, L. E.; Bang, J. J.; Lopez, D. A.; Guerrero, P. A.; Esquivel, E. V.; Choudhuri, A. R.; Subramanya, M.; Morandi, M.; Holian, A., Carbon nanotubes and nanocrystals in methane combustion and the environmental implications. *Journal of Materials Science* **2004,** *39*, (6), 2199-2204.

9. Chijiwa, T.; Arai, T.; Sugai, T.; Shinohara, H.; Kumazawa, M.; Takano, M.; Kawakami, S., Fullerenes found in the Permo-Triassic mass extinction period. *Geophysical Research Letters* **1999,** *26*, (6), 767-770.

10. O'Connell, M. J.; Bachilo, S. M.; Huffman, C. B.; Moore, V. C.; Strano, M. S.; Haroz, E. H.; Rialon, K. L.; Boul, P. J.; Noon, W. H.; Kittrell, C.; Ma, J. P.; Hauge, R. H.; Weisman, R. B.; Smalley, R. E., Band gap fluorescence from individual single-walled carbon nanotubes. *Science* **2002,** *297*, (5581), 593-596.

11. Islam, M. F.; Rojas, E.; Bergey, D. M.; Johnson, A. T.; Yodh, A. G., High weight fraction surfactant solubilization of single-wall carbon nanotubes in water. *Nano Letters* **2003,** *3*, (2), 269-273.

12. O'Connell, M. J.; Boul, P.; Ericson, L. M.; Huffman, C.; Wang, Y. H.; Haroz, E.; Kuper, C.; Tour, J.; Ausman, K. D.; Smalley, R. E., Reversible water-solubilization of single-walled carbon nanotubes by polymer wrapping. *Chemical Physics Letters* **2001,** *342*, (3-4), 265-271.

CHAPTER 2

LITERATURE REVIEW

Structure and Formation of Fullerenes

Fullerenes are the third allotropes of carbon, which have the structure similar to graphene but contain pentagon rings as well as hexagon rings to produce three dimensional structures such as spheres (*e.g.*, C_{60} and C_{70}) and tubes (e.g., carbon nanotubes (CNT)). CNT consist of sheets of carbon atoms covalently bonded in hexagonal arrays that are seamlessly rolled into a hollow, cylindrical shape with both ends rounded through pentagon ring inclusions [1]. They present a highly flexible thread-like structure having an extremely high aspect ratio with the diameter ranging from 1 to 200 nm and the length from 0.1 to 100 μm [2]. Hence, CNT represent a mixture of molecules with different lengths and carbon arrays. CNT are categorized into two main species based on their molecular structures; single-walled carbon nanotubes (SWNT) and multi-walled carbon nanotubes (MWNT), where MWNT form from the co-axial assembly of multiple SWNT.

Since Iijima *et al.* [1] first identified CNT from carbon soot deposited on an electrode during the direct current arc discharge experiment, several methods have been suggested to synthesize CNT. Generally, the methods can be classified into two categories based on the temperature they are synthesized; high temperature methods and low temperature methods [3]. High temperature methods use electric arc discharge, laser

beam, or solar energy to provide energy high enough to sublime graphite while low temperature methods are based on catalytic chemical vapor deposition (CCVD).

In the arc discharge method, from which Iijima *et al.* [1] first discovered CNT, arc discharge is allowed to two graphite electrodes to raise the temperature up to 6000^{o}C. In this high temperature and under a partial pressure of helium or argon, carbon in the electrodes sublimes to form plasma. The carbon plasma finally accumulates on the cold cathode to form CNT. The original apparatus of Iijima *et al.* produces MWNT, but types of CNT are determined by metal catalysts, *i.e.*, MWNT are formed in the absence of catalysts while SWNT are produced in the presence of catalysts such as Fe, Co, Ni or rare metal [3]. Laser ablation method, which was originally devised to produce C_{60} [4], can be also utilized for the production of CNT. Similar to the arc discharge method, the laser ablation method sublimes carbon in the electrodes under low pressure inert gas atmosphere, while it uses pulsed laser [5, 6] or continuous laser [7] to obtain high energy for carbon sublimation. Due to the similarity in principles, the structure CNT produced by the laser ablation method is similar to those produced by the arc discharge method [3].

CNT can be produced at moderate temperature range (800-1200^{o}C) from catalytic chemical vapor deposition (CCVD) method [8]. CCVD utilizes catalytic reaction of carbonaceous gas to grow nanotubes, in which carbonaceous gas decomposes on catalysts and forms graphitic carbons [8]. Carbonaceous gas can be either CO or hydrocarbons such as C_2H_2, CH_4, C_6H_6 and it is generally applied in the reactor with inert gas such as Ar, He, and N_2 which act on the hydrodynamic parameters or modify thermodynamic

conditions [3]. Type of metal catalysts and ambient conditions of synthesis can be important factors to determine the types of CNT. Fe, Co, and Ni [9-11] have been frequently used for the MWNT synthesis while bimetallic catalysts such as Fe/Mo, Co/Mo, and Fe/Mo [12, 13] or organometallic precursors ($FeCO_5$) [14, 15] have been utilized for the SWNT synthesis. In the CCVD, MWNT are favorably produced at relatively low temperature range (600-800^oC) , while SWNT are favored at high temperature (1000-1200^oC) [3].

C_{60} consists of 60 carbon atoms arranged in 20 hexagons and 12 pentagons that form a perfectly symmetrical cage structure of a soccer ball with *ca*. 1 nm size [4]. C_{60} molecule follows Euler's theorem where each fullerene consists of 12 pentagons and M hexagons containing 2(10+M) carbon atoms [16]. Similarly arranged, other carbon cage structures such as $C_{70,}$ $C_{76,}$ C_{78}, C_{84}, and C_{90} have been also identified [17]. Each carbon atom is bonded to 3 other carbon atoms to form sp2 hybridization and, consequently, entire C_{60} molecule is surrounded by π electron clouds[18]. C_{60} has 2 different types of bonds; 6:6 bond which located in between two hexagon rings and 6:5 bond which located in between a hexagon ring and a pentagon ring and 6:6 bonds are considered as double bonds having shorter bonding length than 6:5 bonds [18].

C_{60} molecule was first found in 1985 by Kroto et al. [4] from the ablation of a graphite with energetic pulsed laser. However, mass production of these carbon based nanoparticles was not possible until Kratchmer et al. [19] succeeded in synthesizing C_{60} by resistive heating method. In the method, two graphite rods, which were produced by

compressing (at about 1 kbar) and heating (at about 1300°C) carbon powder, are evaporated in a glass evaporator filled with less than 100 torr of Helium at high temperature (more than 3200°C). The resistive heating method allows for an electrical current across the two rods by maintaining contact of two graphite rods by a spring mechanism. Carbon vapor produced by the resistive heating method reorganized to form black soot which contains *ca.* 8% of C_{60} and C_{70}. Thus formed black soot could be collected on the cold surfaces and dispersed in organic solvent such as benzene [19]. Instead of resistive heating, arc discharge could be adopted to provide the graphite with high energy to make it evaporate and eventually form C_{60} [3]. C_{60} could be synthesized from high temperature combustion of hydrocarbons such as benzene, naphthalene, and acetylene under optimal atmospheric conditions [20-23]. The method is fundamentally different from the resistive heating or the arc discharge method in that, instead of graphite, it utilizes hydrocarbons as initial carbon sources. In the method, fullerenes can be formed from the pyrolysis and the subsequent rearrangement of hydrocarbons [22]. Howard *et al.* [23] combusted benzene at ~1800°C under argon and oxygen mixed atmosphere and found that he mass of C_{60} and C_{70} mixture consists of 0.003-9.0% of total mass of soot generated from the combustion. Based on the initial carbon fuel basis, up to 0.3% yield of C_{60} and C_{70} mixture could be obtained at a pressure of 20 torr and a carbon oxygen ratio of 0.995 with 10% argon. The combustion method made continuous production of C_{60} possible [21] and the current C_{60} mass production process has developed from the modification of the method [24].

Solubility of Fullerenes in Aqueous Phase

Solubility of fullerenes in the aqueous phase is an important factor to predict the eventual fate of the carbon based nanomaterials in the water environment. Due to its extremely high hydrophobicity and large molecular size, CNT cannot be independently dispersed in water without the modification of their chemical structure or the assistance from foreign chemical compounds. Several approaches were suggested to produce stable CNT suspensions in the aqueous phase.

First, CNT can be chemically modified to include hydrophilic functionalities by derivatization reaction. Thus induced functional groups can significantly increase the stability of CNT in the aqueous phase [25-27]. Acid treatment is one of the popular methods to derivatize carbon nanotubes. HNO_3, H_2SO_4, and HNO_3/H_2SO_4 mixture are commonly used acids for the treatment [8, 28, 29]. The acid treatment usually performed in combination with thermal oxidation or ultrasonication and it generally leads to the induction of carbonyl, carboxylic and hydroxyl functional groups at the end caps of CNT [8, 29]. For instance, Zhao *et al.* [27] proposed a method to produce carboxylated SWNT from the treatment of SWNT with concentrated sulfuric acid followed by up to 5 min. of sonication. The stability of the modified SWNT appeared to be due to the electrostatic repulsion between deprotonated carboxylic functional groups. As a result, the stability of SWNT largely depended on pH. For example, at pH less than 3 CNT aggregates formed within minutes. Fluorination is also a common way to functionalize CNT and F_2 gas reacted with CNT is known to lead to side-wall derivatization [30, 31]. However, in the derivatization process disruption of the chemical structure of CNT associated with the

formation of new covalent bonds in the graphene sheet can result in the loss of unique CNT characteristics.

Second, CNT can be stabilized in water from non-covalent surface coating by surfactants and polymers [32-37], which can effectively shield the hydrophobic surface of CNT to provide thermodynamically more favorable surface in water as well as steric or electrostatic repulsions which prevent aggregation of CNT. Surfactants and polymers frequently used for this purpose include sodium dodecyl sulfate (SDS) [38], sodium dodecylbenzene sulfonate [32, 33], Triton X-100 [32, 34, 35], polyvinyl pyrrolidone [36], polystyrene sulfonate [36], and hydrolyzed poly(styrene *alt*-maleic anhydride) [37], poly(vinyl alcohol) [39], amylase [40], or poly(ethylene oxide) [41] among others.

C_{60} is extremely hydrophobic and its solubility in water is very low ($< 10^{-12}$ g/L) [42]. Similar to CNT, aqueous solutions of molecular C_{60} can be produced by derivatization of hydrophilic functional groups [43] or applying surfactants or polymers (*e.g.*, polyvinyl pyrrolidone (PVP)) which can shield hydrophobic surface of C_{60} [44-46]. However, disruption of the chemical structure of C_{60} or the existence of impurities (*e.g*, surfactants and polymers) can prevent wider usage of this novel carbon nanomaterial.

Upon extended contact with water, C_{60} is known to form negatively charged water stable aggregates, commonly called nC_{60} or nano C_{60} [47-49]. nC_{60} has much higher solubility (*ca.* 150 mg/L) in water compared to molecular C_{60} and is known to be the most relevant form of C_{60} in the environment [49]. Hence, in the episodes of spillage of

C_{60} powder or C_{60} dissolved in organic solvents, it is most likely that nC_{60} can be produced [50]. Scrivens *et al.* [47] first suggested a solvent exchange protocol to produce water stable nC_{60} aggregates (nC_{60}). The method begins with toluene containing dissolved C_{60} and diluting in series into THF, acetone and water. Finally, a yellow colored nC_{60} suspension was formed in water. After the first successful production of nC_{60}, several methods have been suggested to produce stable nC_{60} suspension in aqueous phase. Tetrahydrofuran (THF)/nC_{60} method was suggested by Deguchi *et al.* [48] and modified by Fortner *et al.* [49]. In the method, powder C_{60} was first dissolved in THF up to saturation concentration (9 mg/L). After filtering the solution to remove any undissolved particles, the solution was stirred vigorously while an equal volume of water was added at a constant rate. During the process, C_{60} transported to the water phase and formed nC_{60}. THF was then removed by a rotary evaporator to obtain nC_{60} solution. Aqueous suspension of nC_{60} (*ca.* 3-5 mg/L C_{60}) produced by this method showed yellow or brown color and stable for a long period. nC_{60} also could be obtained by sonication of C_{60} dissolved in toluene [44]. DI water was added to toluene solution and then layered solutions were sonicated until all toluene was evaporated. Thus formed brown C_{60} suspension was filtered to remove suspended particles. Recent study by Chen et al. [51] shows that C_{60} can be produced by extended (2-4 weeks) high shear mixing of powder C_{60} with deionized water. Even though it produced a broader size range of aggregates, nC_{60} generated from this method showed similar chemical and physical properties with those prepared by other methods. The formation of nC_{60} from the extended mixing confirms that nC_{60} is the most environmentally relevant form of C_{60}.

Spectroscopic Analysis of Fullerenes in the Aqueous Phase

Raman, Near IR (NIR) absorption, and fluoroscence spectroscopies are three main methods to study the molecular properties of CNT as well as their interaction with molecules in the aqueous phase. Raman spectroscopy can provide important information on physical and electrical properties of CNT. The radial breathing modes (RBM) are generally seen in the 100-500 cm^{-1} range of Raman shift and arises from the radial motion of the carbon atoms [52]. Diameter of SWNT is known to be inversely proportional to the RBM band frequencies and can be calculated using the following correlation [53]:

$$v_{RBM} = 238/d^{0.93}$$

where vRBM is RBM frequency in cm^{-1}, and d is tube diameter in nm. G-band can be observed in the 1500-1600 cm^{-1} region of Raman shift and results from the tangential C-C stretching vibrations both longitudinally and transversally on the CNT axis [54]. The shape of the G-band is different based on the electronic identity of CNT (*i.e.*, metallic versus semiconducting) [55]. D-band also known as the disorder peak can be seen in the 1300-1400 cm^{-1} region. This peak results from the defects in sp^2 carbons [55]. The strength of the peak is related to the amount of disordered graphite and the degree of conjugation disruption in the graphene sheet [55]. The strength of adherence of the polymer or surfactant chains to CNT through hydrophobic interaction can be seen from Raman spectra [56]. Generally, RBM peaks for CNT shifts to higher Raman frequencies

when they are coated with polymers or surfactants [56]. The higher frequency of Raman peaks results from the hydrophobic and van der Waals attraction forces between the polymer and the graphite sheet, which would increase the energy necessary for the vibrations [56].

SWNT shows absorption spectrum at NIR region due to the electronic transition between valence and conduction bands [57]. Three electronic transitions in SWNT includes: the first semiconducting transition (S_{11}) at *ca*. 0.7 eV, the second semiconducting transition (S_{22}) at *ca*. 1.2 eV, and metallic transition (M_{11}) at *ca*. 1.8 eV [57]. The NIR absorption study can give important information on the electronic properties of semiconducting SWNT (*e.g.*, band gap) as well as the interaction between other molecules and nanotubes [57]. Since O'conell *et al.* [38] first found photoluminescence of SWNT surrounded by sodium dodecylsulfate (SDS) micelles in the aqueous phase, photoluminescence spectroscopy has been widely adopted to analyze the effect of surfactants and polymers adsorbed on the SWNT surfaces on the electronic structure of nanotubes [57]. A recent comparative study by Moore *et al.* [58] revealed that the interband electronic transitions in photoluminescence was very sensitive to the types of surfactants and linear relationship existed between the spectral shift of photoluminescence and fluorescent yield. In the same study, polymers adsorbed on CNT generally brought a downshift of photoluminescence peaks by 70 to 200 cm^{-1}. This result indicates that the polymers surrounding the SWNT generate a more polarizable environment, which in turn results in changes in the excitation binding energies.

C_{60} can be characterized using various spectroscopic methods such as UV-vis, IR, and nuclear magnetic resonance (NMR) analysis. Water stable aggregates of C_{60} (nC_{60}) suspension shows characteristic peaks at 227, 280 and 360 nm in UV-vis spectra [47]. However, the shift of the characteristics peaks depends on solvents. For instance, UV-vis spectra of C_{60} dissolved in hexane exhibits blue shift from those in water, showing characteristic peaks at 211, 256, and 328 nm [59]. The nC_{60} suspension also demonstrates four characteristic IR absorption bands at 1,429, 1,183, 577 and 528 cm^{-1}, which correspond to four bonding structures (*i.e.*, C-C(pentagon bond), C=C(hexagon bond), C-C=C(angle) , and C-C-C(angle)) [60]. The IR spectrum indicates highly symmetrical icosahedral molecular structure of C_{60}. The IR spectrum of nC_{60} is consistent with those of molecular C_{60}, confirming chemically unaltered nature of nC_{60} [60]. ^{13}C NMR study of C_{60} shows *ca*. 143 ppm shift from a tetramethylsilane ($(CH_3)_4Si$) reference, confirming icosahedral structure of C_{60} and exact equivalency of carbon atoms [59].

Properties and Usages

Fullerenes are being considered for a range of applications due to their exceptional mechanical, electro-optical, and thermal properties [61, 62]. Examples of such properties include: low threshold emission fields and the excellent emission stability [2, 63, 64]; hydrogen adsorption (storage) capacity [65, 66]; high tensile strength and elasticity [67]; and electronic sensitivity in different chemical environments [68-71].

Field emission phenomenon of CNT has been first found by Rinzler et al. [63] and CNT is known to have right properties to become a good field emitter such as nanometer size diameters, good electrical conductivity, structural integrity, and chemical stability among others [2]. Materials with electron field emission, where electron near the Fermi level escapes to vacuum upon subject to a high electric field, can be used for the production of flat panel displays, electron guns in electron microscopes, and microwave amplifiers [2]. For the industrial application, field emitters necessitate low threshold emission fields and stability at high current densities. Threshold emission fields of SWNT ranged from 2-3 V/μm for a current density of 10 mA/cm^2, while those of MWNT ranged form 3-5 V/μm for the same current density [72]. These values are significantly lower than conventional field emitters such as Mo or Si tips, which show threshold value of 50-100 V/μm for a current density of 10 mA/cm^2 [2]. CNT also exhibit a capability to achieve stable emission of higher electron current densities (>20 mA/cm^2) [64]. With these low threshold emission fields and the good stability, the CNT emitter has advantage over conventional emitters.

Materials with high hydrogen storage capacity are essential for the development of energy storage devices. CNT have been reported to have very high but reversible hydrogen adsorption capacity, ranged from 4 to 10 wt. % of H_2 depending on ambient temperature and pressure [2]. This hydrogen adsorption capacity is considered to be due to the capillary effect, which originated from the cylindrical and hollow structure and the nano-size diameter of SWNT [73]. A study using 0.1-0.2 wt % SWNT showed that SWNT have 5-10 wt. % of hydrogen storage density [65]. Another study on higher

purity SWNT showed ~8 wt. % hydrogen adsorption at 80 K and rather high pressure of 100 atm [74]. This high level of hydrogen adsorption capacity is expected to meet or exceed the benchmark of 6.5 wt % H_2 to system weight ratio set by US Department of Energy, promising future usage in hydrogen storage devices [2].

CNT are known to have exceptionally high stiffness and axial strength mainly due to their seamless cylindrical graphite structure [75]. For instance, Treacy *et al.* [75] showed that SWNT have Young's modulus of 1.8 TPa. The modulus is 2 to 3 times higher than that of carbon fibers, which have been frequently used to produce reinforced composites. Theoretical estimation showed that Young's modulus of SWNT can reach up to5 TPa depending on the diameter and structure of CNT and CNT can be a promising filler material of polymer composites to reinforce the strength and stiffness replacing the traditional carbon fibers [2].

Due to small size, high conductivity, high mechanical strength and flexibility, CNT can be used as nanoprobes and nanosensors. Wong *et al.* [76] attached MWNT to a cantilever of scanning probe microscope to obtain the image of biological molecules. Due to smaller radii of MWNT and flexibility of MWNT, MWNT tip could provide the high resolution images of fibril and protofibril which could not be obtained by conventional Si or metal tips. Kong *et al.* [68] found that the electrical conductance of SWNT changes upon exposure to different gaseous molecules such as NO_2, NH_3, and O_2. Therefore, the presence of different gas molecules could be detected by monitoring change in the electric conductance of the nanotubes [68, 70, 71]. The nanotube-based

sensors showed at least one order faster response time compared to the ones based on currently available technology (solid state metal oxide and polymer) [68].

Due to its good affinity to the organic compounds, C_{60} and its derivatives can be used for the chemical sensors or adsorbents of chemical contaminants [77, 78]. C_{60} and their derivatives can be coated on the surface of some chemical sensors such as quartz crystal microbalance (QCM) [78]. QCM has piezoelectric crystals which are very sensitive to the change of mass in the surface. The sensor coated with C_{60} and their derivatives was used to detect organic molecules using the change of the oscillating frequency of the piezoelectric crystal [78]. Fullerene polymer-like material $C_{60}Pd_n$ shows good adsorption capacity toward volatile aromatic carbons such as toluene, xylene, mercaptan, and formaldehyde in air and this result implies that fullerene can be used for the removal of harmful gases from living environment [77].

Medical and biological application of fullerenes also has been widely studied. C_{60} are considered to have a high potential for the drug delivery system since they can be multifunctionalized, act as drug adsorbents and form particles in nano-scale [79]. For instance, methanofullerene, a derivatized form of fullerenes, was conjugated to paclitaxel and used for the slow released drug delivery system and the conjugate injected into tissue cultures showed significant anti-cancer activity [80]. In another study [81], nanoparticles containing C_{60} were applied for the delivery of erythropoietin to the small intestine and the use of C_{60} in the nanoparticles significantly enhanced the bioavailability of erythropoietin. C_{60} derivatives can be used as the antibacterial and antiviral agents. For

instance, C_{60} derivatized with amine functional groups inhibited the growth of *Escherichia Coli*., presumably from the inhibition of respiratory chain [82]. C_{60}/PVP composites exhibited the inhibition of influenza virus type A, influenza virus type B, and herpes simplex virus [83]. Inhibition of HIV proteases seemingly resulted from the hydrophobic interaction of C_{60} derivative with the active site of enzyme [84]. However, the exact mechanism involved in antimicrobial and antiviral inhibition is not well elucidated.

With increasing commercial interests and industrial scale production facilities currently under construction [85], fullerene supply and demand, by all accounts, are expected to grow rapidly over the next decade [86, 87].

Toxicity

Despite the expected rapid growth in CNT and C_{60} production, information to assess the human health effects of the carbon nanomaterials is not sufficient. However, concerns have risen due to the recent findings that fullerenes can interact with living organisms causing toxic effects that are unique to this class of materials [61, 88-91].

The first comparative toxicity study of SWNT was performed by Lam *et al.* [91] , where carbon black and quartz used as low and high pulmonary toxicity controls, respectively. After 7 and 90 days of exposure to SWNT, which have produced by various methods and containing different amounts of metal catalysts, all SWNT induced

dose-dependent formation of granulomas in rodents. Based on the study, Lam *et al.* concluded that SWNT have higher toxicity than quartz, under their experimental conditions and the same weight-basis. Warheit et al. [90] also observed formation of pulmonary granulomas in rodents following the exposure to SWNT and the formation of granulomas was appeared to be due to the immune response for removal of foreign substances that are not easily degraded.

Kang *et al.* [92] studied microbial toxicity of SWNT using *Escherichia coli*.. To exclude any interference originated from impurities and/or the derivatization of the nanotubes, experiments were performed with highly purified, pristine SWNTs with a narrow diameter distribution. From the result of Scanning Electron Microscopy (SEM) analysis and fluorescence dye test, it is concluded that antimicrobial activity of SWNT originated from the physical damage to the outer membrane of the *Escherichia coli*. cells. The release of intracellular contents by the physical damage was confirmed by the measurement of DNA and RNA concentrations in the culture media after cultivation of cells with and without SWNT. In a recent study, Porter *et al.*[93] investigated the transport of SWNT to a human macrophage cell, which forms the first line of the defense in many human tissues against foreign materials, using Transmission Electron Microscopy (TEM) and Confocal Microscopy. Human monocyte-derived macrophages were contacted with SWNT for 2 and 4 days at SWNT concentrations ranged 0–10 μg/mL. Most significant observation of this research is that at 4 days of exposure, SWNT entered into the nuclear membrane and localized within the nucleus. This translocation of SWNT into the cytoplasm and localization within the cell nucleus appeared to have

caused cell mortality. Even though no significant decrease in cell viability was observed in 2 days, maximum 40 % decrease in cell viability was observed after 4 days of exposure to SWNT. However, the exact mechanism of cell morality is still unclear.

Toxicity of C_{60} also has been studied by various researchers. Sayes *et al*. [89] first reported cytotoxicity of water soluble C_{60} aggregates, which is commonly called as nC_{60}. In the comparative study with derivatized C_{60} using human dermal fibroblasts (HDF) and human liver carcinoma cells (HepG2), nC_{60} showed more than 7 order higher cell lethal dose than derivatized C_{60} even at relatively low concentration level (less that 1 mg/L). The research suggested that cytotoxicity of C_{60} is mainly originated from the leakage of the plasma membrane after oxidative stress and postulated that superoxide anion species generated from nC_{60} is responsible for the membrane damage and eventual cell death. However, recent study from Lee *et al.* [94] suggested that C_{60} can not produce superoxide anions, epecially when they exist as aggregates, and exact mechanism of the cytotoxicity is still not well understood. Toxicity studies [49, 95] on the prokaryotic bacteria showed that nC_{60} have antimicrobial properties against both Gram negative *Escherichia coli* and Gram positive *Bacillus subtilis*, with minimal inhibitory concentrations of 0.5 to 1 mg/L and 1.5 to 3.0 mg/L, respectively [95]. The result was consistent with a respiration study where CO_2 production reduced with the induction of nC_{60} during the exponential growth phase of the bacteria [49].

Preparation methods for nC_{60} suspension affect antibacterial properties of C_{60} [44]. Among four different methods for stable C_{60} suspension production, solvent exchange

method using THF as a solvent (THF/nC60), sonication of C_{60} dissolved in toluene with water (son/nC60), extensive mixing of C_{60} powder in water (aq/nC_{60}), and mixing with a solubilizing polymer (PVP/C_{60}), C_{60} prepared from son/nC_{60}, aq/nC_{60}, and PVP/C_{60} exhibited similar toxicity to *Bacillus subtilis*, while THF/nC_{60} had higher toxicity showing 1 order lower Minimum Inhibitory Concentration (MIC) to *Bacillus subtilis*. However, the higher toxicity of nC_{60} prepared from THF/C_{60} method could have occurred due to residual solvent (THF) during the preparation process [44]. Size of the nC_{60} also influenced the microbial toxicity and nC_{60} with small particle size generally showed higher toxicity compared to their larger counterparts [44].

Currently, the exposure to this carbon based nanomaterials is regulated based on graphite based exposure limit set by National Institute of Occupational Safety and Health Administration (NIOSH). However, the experimental results above imply that toxicity of these novel carbon based nanomaterials cannot be extrapolated from the existing data on particle toxicity.

Literature Cited

1. Iijima, S., Helical Microtubules of Graphitic Carbon. *Nature* **1991,** *354*, (6348), 56-58.
2. Dresselhaus, M. S., *Carbon Nanotubes Synthesis, Structure, Properties, and Applications* Springer: Heidelberg, Germany, 2001.
3. Loiseau, A., *Understanding Carbon nanotubes*. Springer: New York, 2006.
4. Kroto, H. W.; Heath, J. R.; Obrien, S. C.; Curl, R. F.; Smalley, R. E., C-60 - Buckminsterfullerene. *Nature* **1985,** *318*, (6042), 162-163.
5. Guo, T.; Nikolaev, P.; Rinzler, A. G.; Tomanek, D.; Colbert, D. T.; Smalley, R. E., Self-assembly of tubular fullerenes. *Journal of Physical Chemistry* **1995,** *99*, (27), 10694-10697.
6. Thess, A.; Lee, R.; Nikolaev, P.; Dai, H. J.; Petit, P.; Robert, J.; Xu, C. H.; Lee, Y. H.; Kim, S. G.; Rinzler, A. G.; Colbert, D. T.; Scuseria, G. E.; Tomanek, D.; Fischer, J. E.; Smalley, R. E., Crystalline ropes of metallic carbon nanotubes. *Science* **1996,** *273*, (5274), 483-487.
7. Munoz, E.; Maser, W. K.; Benito, A. M.; Martinez, M. T.; de la Fuente, G. F.; Righi, A.; Sauvajol, J. L.; Anglaret, E.; Maniette, Y., Single-walled carbon nanotubes produced by cw CO2-laser ablation: study of parameters important for their formation. *Applied Physics a-Materials Science & Processing* **2000,** *70*, (2), 145-151.

8. Hilding, J.; Grulke, E. A.; Zhang, Z. G.; Lockwood, F., Dispersion of carbon nanotubes in liquids. *Journal of Dispersion Science and Technology* **2003,** *24*, (1), 1-41.

9. Cui, S.; Lu, C. Z.; Qiao, Y. L.; Cui, L., Large-scale preparation of carbon nanotubes by nickel catalyzed decomposition of methane at 600 degrees C. *Carbon* **1999,** *37*, (12), 2070-2073.

10. Ivanov, V.; Fonseca, A.; Nagy, J. B.; Lucas, A.; Lambin, P.; Bernaerts, D.; Zhang, X. B., Catalytic production and purification of nanotubules having fullerene-scale diameters. *Carbon* **1995,** *33*, (12), 1727-1738.

11. Kukovecz, A.; Konya, Z.; Nagaraju, N.; Willems, I.; Tamasi, A.; Fonseca, A.; Nagy, J. B.; Kiricsi, I., Catalytic synthesis of carbon nanotubes over Co, Fe and Ni containing conventional and sol-gel silica-aluminas. *Physical Chemistry Chemical Physics* **2000,** *2*, (13), 3071-3076.

12. Flahaut, E.; Govindaraj, A.; Peigney, A.; Laurent, C.; Rousset, A.; Rao, C. N. R., Synthesis of single-walled carbon nanotubes using binary (Fe, Co, Ni) alloy nanoparticles prepared in situ by the reduction of oxide solid solutions. *Chemical Physics Letters* **1999,** *300*, (1-2), 236-242.

13. Tang, S.; Zhong, Z.; Xiong, Z.; Sun, L.; Liu, L.; Lin, J.; Shen, Z. X.; Tan, K. L., Controlled growth of single-walled carbon nanotubes by catalytic decomposition of CH4 over Mo/Co/MgO catalysts. *Chemical Physics Letters* **2001,** *350*, (1-2), 19-26.

14. Nikolaev, P.; Bronikowski, M. J.; Bradley, R. K.; Rohmund, F.; Colbert, D. T.; Smith, K. A.; Smalley, R. E., Gas-phase catalytic growth of single-walled carbon

nanotubes from carbon monoxide. *Chemical Physics Letters* **1999,** *313*, (1-2), 91-97.

15. Rao, C. N. R.; Sen, R.; Satishkumar, B. C.; Govindaraj, A., Large aligned-nanotube bundles from ferrocene pyrolysis. *Chemical Communications* **1998**, (15), 1525-1526.

16. Hirsch, A.; Brettreich, M., *Fullerenes: Chemistry and Reactions*. Wiley-VCH Verlag GMBH&Co.: Weinheim, 2005.

17. Diederich, F.; Ettl, R.; Rubin, Y.; Whetten, R. L.; Beck, R.; Alvarez, M.; Anz, S.; Sensharma, D.; Wudl, F.; Khemani, K. C.; Koch, A., The higher fullerenes - Isolation and characterization of C76, C84, C90, C94, and C70O, an oxide of D5H-C70. *Science* **1991,** *252*, (5005), 548-551.

18. Buhl, M.; Hirsch, A., Spherical aromaticity of fullerenes. *Chemical Reviews* **2001,** *101*, (5), 1153-1183.

19. Kratschmer, W.; Fostiropoulos, K.; Huffman, D. R., The infrared and ultraviolet-absorption spectra of laboratory-produced carbon dust - evidence for the presence of the C-60 molecule. *Chemical Physics Letters* **1990,** *170*, (2-3), 167-170.

20. Richter, H.; Labrocca, A. J.; Grieco, W. J.; Taghizadeh, K.; Lafleur, A. L.; Howard, J. B., Generation of higher fullerenes in flames. *Journal of Physical Chemistry B* **1997,** *101*, (9), 1556-1560.

21. Taylor, R.; Langley, G. J.; Kroto, H. W.; Walton, D. R. M., Formation of C_{60} by pyrolysis of naphthalene. *Nature* **1993,** *366*, (6457), 728-731.

22. Pope, C. J.; Marr, J. A.; Howard, J. B., Chemistry of fullerenes C-60 and C-70 formation in flames. *Journal of Physical Chemistry* **1993,** *97*, (42), 11001-11013.

23. Howard, J. B.; McKinnon, J. T.; Makarovsky, Y.; Lafleur, A. L.; Johnson, M. E., Fullerenes C_{60} and C_{70} in flames. *Nature* **1991,** *352*, (6331), 139-141.

24. Tremblay, J. F., Mitsubishi chemical aims at breakthrough. *Chemical & Engineering News* **2002,** *80*, (49), 16-17.

25. Ogoshi, T.; Yamagishi, T.; Nakamoto, Y.; Harada, A., Water soluble single-walled carbon nanotubes using inclusion complex of cyclodextrin with an adamantane derivative. *Chemistry Letters* **2007,** *36*, (8), 1026-1027.

26. Zhao, B.; Hu, H.; Yu, A. P.; Perea, D.; Haddon, R. C., Synthesis and characterization of water soluble single-walled carbon nanotube graft copolymers. *Journal of the American Chemical Society* **2005,** *127*, (22), 8197-8203.

27. Zhao, W.; Song, C. H.; Pehrsson, P. E., Water-soluble and optically pH-sensitive single-walled carbon nanotubes from surface modification. *Journal of the American Chemical Society* **2002,** *124*, (42), 12418-12419.

28. Ago, H.; Kugler, T.; Cacialli, F.; Salaneck, W. R.; Shaffer, M. S. P.; Windle, A. H.; Friend, R. H., Work functions and surface functional groups of multiwall carbon nanotubes. *Journal of Physical Chemistry B* **1999,** *103*, (38), 8116-8121.

29. Kuznetsova, A.; Popova, I.; Yates, J. T.; Bronikowski, M. J.; Huffman, C. B.; Liu, J.; Smalley, R. E.; Hwu, H. H.; Chen, J. G. G., Oxygen-containing functional groups on single-wall carbon nanotubes: NEXAFS and vibrational spectroscopic studies. *Journal of the American Chemical Society* **2001,** *123*, (43), 10699-10704.

30. Seifert, G.; Kohler, T.; Frauenheim, T., Molecular wires, solenoids, and capacitors by sidewall functionalization of carbon nanotubes. *Applied Physics Letters* **2000,** *77*, (9), 1313-1315.

31. Mickelson, E. T.; Huffman, C. B.; Rinzler, A. G.; Smalley, R. E.; Hauge, R. H.; Margrave, J. L., Fluorination of single-wall carbon nanotubes. *Chemical Physics Letters* **1998,** *296*, (1-2), 188-194.

32. Islam, M. F.; Rojas, E.; Bergey, D. M.; Johnson, A. T.; Yodh, A. G., High weight fraction surfactant solubilization of single-wall carbon nanotubes in water. *Nano Letters* **2003,** *3*, (2), 269-273.

33. Matarredona, O.; Rhoads, H.; Li, Z. R.; Harwell, J. H.; Balzano, L.; Resasco, D. E., Dispersion of single-walled carbon nanotubes in aqueous solutions of the anionic surfactant NaDDBS. *Journal of Physical Chemistry B* **2003,** *107*, (48), 13357-13367.

34. Chen, Q.; Saltiel, C.; Manickavasagam, S.; Schadler, L. S.; Siegel, R. W.; Yang, H. C., Aggregation behavior of single-walled carbon nanotubes in dilute aqueous suspension. *Journal of Colloid and Interface Science* **2004,** *280*, (1), 91-97.

35. Wang, H.; Zhou, W.; Ho, D. L.; Winey, K. I.; Fischer, J. E.; Glinka, C. J.; Hobbie, E. K., Dispersing single-walled carbon nanotubes with surfactants: A small angle neutron scattering study. *Nano Letters* **2004,** *4*, (9), 1789-1793.

36. O'Connell, M. J.; Boul, P.; Ericson, L. M.; Huffman, C.; Wang, Y. H.; Haroz, E.; Kuper, C.; Tour, J.; Ausman, K. D.; Smalley, R. E., Reversible water-solubilization of single-walled carbon nanotubes by polymer wrapping. *Chemical Physics Letters* **2001,** *342*, (3-4), 265-271.

37. Carrillo, A.; Swartz, J. A.; Gamba, J. M.; Kane, R. S.; Chakrapani, N.; Wei, B. Q.; Ajayan, P. M., Noncovalent functionalization of graphite and carbon nanotubes

with polymer multilayers and gold nanoparticles. *Nano Letters* **2003,** *3*, (10), 1437-1440.

38. O'Connell, M. J.; Bachilo, S. M.; Huffman, C. B.; Moore, V. C.; Strano, M. S.; Haroz, E. H.; Rialon, K. L.; Boul, P. J.; Noon, W. H.; Kittrell, C.; Ma, J. P.; Hauge, R. H.; Weisman, R. B.; Smalley, R. E., Band gap fluorescence from individual single-walled carbon nanotubes. *Science* **2002,** *297*, (5581), 593-596.

39. Zhang, J.; Lee, J. K.; Wu, Y.; Murray, R. W., Photoluminescence and electronic interaction of anthracene derivatives adsorbed on sidewalls of single-walled carbon nanotubes. *Nano Letters* **2003,** *3*, (3), 403-407.

40. Kim, O. K.; Je, J. T.; Baldwin, J. W.; Kooi, S.; Pehrsson, P. E.; Buckley, L. J., Solubilization of single-wall carbon nanotubes by supramolecular encapsulation of helical amylose. *Journal of the American Chemical Society* **2003,** *125*, (15), 4426-4427.

41. Chen, R. J.; Bangsaruntip, S.; Drouvalakis, K. A.; Kam, N. W. S.; Shim, M.; Li, Y. M.; Kim, W.; Utz, P. J.; Dai, H. J., Noncovalent functionalization of carbon nanotubes for highly specific electronic biosensors. *Proceedings of the National Academy of Sciences of the United States of America* **2003,** *100*, (9), 4984-4989.

42. Heymann, D., Solubility of fullerenes C-60 and C-70 in seven normal alcohols and their deduced solubility in water. *Fullerene Science and Technology* **1996,** *4*, (3), 509-515.

43. Arrais, A.; Boccaleri, E.; Diana, E., Efficient direct water-solubilisation of single-walled carbon nanotube derivatives. *Fullerenes Nanotubes and Carbon Nanostructures* **2004,** *12*, (4), 789-809.

44. Lyon, D. Y.; Adams, L. K.; Falkner, J. C.; Alvarez, P. J. J., Antibacterial activity of fullerene water suspensions: Effects of preparation method and particle size. *Environmental Science & Technology* **2006,** *40*, (14), 4360-4366.

45. Yamakoshi, Y. N.; Yagami, T.; Fukuhara, K.; Sueyoshi, S.; Miyata, N., Solubilization of fullerenes into water with polyvinylpyrrolidone applicable to biological tests. *Journal of the Chemical Society-Chemical Communications* **1994**, (4), 517-518.

46. Murthy, C. N.; Choi, S. J.; Geckeler, K. E., Nanoencapsulation of [60]fullerene by a novel sugar-based polymer. *Journal of Nanoscience and Nanotechnology* **2002,** *2*, (2), 129-132.

47. Scrivens, W. A.; Tour, J. M.; Creek, K. E.; Pirisi, L., Synthesis of C-14-labeled C-60, its suspension in water, and its uptake by human keratinocytes. *Journal of the American Chemical Society* **1994,** *116*, (10), 4517-4518.

48. Deguchi, S.; Alargova, R. G.; Tsujii, K., Stable dispersions of fullerenes, C-60 and C-70, in water. Preparation and characterization. *Langmuir* **2001,** *17*, (19), 6013-6017.

49. Fortner, J. D.; Lyon, D. Y.; Sayes, C. M.; Boyd, A. M.; Falkner, J. C.; Hotze, E. M.; Alemany, L. B.; Tao, Y. J.; Guo, W.; Ausman, K. D.; Colvin, V. L.; Hughes, J. B., C-60 in water: Nanocrystal formation and microbial response. *Environmental Science & Technology* **2005,** *39*, (11), 4307-4316.

50. Brant, J.; Lecoanet, H.; Hotze, M.; Wiesner, M., Comparison of electrokinetic properties of colloidal fullerenes (n-C-60) formed using two procedures. *Environmental Science & Technology* **2005,** *39*, (17), 6343-6351.

51. Cheng, X. K.; Kan, A. T.; Tomson, M. B., Naphthalene adsorption and desorption from Aqueous C-60 fullerene. *Journal of Chemical and Engineering Data* **2004,** *49*, (3), 675-683.

52. Rao, A. M.; Richter, E.; Bandow, S.; Chase, B.; Eklund, P. C.; Williams, K. A.; Fang, S.; Subbaswamy, K. R.; Menon, M.; Thess, A.; Smalley, R. E.; Dresselhaus, G.; Dresselhaus, M. S., Diameter-selective Raman scattering from vibrational modes in carbon nanotubes. *Science* **1997,** *275*, (5297), 187-191.

53. Jacquemin, R.; Kazaoui, S.; Yu, D.; Hassanien, A.; Minami, N.; Kataura, H.; Achiba, Y., Doping mechanism in single-wall carbon nanotubes studied by optical absorption. *Synthetic Metals* **2000,** *115*, (1-3), 283-287.

54. Kukovecz, A.; Kramberger, C.; Georgakilas, V.; Prato, M.; Kuzmany, H., A detailed Raman study on thin single-wall carbon nanotubes prepared by the HiPCO process. *European Physical Journal B* **2002,** *28*, (2), 223-230.

55. Dresselhaus, M. S.; Dresselhaus, G.; Jorio, A.; Souza, A. G.; Saito, R., Raman spectroscopy on isolated single wall carbon nanotubes. *Carbon* **2002,** *40*, (12), 2043-2061.

56. Sinani, V. A.; Gheith, M. K.; Yaroslavov, A. A.; Rakhnyanskaya, A. A.; Sun, K.; Mamedov, A. A.; Wicksted, J. P.; Kotov, N. A., Aqueous dispersions of single-wall and multiwall carbon nanotubes with designed amphiphilic polycations. *Journal of the American Chemical Society* **2005,** *127*, (10), 3463-3472.

57. Britz, D. A.; Khlobystov, A. N., Noncovalent interactions of molecules with single walled carbon nanotubes. *Chemical Society Reviews* **2006,** *35*, (7), 637-659.

58. Moore, V. C.; Strano, M. S.; Haroz, E. H.; Hauge, R. H.; Smalley, R. E.; Schmidt, J.; Talmon, Y., Individually suspended single-walled carbon nanotubes in various surfactants. *Nano Letters* **2003,** *3*, (10), 1379-1382.

59. Ajie, H.; Alvarez, M. M.; Anz, S. J.; Beck, R. D.; Diederich, F.; Fostiropoulos, K.; Huffman, D. R.; Kratschmer, W.; Rubin, Y.; Schriver, K. E.; Sensharma, D.; Whetten, R. L., Characterization of the soluble all-carbon molecules C_{60} and C_{70}. *Journal of Physical Chemistry* **1990,** *94*, (24), 8630-8633.

60. Weeks, D. E.; Harter, W. G., Vibrational frequencies and normal-modes of buckminsterfullerene. *Chemical Physics Letters* **1988,** *144*, (4), 366-372.

61. Dreher, K. L., Health and environmental impact of nanotechnology: Toxicological assessment of manufactured nanoparticles. *Toxicological Sciences* **2004,** *77*, (1), 3-5.

62. Ajayan, P. M.; Charlier, J. C.; Rinzler, A. G., Carbon nanotubes: From macromolecules to nanotechnology. *Proceedings of the National Academy of Sciences of the United States of America* **1999,** *96*, (25), 14199-14200.

63. Rinzler, A. G.; Hafner, J. H.; Nikolaev, P.; Lou, L.; Kim, S. G.; Tomanek, D.; Nordlander, P.; Colbert, D. T.; Smalley, R. E., Unraveling Nanotubes - Field-Emission from an Atomic Wire. *Science* **1995,** *269*, (5230), 1550-1553.

64. Zhu, W.; Bower, C.; Zhou, O.; Kochanski, G.; Jin, S., Large current density from carbon nanotube field emitters. *Applied Physics Letters* **1999,** *75*, (6), 873-875.

65. Dillon, A. C.; Jones, K. M.; Bekkedahl, T. A.; Kiang, C. H.; Bethune, D. S.; Heben, M. J., Storage of hydrogen in single-walled carbon nanotubes. *Nature* **1997,** *386*, (6623), 377-379.

66. Cheng, H. M.; Yang, Q. H.; Liu, C., Hydrogen storage in carbon nanotubes. *Carbon* **2001,** *39*, (10), 1447-1454.

67. Ajayan, P. M.; Zhou, O. Z., Applications of carbon nanotubes. *Carbon Nanotubes* **2001,** *80*, 391-425.

68. Kong, J.; Franklin, N. R.; Zhou, C.; Chapline, M. G.; Peng, S.; Cho, K.; Dai, H., Nanotube Molecular Wires as Chemical Sensors. *Science* **2000,** *287*, 622-625.

69. Collins, P. G.; Bradley, K.; Ishigami, M.; Zettl, A., Extreme oxygen sensitivity of electronic properties of carbon nanotubes. *Science* **2000,** *287*, (5459), 1801-1804.

70. Chopra, S.; McGuire, K.; Gothard, N.; Rao, A. M.; Pham, A., Selective gas detection using a carbon nanotube sensor. *Applied Physics Letters* **2003,** *83*, (11), 2280-2282.

71. Chopra, S.; Pham, A.; Gaillard, J.; Parker, A.; Rao, A. M., Carbon-nanotube-based resonant-circuit sensor for ammonia. *Applied Physics Letters* **2002,** *80*, (24), 4632-4634.

72. Bower, C.; Zhou, O.; Zhu, W.; Ramirez, A. G.; Kochanski, G. P.; Jin, S. In Amorphous and Nanostructured Carbon 2000; Material Ressearch Society: 2000.

73. Pederson, M. R.; Broughton, J. Q., Nanocapillarity in fullerene tubules. *Physical Review Letters* **1992,** *69*, (18), 2689-2692.

74. Ye, Y.; Ahn, C. C.; Witham, C.; Fultz, B.; Liu, J.; Rinzler, A. G.; Colbert, D.; Smith, K. A.; Smalley, R. E., Hydrogen adsorption and cohesive energy of single-walled carbon nanotubes. *Applied Physics Letters* **1999,** *74*, (16), 2307-2309.

75. Treacy, M. M. J.; Ebbesen, T. W.; Gibson, J. M., Exceptionally high Young's modulus observed for individual carbon nanotubes. *Nature* **1996,** *381*, (6584), 678-680.

76. Wong, S. S.; Harper, J. D.; Lansbury, P. T.; Lieber, C. M., Carbon nanotube tips: High-resolution probes for imaging biological systems. *Journal of the American Chemical Society* **1998,** *120*, (3), 603-604.

77. Hayashi, A.; Yamamoto, S.; Suzuki, K.; Matsuoka, T., The first application of fullerene polymer-like materials, $C_{60}Pd_n$, as gas adsorbents *R&D Review of Toyota CRDL* **2004,** *40*, (1), 14-21.

78. Lin, H.-B.; Shih, J.-S., Fullerene C60-cryptand coated surface acoustic wave quartz crystal sensor for organic vapors. *Sensors and Actuators B: Chemical* **2003,** *92*, (3), 243-254.

79. Langa, F.; Nierengarten, J., *Fullerenes Principles and Applications*. RCS Publishing: Cambridge, UK, 2007.

80. Zakharian, T. Y.; Seryshev, A.; Sitharaman, B.; Gilbert, B. E.; Knight, V.; Wilson, L. J., A Fullerene-Paclitaxel Chemotherapeutic: Synthesis, Characterization, and Study of Biological Activity in Tissue Culture. *Journal of the American Chemical Society* **2005,** *127*, (36), 12508-12509.

81. Venkatesan, N.; Yoshimitsu, J.; Ito, Y.; Shibata, N.; Takada, K., Liquid filled nanoparticles as a drug delivery tool for protein therapeutics. *Biomaterials* **2005,** *26*, (34), 7154-7163.

82. Mashino, T.; Usui, N.; Okuda, K.; Hirota, T.; Mochizuki, M., Respiratory chain inhibition by fullerene derivatives: hydrogen peroxide production caused by

fullerene derivatives and a respiratory chain system. *Bioorganic & Medicinal Chemistry* **2003,** *11*, (7), 1433-1438.

83. Piotrovsky, L. B.; Kiselev, O. I., Fullerenes and Viruses. *Fullerenes Nanotubes and Carbon Nanostructures* **2004,** *12*, (1/2), 397-403.

84. Sijbesma, R.; Srdanov, G.; Wudl, F.; Castoro, J. A.; Wilkins, C.; Friedman, S. H.; DeCamp, D. L.; Kenyon, G. L., Synthesis of a fullerene derivative for the inhibition of HIV enzymes. *Journal of the American Chemical Society* **1993,** *115*, (15), 6510-6512.

85. Colvin, V. L., The potential environmental impact of engineered nanomaterials *Nature Biotechnology* **2004,** *22*, (6), 760-760.

86. Lee, B. I.; Qi, L.; Copeland, T., Nanoparticles for materials design: present & future. *Journal of Ceramic Processing Research* **2005,** *6*, (1), 31-40.

87. Ball, P., Roll up for the revolution. *Nature* **2001,** *414*, (6860), 142-144.

88. Cui, D. X.; Tian, F. R.; Ozkan, C. S.; Wang, M.; Gao, H. J., Effect of single wall carbon nanotubes on human HEK293 cells. *Toxicology Letters* **2005,** *155*, (1), 73-85.

89. Sayes, C. M.; Fortner, J. D.; Guo, W.; Lyon, D.; Boyd, A. M.; Ausman, K. D.; Tao, Y. J.; Sitharaman, B.; Wilson, L. J.; Hughes, J. B.; West, J. L.; Colvin, V. L., The differential cytotoxicity of water-soluble fullerenes. *Nano Letters* **2004,** *4*, (10), 1881-1887.

90. Warheit, D. B.; Laurence, B. R.; Reed, K. L.; Roach, D. H.; Reynolds, G. A.; Webb, T. R., Comparative pulmonary toxicity assessment of single-wall carbon nanotubes in rats. *Toxicological Sciences* **2004,** *77*, (1), 117-25.

91. Lam, C. W.; James, J. T.; McCluskey, R.; Hunter, R. L., Pulmonary toxicity of single-wall carbon nanotubes in mice 7 and 90 days after intratracheal instillation. *Toxicological Sciences* **2004,** *77*, (1), 126-134.

92. Kang, S.; Pinault, M.; Pfefferle, L. D.; Elimelech, M., Single-walled carbon nanotubes exhibit strong antimicrobial activity. *Langmuir* **2007,** *23*, (17), 8670-8673.

93. Porter, A. E.; Gass, M.; Muller, K.; Skepper, J. N.; Midgley, P. A.; Welland, M., Direct imaging of single-walled carbon nanotubes in cells. *Nature Nanotechnology* **2007,** *2*, (11), 713-717.

94. Lee, J.; Fortner, J. D.; Hughes, J. B.; Kim, J. H., Photochemical production of reactive oxygen species by C-60 in the aqueous phase during UV irradiation. *Environmental Science & Technology* **2007,** *41*, (7), 2529-2535.

95. Lyon, D. Y.; Fortner, J. D.; Sayes, C. M.; Colvin, V. L.; Hughes, J. B., Bacterial cell association and antimicrobial activity of a C-60 water suspension. *Environmental Toxicology and Chemistry* **2005,** *24*, (11), 2757-2762.

CHAPTER 3*
NATURAL ORGANIC MATTER STABILIZES CARBON NANOTUBES IN THE AQUEOUS PHASE

Abstract

This study investigates the aqueous stability of multi-walled carbon nanotubes (MWNTs) in the presence of natural organic matter (NOM). MWNTs were readily dispersed as an aqueous suspension in both model NOM (Suwannee River NOM (SR-NOM)) solutions and natural surface water (actual Suwannee River water with unaltered NOM background) which remained stable for over one month. Microscopic analyses suggested that the suspension consisted primarily of individually dispersed MWNTs. Concentrations of MWNTs suspended in the aqueous phase, quantified using thermal optical transmission analysis (TOT), ranged from 0.6 mg/L to 6.9 mg/L as initial concentrations of MWNT and SR-NOM were varied from 50 to 500 mg/L and 10 to 100 mg/L, respectively. Suwannee River water showed the similar MWNT stabilizing capacity compared to the model SR-NOM solutions. For the same initial MWNT concentrations, the concentrations of suspended MWNT in SR-NOM solutions and Suwannee River water were considerably higher than that in a solution of 1 % sodium dodecyl sulfate, a commonly used surfactant to stabilize CNTs in the aqueous phase. These findings suggest that dispersal of carbon based nano-materials in the natural, aqueous environment might occur to unexpected extent following a mechanism that has not been previously considered in environmental fate and transport studies.

*This chapter is published in Environmental Science and Technology, vol. 41, page 179-184 in 2007.

Introduction

Carbon nanotubes (CNTs) are pure carbon macromolecules consisting of sheets of carbon atoms covalently bonded in hexagonal arrays that are seamlessly rolled into a hollow, cylindrical shape with both ends rounded through pentagon ring inclusions. Variable CNT architectures with diameters in the nanometer range (*ca*. 1 to 100 nm) and lengths up to several tens of micrometers give rise to high length to diameter aspect ratios compared to other carbon fullerenes such as C_{60} (1). Based on their structure, CNTs are categorized into two main species; single-walled nanotubes (SWNTs) and multi-walled nanotubes (MWNTs). The latter results from a co-axial assembly of the multiple SWNTs (2).

CNTs are being considered for a range of applications due to their exceptional mechanical, electro-optical, and thermal properties (3,4). Examples of such properties and corresponding applications include: high tensile strength and elasticity suitable for aerospace and fiber industries (5); electronic conductance and unique semi-conducting capacities ideal for nano-electronics and semiconductors (5-7); hydrogen adsorption (storage) capacity for application in hydrogen based fuel cells (8,9); and electronic sensitivity in different chemical environments allowing for novel environmental sensors (10-13). With increasing commercial interests and industrial scale production facilities currently under construction (14), CNT supply and demand, by all accounts, are expected to grow very rapidly over the next decade (15,16).

Unfortunately, a limited amount of information is currently available regarding the fate and transport of CNTs in the natural and engineering environment and the ultimate human health effects (14). To date, studies have shown that CNTs are biologically active as demonstrated by a pulmonary response via induction of pulmonary granulomas (17,18) at greater instance than quartz (1-3 μm crystalline silica), which is a recognized chronic occupational health hazard (via inhalation routes). Both SWNT and MWNT were also attributed to cause the loss of the phagocytic ability and ultrastructure damage to alveola macrophages (19). Furthermore, CNT have induced observable toxic responses in other cell cultures (20,21).

When considering industrial scale production and use, observed biological activities, and the fact that CNT and other fullerene structures have been identified in the soot from common hydrocarbon combustion processes (22,23), understanding their fate in the natural environment is necessary to assess possible routes for exposure to human and ecosystem. The CNTs have seldom been considered as potential contaminants in the aqueous phase. They are extremely hydrophobic and prone to aggregation, as they are subject to high Van der Waals interaction forces along the length axis, thus not readily dispersed (24,25). However, facile dispersion of CNT in aqueous phase can be achieved by augmenting the surface of the carbon structure through the addition of surfactants and polymers such as sodium dodecyl sulfate (SDS) (26-33), sodium dodecylbenzene sulfonate (NaDDBS) (34,35), Triton X-100 (34,36,37) and polyvinyl pyrrolidone (PVP) (38) among others (34,39). These surfactants and polymers not only create a

thermodynamically suitable surface in water but also provide steric or electrostatic repulsion among dispersed CNTs thus preventing aggregation (27,30,35,36).

Given the previous observations that CNTs are stabilized in the aqueous phase by well characterized surfactants and polymers, it is possible that similar interactions between CNTs and organic molecules present in natural systems will occur. This may result in aqueous dispersion and stabilization of CNTs following a demonstrated mechanism of hydrophobic surface shielding that has not been widely considered in environmental fate and transport studies to date. The objectives of this study were to verify MWNT stabilization, as an aqueous suspension, in both synthetic solutions containing model natural organic matter (NOM) and natural surface water with high NOM background (Suwannee River) and to develop a method to quantify MWNTs suspended in NOM solutions based on thermal optical analysis.

Experimental

MWNTs, produced by chemical vapor deposition (CVD) method with purity greater than 90 %, were obtained from the MER Corporation (Tucson, AZ). Average diameter and average length were reported by the manufacturer to be 140 ± 30 nm (approximately 100 graphene layers per each molecules on average) and 7 ± 2 μm, respectively. Standard Suwannee River NOM (SR-NOM) obtained from International Humic Substances Society (IHSS) (St. Paul, MN) was used as model NOM. Number average and weight average molecular weights of SR-NOM determined by gel permeation chromatography (GPC) were reported as 1,718 Da and 2,703 Da, respectively (40). Based on the analytical information provided by IHSS, the SR-NOM is composed of 52.47 wt % of carbon, 4.19 wt % of hydrogen, 42.69 wt % of oxygen, 1.10 wt % of nitrogen, 0.65 wt % of sulfur and 0.02 wt % of phosphate and ash content is 7.0 wt %. Significant amount of carbon in the SR-NOM is distributed at the carboxylic group (20 %), which provides acidic moiety to the SR-NOM, as well as aromatic (23 %), aliphatic (27 %) and heteroaliphatic (15 %) groups. A 100 mg-Carbon/L (C/L) stock solution was prepared by dissolving SR-NOM for 24 hours and filtering the solution through a 0.2 μm nylon membrane filter (Cole Parmer, Chicago, IL). For comparison with model SR-NOM, a grab sample of actual Suwannee River water was obtained from the official sampling site of the IHSS, located in the Okefenokee National Wildlife Refugee in the State of Georgia (41). The water sample was transported in a cooler packed with ice from the sampling location and preserved in a 4 ^{o}C temperature room after filtered with a 0.2 μm nylon membrane filter (Cole Parmer, Chicago, IL). ACS reagent grade (>99 %) Sodium

dodecyl sulfate (SDS, $CH_3(CH_2)_{11}OSO_3Na$, FW 288.38) (Aldrich Chemical Company, Milwaukee, WI), which has critical micelle concentration of 0.24 % at 25 ^oC, was used as a representative surfactant to stabilize MWNTs in water. Ultrapure water (>18 MΩ) produced by the Milli-Q water purification system (Millipore, Billerica, MA) was used for the preparation of all solutions.

MWNT suspensions were prepared by adding varying amounts of MWNT into 100 mL of Milli-Q water, 1% SDS solution, a well known surfactant to stabilize CNTs, as a positive control, the solutions containing varying concentrations SR-NOM, and Suwannee River water in Erlenmeyer flasks and vigorously agitating the solutions for one hour. After settling for four days, the unsettled supernatant (*ca*. 60 % of total volume) was carefully removed by syringe from the top of the flask. The solution was then filtered using a Whatman Model 541 filter paper (20-25 μm, Florham Park, NJ) to remove any undispersed MWNT agglomerates and the filtrate was collected for further analyses.

In situ images (i.e. suspended in the water phase) of MWNTs in suspension were obtained using a Leica DM IRM Differential Interference Contrast (DIC) Microscope (Wetzlar, Germany) operated in a reflective index mode and recorded with a Hamamatsu EM-CCD C9100 Camera (Hamamatsu City, Japan). The point-to-point resolution of the resulting image was 0.053 μm. Suspended MWNTs were particularly easy to identify and record due to the contrasting reflective indexes of MWNT compared to the aqueous background. Electron microscopic images were analyzed by a JEM 100C transmission

electron microscope (TEM) (Jeol, Peabody, MA) using 100 kV electron beam at magnifications of 7,200 and 100,000. TEM samples were prepared by placing a droplet of MWNT aqueous suspension on the 300 mesh copper carbon grid (Electron Microscopy Science, Hatfield, PA) and dried overnight at room temperature.

Concentrations of suspended MWNTs were determined by a Thermal Optical Transmittance Analyzer (TOT) (Sunset Laboratory, Tigard, OR), UV-Vis absorbance, and turbidity measurements. TOT analysis was performed following the method described by NIOSH (National Institute for Occupational Safety and Health) (42). Samples for the TOT were prepared by filtering a known volume of MWNT suspension through a 25 mm diameter disc type Pallflex 2500 quartz filter (Pall Corporation, Ann Arbor, MI) with nominal pore size of 0.3 μm, which has good durability at high temperature condition of TOT, and drying the filter for 24 hours at 90 ^{o}C. Independent control test confirmed that virtually all MWNTs stabilized in the aqueous suspension were retained by this filter (*i.e*. the concentration of MWNT in the filtrate was less than the detection limit of the analytical methods used in this study). NOM and SDS that were not associated with MWNTs were also removed as filtrate during this step. After drying, each TOT specimen was prepared by cutting a 1.5 cm^2 rectangular area from the center of the glass filter and loading it on a glass sampling boat of the TOT. Before each set of measurements, the equipment was calibrated using a 10 μL of 5.0 mg/L sucrose solution. For each measurement, the flame ionization detector (FID) was calibrated using a known volume of CH_4. UV-Vis absorbance and turbidity of MWNT suspensions were measured by an Agilent 8453 UV-Vis spectroscopy system (Palo Alto, CA) and a Hach 2100N

turbidimeter (Loveland, CO), respectively. Concentrations of NOM remaining in the solution phase, which did not adsorb onto MWNT, were quantified by UV-Vis absorbances at 254 nm (UV_{254}) after removing the suspended MWNT and associated NOM with a GHP Acrodisc 0.2 μm syringe filter (Pall Corporation, Ann Arbor, MI). UV_{254} measurements were calibrated with DOC analysis (TOC-Vw analyzer, Shimadzu, Columbia, MD).

Results and Discussion

The stability of MWNTs in the aqueous phase was largely dependent on the presence of SDS or NOM (Figure 3.1). The MWNTs added to organic-free Milli-Q water at 500 mg/L (50 mg of MWNTs added to 100 mL Milli-Q water) settled quickly and the water became completely transparent in less than an hour (Figure 3.1a). Upon the addition of the MWNT at the same (equivalent) concentration, a 1% SDS solution immediately became dark and turbid. The solution gradually changed to a light grey suspension after one day of settling and the color of the solution did not noticeably change for over a month (Figure 3.1b). The solution of 100 mg-C/L SR-NOM originally appeared dark and turbid upon equivalent MWNT addition and gradually lightened with a corresponding loss of turbidity during the first four days of settling. However, after four days, the dark solution, which appeared to be due to the presence of MWNTs, with yellowish background remained stable for over a month (Figure 3.1c).

In-situ microscopic images of MWNTs suspended in the SDS and SR-NOM solutions are presented in Figure 2. Negligible morphological differences were observed between the MWNTs stabilized by SDS (Figure 3.2a) and those by SR-NOM (Figure 3.2b). Both samples contained relatively well dispersed rod-shaped MWNTs as well as larger size flocs albeit in much less frequency. A closer examination of MWNTs in SR-NOM solution by TEM suggested that the majority of MWNTs were suspended as a single tube (a representative image shown in Figure 3.2c), as evidenced by the presence of single hollow core (approximately 2 nm in diameter according to the manufacturer) in

single fibrous structure in these images. Bundles of MWNTs (*i.e.* pairing of several MWNTs along the length axis) were seldom observed. Bubble-like artifacts adjacent to MWNT surfaces might have originated from the sublimation of organic matter due to high energy electron beam irradiation during TEM analysis. The agglomerates of MWNTs in which single MWNT appeared to be connected to another MWNT, potentially by bridging through NOM, were also observed during TEM examination. While it is possible that some of these bridged structures might have been additionally generated during a drying process for TEM sample preparation, the similar structures were also observed in the *in-situ* images.

In the presence of complex and undefined NOM, analytical approaches utilizing elemental and molecular characteristics may prove challenging to quantify the amount of CNT suspended in the aqueous phase. It should also be noted that CNT sample used in this study consists of a mixture of molecules with different sizes. A method of using TOT relies on the fact that thermal stability of organic carbon (NOM) and elemental carbon (CNT) are different such that they can be differentially quantified (43-46). This instrument is widely used to examine carbon content and composition in various atmospheric samples (47-51).

The TOT analysis typically proceeds in two distinct stages (52). In the first stage, temperature increases stepwise up to 820 ^{o}C in a He atmosphere to volatilize organic carbon (OC) which is then oxidized to CO_2 via granular MnO_2 at 900 °C. CO_2 is subsequently reduced to CH_4 by a Ni/firebrick methanator at 450 °C and quantified by a

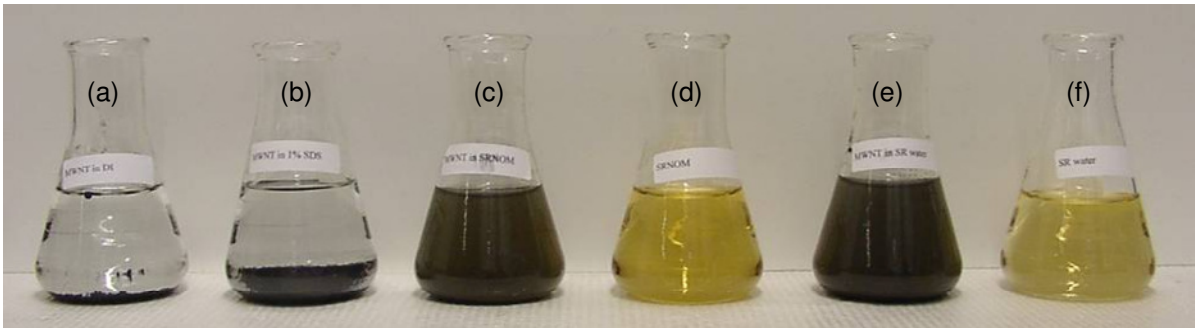

Figure 3.1. Visual examination of (a) organic-free water, (b) 1 % SDS solution, and (c) 100 mg-C/L SR-NOM solution and (e) Suwannee River water after adding 500 mg/L of MWNTs, agitating for one hour, and quiescent settling for four days. 100 mg-C/L SR-NOM solution and Suwannee River water without MWNT addition are also shown in (d) and (f).

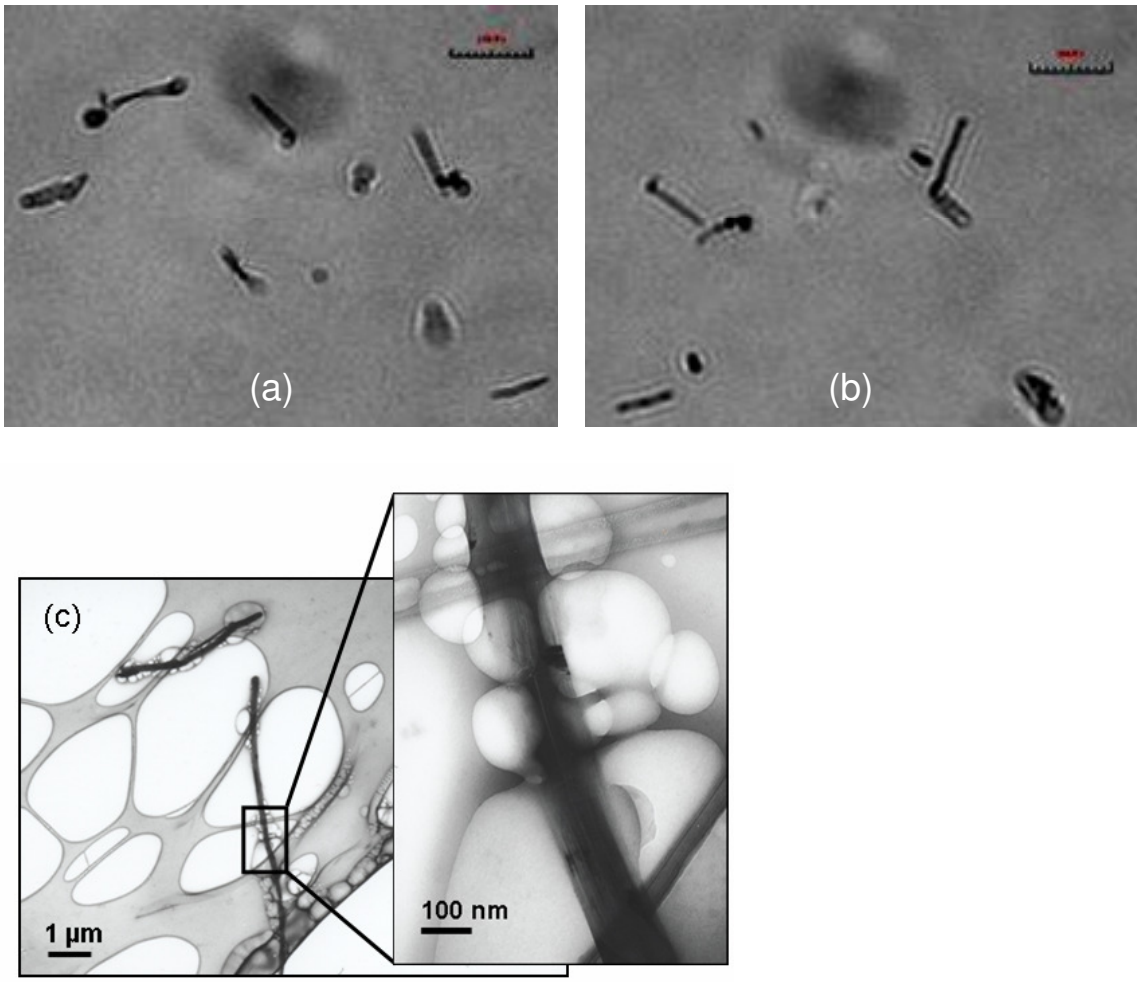

Figure 3.2. (a) *In-situ* microscope images of MWNTs suspended in 1 % SDS solution and (b) 100 mg-C/L SR-NOM solution (from Figure 1). The scale bars in the upper right corner of each image correspond to 5.3 µm. (c) A representative transmission electron microscopy image of MWNTs stabilized in the SR-NOM solution.

flame ionization detector (FID). However, not all of OC is volatilized, as some becomes pyrolized in the O_2 deficient atmosphere. Elemental carbon (EC) measurement along with pyrolized organic carbon (PC) correction is performed in the next stage. The temperature is again raised stepwise in an O_2 (10 %) and He (90 %) mixed atmosphere. The total amount of thermally oxidized EC and PC is measured by the FID after reduction to CH_4. Utilizing He-Ne laser transmittance through the sample, EC from the original sample is differentiated from PC. In the first stage, as PC is generated and absorbs the light, the laser transmittance is decreased. However as both EC and PC are volatilized, the laser transmittance increases in the second stage. The point at which the laser transmittance reaches the initial value (time = 0) is the separation point between PC and EC. CH_4 detected before this point is attributed to carbon originating from OC and that detected after this point is from EC.

Profiles of temperature, laser transmittance, and FID signal for an entire cycle of a TOT measurement are presented in Figure 3.3 along with the split point between OC and EC. Control experiments were first performed with only SR-NOM (Figure 3.3a) and only MWNT (Figure 3.3b) samples. The sample containing only SR-NOM was prepared by placing 1 mL of 500 mg/L SR-NOM stock solution on top of the quartz filter without suction and drying at 90 ^{o}C. The sample with only MWNT was prepared by adding MWNT to Milli-Q water, retrieving an arbitrary fraction onto the quartz filter, and drying it overnight at 90 ^{o}C. Therefore, the exact concentrations of MWNT were unknown and quantitative comparison was not made for these samples. Nevertheless, these experiments confirmed that signals from these different carbon classes do not overlap,

allowing for quantitative differentiation between MWNT and SR-NOM. During the analysis of SR-NOM only control (Figure 3.3a), peaks were generated in both the first and second stages of analysis and the second stage peak appeared to be due to the generation of PC, as the concentration estimated from the sum of two peaks agreed with a concentration measured as DOC. For the MWNT-only sample (Figure 3.3b), peaks were observed only in the second stage as EC (with O_2 present). When the sample specimen after one cycle was subject to another entire TOT cycle, no further change in laser transmittance was observed and no more CH_4 was produced, confirming that MWNT conversion to CH_4 was complete, consistent with observations reported in the literature under similar combustion conditions (53,54).

A representative TOT thermogram for the MWNT and SR-NOM adduct is shown in Figure 3.3c. Following this direct quantification method, concentrations of suspended MWNTs in synthetic solutions, prepared according to an orthogonal matrix of varying initial SR-NOM concentrations (10, 25, 50, and 100 mg-C/L) and varying MWNT mass initially added (50, 100, 250, and 500 mg/L), were analyzed. Results summarized in Table 3.1 demonstrate that approximately 0.25 to 1.4 % of MWNTs initially added to the SR-NOM solution became suspended for the range of solution compositions investigated. The fraction of suspended MWNT to the initial mass increased as more NOM was available. However, NOM availability was certainly not a limiting factor since the concentration of suspended MWNT also increased as initial MWNT dose increased for the same NOM concentration. This observation suggests that NOM association with

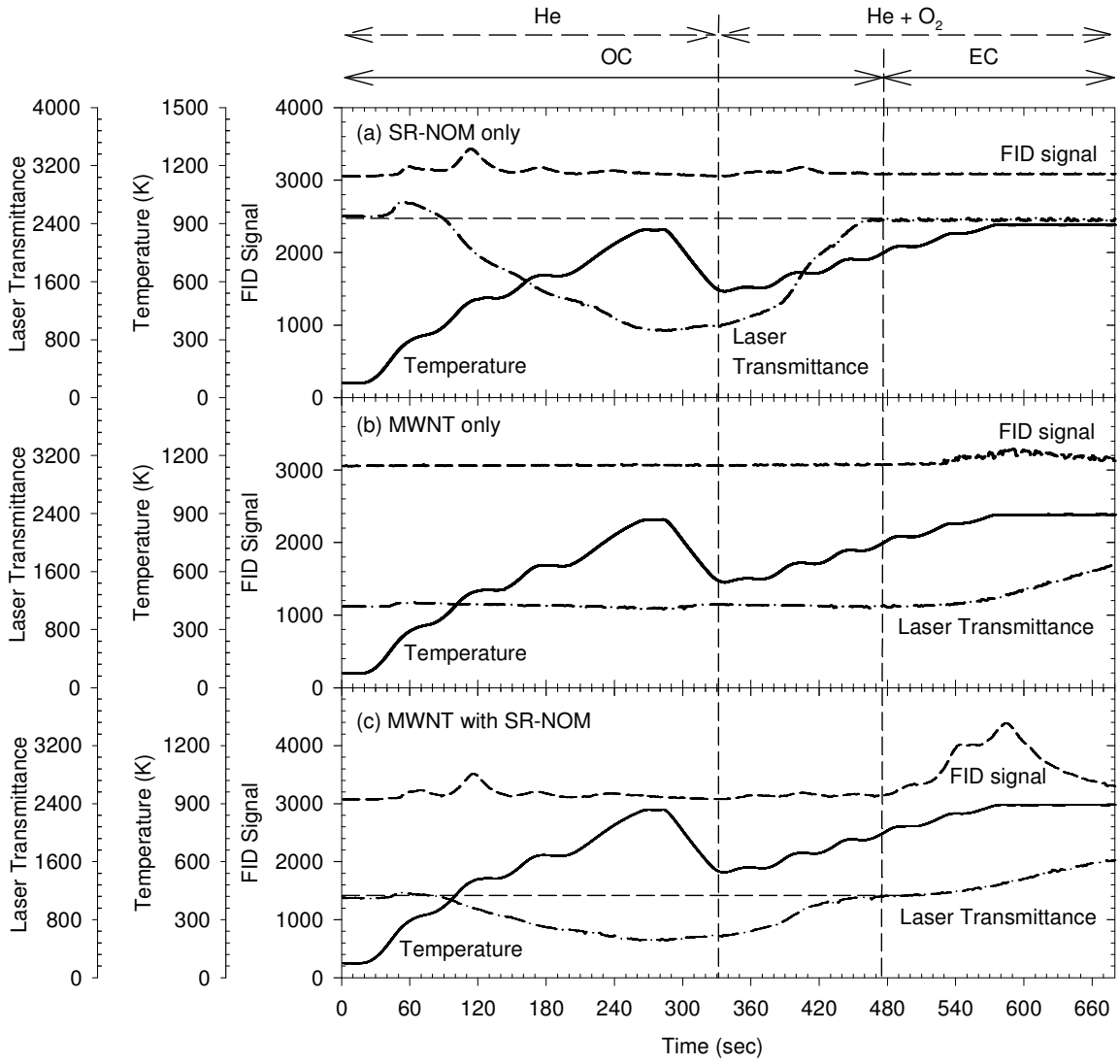

Figure 3.3. Representative TOT thermograms for (a) SR-NOM only (b) MWNT only and (c) MWNT associated with SR-NOM.

mass of MWNT added decreased). These results, taken with the TOT results, suggest that the MWNT-NOM suspension formation has two aspects of consideration: 1) the physical dispersion of the MWNT added to solution and 2) the association/equilibrium processes of NOM to the surface of MWNTs rendering them stable in the aqueous phase.

A spectral analysis of MWNT in SR-NOM solution showed a distinct, broad increase in the baseline of absorbance spectrum in visible range (over 500 nm), which was not observed in the solution containing only SR-NOM. Since the increase in baselines appears to be a function of light scattering by MWNT suspension and no specific absorption peak was identified, the absorbance at 800 nm was arbitrary selected and plotted against the suspended MWNT concentrations determined from TOT analyses, which resulted in a linear correlation (r^2=0.987) (Figure 3.4). Similarly, simple turbidity measurements resulted in a reasonable correlation (r^2=0.952) with the suspended MWNT concentration (results not shown).

The stability of MWNT was further investigated using an actual Suwannee River water sample (collected *in situ* as described above) in order to exclude any potential artifacts that might have originated from the use of a model compound. The pH, conductivity and, DOC of the 0.2 μm filtered sample were 3.42, 69.4 μS, and 59.1 mg-C/L, respectively. Figure 3.1e shows 500 mg/L of MWNT added to Suwannee River water compared to filtered Suwannee River water (Figure 3.1f). This picture was taken after agitation for one hour and quiescent settling for four days. Similar to the model SR-NOM, the Suwannee River water quickly dispersed MWNT and the resulting suspension

was stable for over one month. When initial amount of MWNT added to the Suwannee River water was varied at 500, 250, 100, and 50 mg/L, the concentration of suspended MWNT was determined at 6.9, 5.45, 2.27, and 1.76 mg/L, respectively, which was consistent with observation made with model SR-NOM in that suspended MWNT increased as initial MWNT dose increased. The amount of NOM adsorbed per unit mass of MWNT was 0.033, 0.042, 0.060, and 0.104 mg-C/mg for initial MWNT concentration of 500, 250, 100, and 50 mg/L, which were also in reasonable agreement with the results obtained with the model NOM (Table 3.1).

The observed similarity in the dispersion nature of the MWNT in solutions containing NOM and SDS suggests that MWNT stabilization in the presence of NOM might follow a similar stabilization mechanism of MWNT surface shielding by these molecules which not only leads to more thermodynamically favorable surfaces but also induces electrostatic and steric stabilization (27,30,35,36). Consequently, an amphiphilic, surfactant-like fraction of NOM with non-polar groups coexisting with polar, charged groups might play a critical role. It is noteworthy that NOM appeared to be a better stabilizing agent than SDS as clearly demonstrated in Figure 3.1. TOT analysis also suggested that approximately 1.78 mg/L of MWNT would be suspended when 200 mg/L of MWNT was added to 1% (10,000 mg/L) SDS solution. This value was approximately three times lower than that of a solution containing 100 mg-C/L of SR-NOM, which was only 1/100 of the compared SDS concentration by mass.

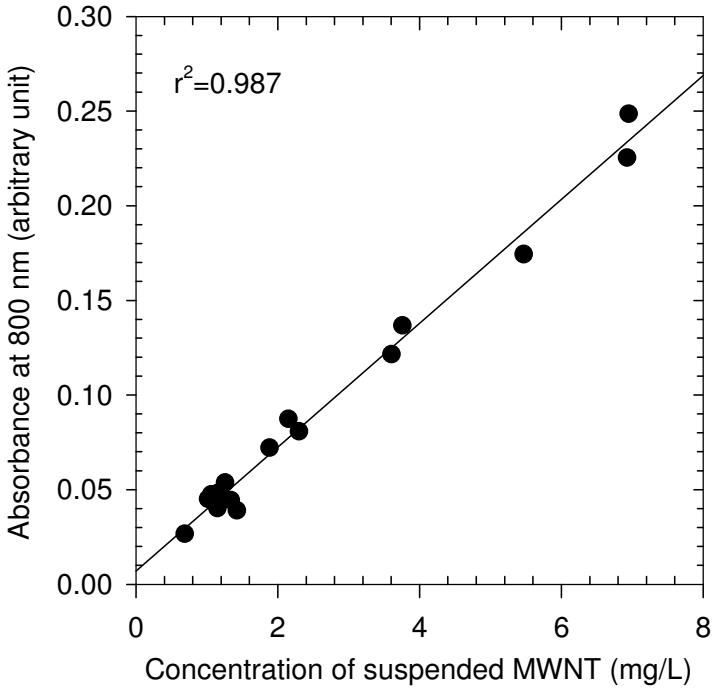

Figure 3.4. Comparison of light absorbance of MWNTs dispersed in SR-NOM solution at 800 nm and concentration of suspended MWNTs measured by TOT.

Table 3.1. Concentration of Suspended MWNT in SR-NOM Solutions and Mass of SR-NOM Bound to Unit Mass of MWNT Prepared with Varying Initial SR-NOM and MWNT Concentrations.

	Initial SR-NOM concentration (mg/L)	MWNT initially added (mg/L)			
		500	250	100	50
Suspended MWNT (mg/L)	100	6.92	6.95	3.75	1.42
	50	5.47	3.6	2.15	1.34
	25	2.31	1.88	1.02	1.15
	10	1.26	1.06	1.17	0.68
NOM mass per unit MWNT mass (mg/mg)	100	0.039	0.053	0.114	0.338
	50	0.029	0.031	0.048	0.072
	25	0.02	0.024	0.027	0.036
	10	0.012	0.014	0.013	0.011

Enhanced stabilizing propensity might be attributed to the presence of aromatic fractions of NOM, compared to SDS which is aliphatic, as aromaticity and resulting π-π interactions have been identified as an important parameter in MWNT stabilization by various surfactant molecules (34,39). Generally, ubiquitous aromatic fractions of NOM can range from *ca.* 10-40 % (C/C) depending on the source and age; with SR-NOM composition estimated to be 23% aromatic carbon via ^{13}C-NMR analysis (55). Furthermore, a relatively high percent of charged functional groups, such as carboxyl moieties (20% carbon as carboxyl for SR-NOM (55)) might contribute to enhanced dispersion of resulting NOM-MWNT complexes. However, the exact mechanism for CNT interaction with NOM will depend on both NOM characteristics including aromaticity, charge density, and size as well as CNT characteristics such as aspect ratio (*e.g.* SWNT) and functional derivatization (*e.g.* through a commonly used acid-treatment that induces tube shortening and end-group carboxylation as a way of stabilizing SWNT in the aqueous phase (36)). Understanding these interactions presents a challenge, especially as NOM is largely undefined and variable depending on the source, warranting further in-depth investigations.

Acknowledgements

This research was supported by the United States Environmental Protection Agency (USEPA) STAR Grant #D832526. The authors acknowledge Jaekyu Cho at School of Chemical and Biomolecular Engineering in Georgia Institute of Technology and Sangil

Lee and Evan Cobb at School of Civil and Environmental Engineering in Georgia Institute of Technology for their assistance during some of the instrumental analyses.

Literature Cited

(1) Iijima, S. Helical microtubules of graphitic carbon. *Nature* **1991**, *354*, 56-58.

(2) Cowley, J. M.; Liu, M. Q. The structure of carbon nanotubes impregnated with yttrium. *Micron* **1994**, *25*, 53-61.

(3) Dreher, K. L. Health and environmental impact of nanotechnology: Toxicological assessment of manufactured nanoparticles. *Toxicol. Sci.* **2004**, *77*, 3-5.

(4) Ajayan, P. M.; Charlier, J. C.; Rinzler, A. G. Carbon nanotubes: From macromolecules to nanotechnology. *Proceedings of the National Academy of Sciences of the United States of America* **1999**, *96*, 14199-14200.

(5) Ajayan, P. M.; Zhou, O. Z. Applications of carbon nanotubes. *Carbon Nanotubes* **2001**, *80*, 391-425.

(6) Dai, H.; Wong, E. W.; Liebert, C. M. Probing electrical transport in nanomaterials: conductivity of individual carbon nanotubes. *Science* **1996**, *272*, 523-526.

(7) Rueckes, T.; Kim, K.; Joselevich, E.; Tseng, G. Y.; Cheung, C.-L.; Lieber, C. Carbon nanotube-based nonvolatile randon access memory for molecular computing. *Science* **2000**, *289*, 94-97.

(8) Dillon, A. C.; Jones, K. M.; Bekkedahl, T. A.; Kiang, C. H.; Bethune, D. S.; Heben, M. J. Storage of hydrogen in single-walled carbon nanotubes. *Nature* **1997**, *386*, 377-379.

(9) Cheng, H. M.; Yang, Q. H.; Liu, C. Hydrogen storage in carbon nanotubes. *Carbon* **2001**, *39*, 1447-1454.

(10) Kong, J.; Franklin, N. R.; Zhou, C.; Chapline, M. G.; Peng, S.; Cho, K.; Dai, H. Nanotube molecular wires as chemical sensors. *Science* **2000**, *287*, 622-625.

(11) Collins, P. G.; Bradley, K.; Ishigami, M.; Zettl, A. Extreme oxygen sensitivity of electronic properties of carbon nanotubes. *Science* **2000**, *287*, 1801-1804.

(12) Chopra, S.; McGuire, K.; Gothard, N.; Rao, A. M.; Pham, A. Selective gas detection using a carbon nanotube sensor. *Appl. Phys. Lett.* **2003**, *83*, 2280-2282.

(13) Chopra, S.; Pham, A.; Gaillard, J.; Parker, A.; Rao, A. M. Carbon-nanotube-based resonant-circuit sensor for ammonia. *Appl. Phys. Lett.* **2002**, *80*, 4632-4634.

(14) Colvin, V. L. The potential environmental impact of engineered nanomaterials. *Nat. Biotechnol.* **2004**, *22*, 760-760.

(15) Lee, B. I.; Qi, L.; Copeland, T. Nanoparticles for materials design: present & future. *J. Ceram. Process. Res.* **2005**, *6*, 31-40.

(16) Ball, P. Roll up for the revolution. *Nature* **2001**, *414*, 142-144.

(17) Warheit, D. B.; Laurence, B. R.; Reed, K. L.; Roach, D. H.; Reynolds, G. A.; Webb, T. R. Comparative pulmonary toxicity assessment of single-wall carbon nanotubes in rats. *Toxicol. Sci.* **2004**, *77*, 117-125.

(18) Lam, C. W.; James, J. T.; McCluskey, R.; Hunter, R. L. Pulmonary toxicity of single-wall carbon nanotubes in mice 7 and 90 days after intratracheal instillation. *Toxicol. Sci.* **2004**, *77*, 126-134.

(19) Jia, G.; Wang, H. F.; Yan, L.; Wang, X.; Pei, R. J.; Yan, T.; Zhao, Y. L.; Guo, X. B. Cytotoxicity of carbon nanomaterials: Single-wall nanotube, multi-wall nanotube, and fullerene. *Environ. Sci. Technol.* **2005**, *39*, 1378-1383.

(20) Magrez, A.; Kasas, S.; Salicio, V.; Pasquier, N.; Seo, J. W.; Celio, M.; Catsicas, S.; Schwaller, B.; Forro, L. Cellular toxicity of carbon-based nanomaterials. *Nano Lett.* **2006**, *6*, 1121-1125.

(21) Chen, X.; Tam, U. C.; Czlapinski, J. L.; Lee, G. S.; Rabuka, D.; Zettl, A.; Bertozzi, C. R. Interfacing carbon nanotubes with living cells. *J. Am. Chem. Soc.* **2006**, *128*, 6292-6293.

(22) Murr, L. E.; Soto, K. F.; Esquivel, E. V.; Bang, J. J.; Guerrero, P. A.; Lopez, D. A.; Ramirez, D. A. Carbon nanotubes and other fullerene-related nanocrystals in the environment: A TEM study. *Jom* **2004**, *56*, 28-31.

(23) Utsunomiya, S.; Jensen, K. A.; Keeler, G. J.; Ewing, R. C. Uraninite and fullerene in atmospheric particles. *Environ. Sci. Technol.* **2002**, *36*, 4943-4947.

(24) Wang, H.; Hobbie, E. K. Amphiphobic carbon nanotubes as macroemulsion surfactants. *Langmuir* **2003**, *19*, 3091-3093.

(25) Girifalco, L. A.; Hodak, M.; Lee, R. S. Carbon nanotubes, buckyballs, ropes, and a universal graphitic potential. *Phys. Rev. B* **2000**, *62*, 13104-13110.

(26) Fu, K. F.; Sun, Y. P. Dispersion and solubilization of carbon nanotubes. *J. Nanosci. Nanotechnol.* **2003**, *3*, 351-364.

(27) Jiang, L. Q.; Gao, L.; Sun, J. Production of aqueous colloidal dispersions of carbon nanotubes. *J. Colloid Interf. Sci.* **2003**, *260*, 89-94.

(28) Huang, L. M.; Cui, X. D.; Dukovic, G.; O'Brien, S. P. Self-organizing high-density single-walled carbon nanotube arrays from surfactant suspensions. *Nanotechnology* **2004**, *15*, 1450-1454.

(29) Shen, K.; Curran, S.; Xu, H. F.; Rogelj, S.; Jiang, Y. B.; Dewald, J.; Pietrass, T. Single-walled carbon nanotube purification, pelletization, and surfactant-assisted dispersion: A combined TEM and resonant micro-Raman spectroscopy study. *J. Phys. Chem. B* **2005**, *109*, 4455-4463.

(30) O'Connell, M. J.; Bachilo, S. M.; Huffman, C. B.; Moore, V. C.; Strano, M. S.; Haroz, E. H.; Rialon, K. L.; Boul, P. J.; Noon, W. H.; Kittrell, C.; Ma, J. P.; Hauge, R. H.; Weisman, R. B.; Smalley, R. E. Band gap fluorescence from individual single-walled carbon nanotubes. *Science* **2002**, *297*, 593-596.

(31) Lecoanet, H. F.; Bottero, J. Y.; Wiesner, M. R. Laboratory assessment of the mobility of nanomaterials in porous media. *Environ. Sci. Technol.* **2004**, *38*, 5164-5169.

(32) Lecoanet, H. F.; Wiesner, M. R. Velocity effects on fullerene and oxide nanoparticle deposition in porous media. *Environ. Sci. Technol.* **2004**, *38*, 4377-4382.

(33) Weisman, R. B.; Bachilo, S. M.; Tsyboulski, D. Fluorescence spectroscopy of single-walled carbon nanotubes in aqueous suspension. *Appl. Phys. A-Mater.* **2004**, *78*, 1111-1116.

(34) Islam, M. F.; Rojas, E.; Bergey, D. M.; Johnson, A. T.; Yodh, A. G. High weight fraction surfactant solubilization of single-wall carbon nanotubes in water. *Nano Lett.* **2003**, *3*, 269-273.

(35) Matarredona, O.; Rhoads, H.; Li, Z. R.; Harwell, J. H.; Balzano, L.; Resasco, D. E. Dispersion of single-walled carbon nanotubes in aqueous solutions of the anionic surfactant NaDDBS. *J. Phys. Chem. B* **2003**, *107*, 13357-13367.

(36) Chen, Q.; Saltiel, C.; Manickavasagam, S.; Schadler, L. S.; Siegel, R. W.; Yang, H. C. Aggregation behavior of single-walled carbon nanotubes in dilute aqueous suspension. *J. Colloid Interf. Sci.* **2004**, *280*, 91-97.

(37) Wang, H.; Zhou, W.; Ho, D. L.; Winey, K. I.; Fischer, J. E.; Glinka, C. J.; Hobbie, E. K. Dispersing single-walled carbon nanotubes with surfactants: A small angle neutron scattering study. *Nano Lett.* **2004**, *4*, 1789-1793.

(38) O'Connell, M. J.; Boul, P.; Ericson, L. M.; Huffman, C.; Wang, Y. H.; Haroz, E.; Kuper, C.; Tour, J.; Ausman, K. D.; Smalley, R. E. Reversible water-solubilization of single-walled carbon nanotubes by polymer wrapping. *Chem. Phys. Lett.* **2001**, *342*, 265-271.

(39) Tan, Y.; Resasco, D. E. Dispersion of single-walled carbon nanotubes of narrow diameter distribution. *J. Phys. Chem. B* **2005**, *109*, 14454-14460.

(40) Thapa, P. B.; Nakajima, F.; Furumai, H. Characterization of natural organic matter in a shallow eutrophic lake. *Water Sci. Technol.* **2002**, *46*, 465-471.

(41) Perdue, M., Personal Communication.

(42) Birch, M. E. *Elemental Carbon (Diesel Particulate): Method 5040*; NIOSH, 2003

(43) Itkis, M. E.; Perea, D. E.; Jung, R.; Niyogi, S.; Haddon, R. C. Comparison of analytical techniques for purity evaluation of single-walled carbon nanotubes. *J. Am. Chem. Soc.* **2005**, *127*, 3439-3448.

(44) Landi, B. J.; Cress, C. D.; Evans, C. M.; Raffaelle, R. P. Thermal oxidation profiling of single-walled carbon nanotubes. *Chem. Mater.* **2005**, *17*, 6819-6834.

(45) Pang, L. S.; Saxby, J. D.; Chatfield, S. P. Thermogravimetric analysis of carbon nanotubes and nanoparticles. *J. Phys. Chem. A* **1993**, *97*, 6941-6942.

(46) Young, k. D.; Leboeuf, E. J. Glass transistion behavior in a peat humic acid and an aquatic fulvic acid. *Environ. Sci. Technol.* **2000**, *34*, 4549-4553.

(47) Chow, J. C.; Watson, J. G.; Chen, L. W. A.; Arnott, W. P.; Moosmuller, H. Equivalence of elemental carbon by thermal/optical reflectance and transmittance with different temperature protocols. *Environ. Sci. Technol.* **2004**, *38*, 4414-4422.

(48) Bae, M. S.; Schauer, J. J.; DeMinter, J. T.; Turner, J. R.; Smith, D.; Cary, R. A. Validation of a semi-continuous instrument for elemental carbon and organic carbon using a thermal-optical method. *Atmos. Environ.* **2004**, *38*, 2885-2893.

(49) Viidanoja, J.; Sillanpaa, M.; Laakia, J.; Kerminen, V. M.; Hillamo, R.; Aarnio, P.; Koskentalo, T. Organic and black carbon in PM2.5 and PM10: 1 year of data from an urban site in Helsinki, Finland. *Atmos. Environ.* **2002**, *36*, 3183-3193.

(50) Wierzbicka, A.; Lillieblad, L.; Pagels, J.; Strand, M.; Gudmundsson, A.; Gharibi, A.; Swietlicki, E.; Sanati, M.; Bohgard, M. Particle emissions from district heating units operating on three commonly used biofuels. *Atmos. Environ.* **2005**, *39*, 139-150.

(51) Conny, J. M.; Klinedinst, D. B.; Wight, S. A.; Paulsen, J. L. Optimizing thermal-optical methods for measuring atmospheric elemental (black) carbon: A response surface study. *Aerosol Sci. Tech.* **2003**, *37*, 703-723.

(52) Birch, M. E.; Cary, R. A. Elemental carbon-based method for monitoring occupational exposures to particulate diesel exhaust. *Aerosol Sci. Tech.* **1996**, *25*, 221-241.

(53) Catalado, F. A study on the thermal stability to 1000°C of various carbon allotopes and carbonaceous matter both under nitrogen and in air. *Fuller. Nanotub. Carb. N.* **2002**, *10*, 293-311.

(54) Illekova, E.; Csomorova, K. Kinetics of oxidation in various forms of carbon. *J. Therm. Anal. Calorim.* **2005**, *80*, 103-108.

(55) Thorn, K. A.; Folan, D. W.; MacCarthy, P. *Characterization of the International Humic Substances Society Standard and Reference Fulvic and Humic Acids by Solution State Carbon-13 (13C) and Hydrogen-1 (1H) Nuclear Magnetic Resonance Spectrometry*; U.S. Geological Survey; US Department of Interior: Denver, 1989.

CHAPTER 4
NATURAL ORGANIC MATTER (NOM) ADSORPTION TO MULTI-WALLED CARBON NANOTUBES: EFFECT OF NOM CHARACTERISTICS AND WATER QUALITY PARAMETERS

Abstract

The effect of natural organic matter (NOM) characteristics and water quality parameters on NOM adsorption to multi-walled carbon nanotubes (MWNTs) was investigated. Isotherm experimental results fitted well with a modified Freundlich isotherm model that took into account of the heterogeneous nature of NOM. Accordingly, the preferential adsorption of the higher molecular weight fraction of NOM was observed by a size exclusion chromatographic analysis. Experiments performed with various NOM samples suggested that the degree of NOM adsorption varied greatly depending on the type of NOM and was proportional to the aromatic carbon content of NOM. The NOM adsorption to MWNT was also dependent on water quality parameters: adsorption increased as pH decreased and ionic strength increased. As a result of NOM adsorption to MWNT, a fraction of MWNT formed a stable suspension in water, the concentration of which depended on the amount of NOM adsorbed per unit mass of MWNT. The amount of MWNT suspended in water was also affected by ionic strength and pH. The findings in this study suggested that the fate and transport of MWNT in the natural system would be largely influenced by NOM characteristics and water quality parameters.

*This chapter is accepted for publication in Environmental Science and Technology when this thesis is prepared.

Introduction

As the evidence for toxicological effects of carbon nanotubes (CNT) is rapidly accumulating [1-3], understanding the fate and transport characteristics of CNT in the natural environment during unintended discharge is becoming an important issue. In particular, an exposure route involving natural waterways, which has traditionally not been considered as these molecules are extremely hydrophobic, has been receiving a widespread interest. Our recent study [4] showed that pristine multi-walled carbon nanotubes (MWNT) could be stabilized (suspended) in the aqueous phase by natural organic matter (NOM) which might provide sterically and electrostatically stable surfaces to MWNT after adsorption to MWNT. This finding suggested that the dispersal of carbon based nanomaterials, CNT in particular, in the natural aquatic environment might occur to a higher extent than predicted based only on the hydrophobicity of these materials. In order to accurately predict the behaviors of MWNT in the environment, the mechanism of interaction between NOM and CNT and the effect of water quality on this interaction need to be elucidated.

NOM is a mixture of chemically complex polyelectrolytes with varying molecular weights, produced mainly from the decomposition of plant and animal residues [5]. Due to the carboxylic and phenolic moieties distributed throughout the entire molecule, NOM generally carries a negative charge in the natural environment [6]. These physical and chemical characteristics of NOM are likely to be closely related to the mechanism of NOM interaction with CNT. Compared to NOM adsorption onto CNT, the mechanism of NOM adsorption onto activated carbon is relatively well known due to the rich history

of application to water treatment. A few characteristics of NOM interaction with activated carbon are noteworthy and might be helpful for interpretation of CNT-NOM interaction.

First, the adsorption capacity and strength strongly depend on the type of NOM and the type of activated carbon. Factors affecting adsorption have been reported to include size and chemical characteristics of NOM as well as pore structure and surface chemistry of activated carbon [5-8, 11]. Second, due to the polydisperse nature of NOM, different fractions of NOM tend to have a different degrees of adsorptive interactions with the adsorbent [7]. This preferential adsorption is reflected by the occurrence of dose dependent isotherm relationship. For example, the strongly adsorbable fraction of NOM exhibits a more favorable adsorption at lower activated carbon dose. Finally, NOM adsorption is affected by water quality parameters such as ionic strength and pH which influence the charge and configuration of NOM [6]. Specifically, the adsorption of negatively charged NOM to the activated carbon surface generally increases as ionic strength increases and pH decreases [5, 8-11].

Differences between activated carbon and CNTs need to be also recognized for the proper interpretation of CNT-NOM adsorption phenomena. First, the activated carbon consists of micropores with different sizes which provide sites for NOM adsorption. CNTs in contrast provide adsorption sites only along the surface of a cylindrical structure [12]. Second, the chemical structure of the activated carbon, which contains carbons of varying degree of saturation and oxidation state as well as functional

groups formed during activation process [7], is fundamentally different from that of CNT, which consists only of globally conjugated unsaturated carbons in three dimensional arrays.

The objective of this study was to investigate the effect of NOM characteristics and water quality parameters on adsorptive interaction between MWNT and NOM in water. The characteristics of NOM adsorption to MWNT was studied from batch isotherm experiments, which were performed with various NOM samples under different pH and ionic strength conditions. The experimental result was analyzed using Freundlich isotherm model and critically compared to the adsorption of activated carbon. Finally, the amount of stable MWNT suspension formed in water as a result of NOM adsorption under varying conditions was quantitatively analyzed.

Experimental

Materials. MWNT (10-20 nm diameter × 10-30 μm length) with over 95% purity was obtained from the Cheap Tubes Inc. (Brattleboro, VT). Suwannee River natural organic matter (SRNOM), Suwannee River humic acid standard II (SRHA), Suwannee River fulvic acid standard II (SRFA), Leonardite humic acid standard (LHA), Elliott soil humic acid standard (ESHA), Nordic lake humic acid reference (NLHA), Nordic lake fulvic acid reference (NLFA), Waskish peat humic acid standard (WPHA), and Waskish peat fulvic acid standard (WPFA) were purchased from the International Humic Substances Society (IHSS) (St. Paul, MN). Elemental and carbon compositions of the NOMs are provided in Table 4.S1 (Supporting Information). NOM stock solution was prepared by mixing a known amount of NOM with ultrapure water for 24 hours. Dissolution of NOM was facilitated by adding NaOH to increase the solution pH to 7. After measuring the total organic carbon (TOC) content of the stock solution by a TOC-Vw analyzer (Shimadzu, Columbia, MD), the solution was diluted to target NOM concentrations. Ultrapure water produced by a Milli-Q water filtration system (Millipore, Billerica, MA) was used for the preparation of all the solutions.

Isotherm test. Isotherm relationship for NOM adsorption to MWNT was evaluated by a modified bottle-point technique [5], where each data point of the isotherm was determined by an individual batch experiment. Both constant adsorbent method and constant adsorbate method were adopted. For all the isotherm experiments, NOM solution was buffered with 1 mM phosphate (NaH_2PO_4) and ionic strength was adjusted

with NaCl. The solution pH was adjusted using NaOH and HCl. The mixture of MWNT powder and NOM solution in a 40 mL vial was agitated using a magnetic stirrer for 6 days. Independent kinetic study suggested that the adsorption of NOM reached saturation within 2 days of mixing. Control experiments with blank samples confirmed that the loss of NOM in the solution resulted only from adsorption to MWNT. After 2 days of quiescent settling, samples were taken for the further analyses. All the isotherm experiments were performed at 22°C. Further details on adsorption experimental conditions are provided in Table 4.S2.

Analysis. The concentration of NOM was measured by a TOC-Vw analyzer (Shimadzu, Columbia, MD). The equilibrium NOM concentration after adsorption (C_e) was analyzed after removing MWNT with a 0.2 μm Acrodisc nylon membrane syringe filter (Pall Corporation, Ann Arbor, MI). Once C_e was determined, the equilibrium concentration of NOM adsorbed on the unit mass of MWNT, q_e (mg C/g MWNT), was obtained by the following equation:

$$q_e = \frac{C_0 - C_e}{D} \quad (1)$$

where C_0 (mg C/L) = the initial concentration of NOM and D (g MWNT/L) = dosage of MWNT.

Stability of MWNT in the NOM solution, the quantitative measurement of stable suspension of MWNT due to the NOM adsorption, was determined by visible light absorbance at 800 nm (VIS_{800}) (8453 UV-Vis Spectroscopy System, Agilent, Palo Alto, CA) after 6 days of mixing and 2 days of settling. VIS_{800} was measured after separating the stable MWNT suspension from the bulk using Whatman 541 filter (20-25 μm nominal pore size, Florham Park, NJ). Our previous study verified that VIS_{800} (*i.e.*, transmittance decrease due to light scattering by suspended MWNT) was linearly correlated with the MWNT concentration measured by a Thermal Optical Transmittance (TOT) analyzer [4]. The study also verified that the TOT analysis accurately measure the concentration of MWNT in a solution containing both MWNT and NOM [4]. In this study, VIS_{800} were also calibrated with those obtained using a TOT analyzer (Sunset Laboratory, Tigard, OR).

The molecular weight distribution of NOM was analyzed by a Hewlett-Packard 1100 high performance liquid chromatography (HPLC) system (Wilmington, DE) equipped with a Waters Protein-Pak^{TM} 125 SEC column (Milford, MA), a commonly used column for NOM fractionation [13-15] (mobile phase = 0.1 M NaCl solution buffered with 1 mM phosphate at pH 6.8, flow rate = 1 mL/min at 40^{o}C). UV absorbance at 254 nm (UV_{254}) of eluent was monitored by a diode-array detector (DAD). Electron microscopic images were analyzed by a Philips 120 transmission electron microscope (TEM) (New York, NY). A TEM specimen was prepared by placing a droplet of fullerene suspension on a copper carbon grid (Electron Microscopy Science, Hatfield, PA) and drying overnight at room temperature.

Results and Discussion

Adsorption Isotherm. Results from isotherm experiments performed under varying initial concentrations of SRNOM and MWNT are shown in Figure 4.1a. The isotherms were adsorbent-dose dependent, *i.e.*, different adsorption isotherms, which were linear in a log scale, were obtained at different MWNT doses. Similar adsorbent-dose dependence phenomenon has been observed in previous studies on the adsorption of NOM onto activated carbon [5, 10]. Each isotherm at the same MWNT dose fitted well with the following Freundlich isotherm model which has been commonly used to represent aqueous phase adsorption phenomena:

$$q_e = K_F C_e^{1/n} \tag{2}$$

where, K_F ((mg C/g MWNT)/(mg C/L)$^{1/n}$) and $1/n$ (dimensionless) represent Freundlich constant and Freundlich exponent, respectively. Generally, K_F increases as the adsorption capacity of the adsorbent increases and $1/n$ decreases as the adsorption strength increases. As the initial MWNT dose decreased, more SRNOM adsorbed per unit mass of MWNT and consequently q_e increased. This increase was less pronounced when equilibrium SRNOM concentration (C_e) increased, and the isotherms merged at the highest C_e.

Deviation from a single solute isotherm, where a unique isotherm can be obtained regardless of the initial adsorbate concentration or adsorbent dose, is attributed to the

heterogeneity of NOM and consequential occurrence of preferential adsorption [16, 17]. NOM is a mixture of natural polymers with different adsorption capacity. Therefore, at small adsorbent dosage, highly adsorbable portions of NOM preferentially adsorb onto adsorbent and they would dominate the adsorption behavior of NOM. However, as adsorbent dosage increases, less adsorbable portions start to participate in adsorption and overall adsorption would be also influenced by less adsorbable portions. In such a case, it is known that a unique isotherm is obtained by normalizing the equilibrium adsorbate concentration (C_e) by adsorbent dose (D) as follows [5]:

$$q_e = K_F \left(\frac{C_e}{D}\right)^{1/n} \tag{3}$$

A normalized Freundlich isotherm model fitted with experimental data (Figure 4.1b) could reasonably well incorporate dose dependency of NOM adsorption. The experimental results obtained with the other NOMs used in this study also matched reasonably well with the normalized Freundlich model (Figure 4.S1). The fitted model parameters for all the NOMs are summarized in Table 4.1. Some deviations of experimental data at low/high ends of isotherms in the figures could have resulted from the adsorbate concentration dependency of Freundlich isotherm model [7]. Experimental results were also analyzed using a Langmuir isotherm (results not shown) after dose normalization, but fitting accuracy was comparable to the normalized Freundlich model at best.

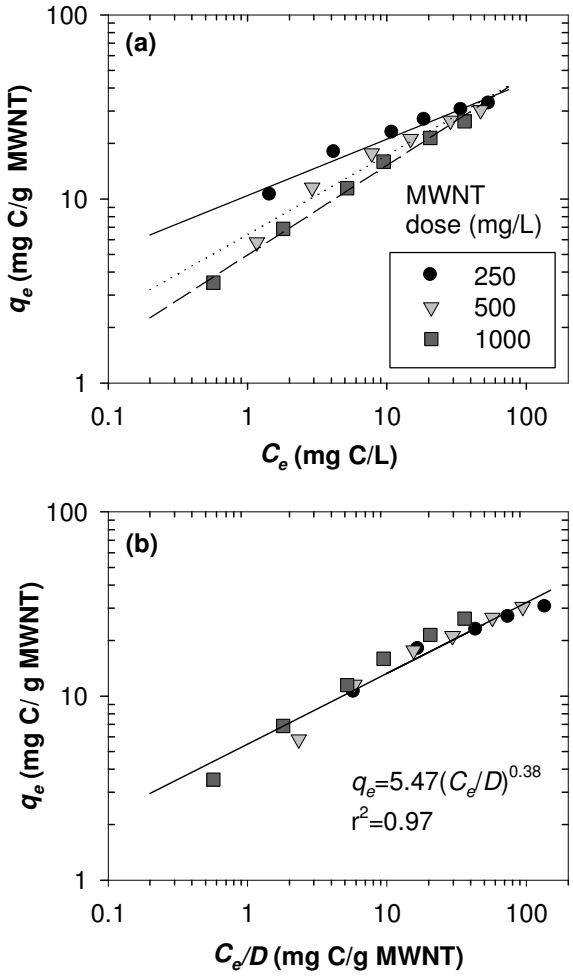

Figure 4.1. Adsorption of SRNOM to MWNT. (a) Isotherm experimental data and Freundlich adsorption isotherm model fit. (b) Normalized data and normalized Freundlich adsorption isotherms model fit. (both at 22 ^{o}C, pH=7.0, [NaCl] = 5 mM, [NaH_2PO_4] = 1 mM)

Table 4.1. Freundlich Adsorption Model Parameters for Various NOMs [c].

	K_F [a]	$1/n$ [b]
SRNOM	5.471 (4.644-6.445)[c]	0.384 (0.333-0.435)
SRHA	9.825 (7.736-12.477)	0.2 (0.122-0.277)
SRFA	5.449 (4.598-6.460)	0.348 (0.294-0.400)
ESHA	11.341 (9.419-13.654)	0.225 (0.163-0.287)
LHA	13.088 (10.899-15.718)	0.212 (0.151-0.274)
NLHA	11.633 (9.617-14.072)	0.222 (0.159-0.286)
NLFA	6.94 (5.890-8.176)	0.324 (0.271-0.376)
WPHA	12.422 (10.644-14.497)	0.225 (0.173-0.276)
WPFA	8.437 (6.620-10.751)	0.278 (0.198-0.357)

[a] (mg C/g MWNT)$^{(1-1/n)}$

[b] dimensionless

[c] Values in the parentheses for K_F and n are 95% confidence intervals. Number of observation (N) is 15 for each NOM.

Effect of NOM Type. Results summarized in Table 4.1 suggest that the adsorptive interaction between NOM and MWNT was strongly dependent on the type of NOM. For example, less soluble, higher molecular weight humic acids had generally higher adsorption capacity than fulvic acids. Various functionalities of the NOMs identified in the previous study [21] using ^{13}C NMR were compared with adsorption characteristics. Among various carbon functionalities present in NOM (*e.g.*, carbonyl, carboxyl, aromatic, acetal, heteroaliphatic, and aliphatic carbons), aromatic carbon content showed the most strong linear relationship with K_F (Figure 4.2) regardless of source (*i.e.*, lake, soil, or river) and type (*i.e.*, bulk, fulvic or humic) of NOMs. Some deviation from the linearity, which might originate from the existence of different elemental composition and functional groups in NOMs, was also observed. Nevertheless, the finding that the adsorption capacity is closely related to the aromatic functional group content in NOM is consistent with past studies which reported that the attractive interaction between chemical compounds containing the aromatic moiety and CNT was largely driven by π-π interactions [22, 23]. Specifically, a previous study [22] suggests that a benzene ring present in a surfactant that shielded the CNT surface would stack upon benzene ring present in the CNT. Gotovac et al. [24] reported that the adsorption of the tetracene (4 benzene rings) was 6 times greater than that with phenanthrene (3 benzene rings). The strong correlation between adsorption capacity and aromatic content of NOM implies that aromatic fractions of NOM, which can range from *ca.* 10-40 % (C/C) depending on the source and age [21] could be a useful measure to evaluate the level of NOM adsorption onto MWNT and consequently the dispersion of MWNT in natural waters.

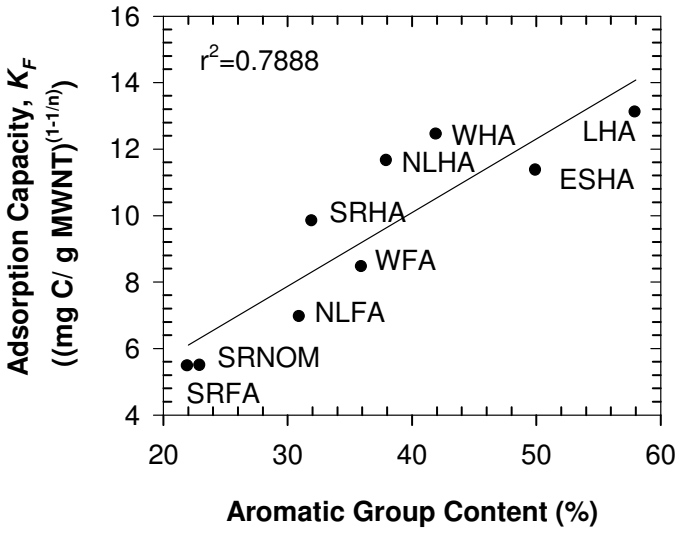

Figure 4.2. Relationship between the aromatic group content of NOM and NOM-MWNT adsorption capacity (K_F).

From the isotherm parameters calculated for each NOM (Table 4.1), it is also notable that K_F is inversely proportional to $1/n$ for all the NOMs tested in this study (Figure 4.S2). This suggests that the capacity and adsorption strength of NOM adsorption are proportional to each other, which is not always the case for NOM adsorption to activated carbons. In case of activated carbon, adsorption capacity is mainly determined by surface area of carbon's porous structure available for adsorption, and many of the smaller pores are not accessible to the larger, more strongly adsorbing NOM molecules. Even for the same activated carbon, the area available for adsorption varies with molecular size distribution and characteristics of NOM. Such variation is not necessarily related to chemical composition of NOM that governs adsorption strength between the NOM and the surface. In contrast, MWNT do not have pores available for adsorption and, therefore, NOM adsorption is less influenced by the physical structure of the adsorbent. Consequently, NOMs with greater adsorption strength are likely to have greater adsorption capacity to MWNT as experimental results suggested.

Preferential Adsorption. Preferential adsorption of the higher molecular weight faction of SRNOM to MWNT was evident when size exclusion chromatograms of the non-adsorbed portion of NOM at different MWNT doses were examined (Figure 4.3). As MWNT dose was increased, higher molecular weight faction (*i.e.*, fractions appearing at lower retention time) was removed to a greater extent. Similar phenomena were observed from the SEC analysis performed with other types of NOM such as SRHA and SRFA (Figure 4.S3). This observation is in accordance with previous studies performed with the polydispersed polymers and non-porous adsorbents where preferential

adsorption of high molecular weight fractions was observed [16, 17]. However, the opposite molecular weight dependence was reported when adsorbent was porous (*e.g.*, activated carbon). From the SEC study on the Laurentian humic acid adsorbed to activated carbon, Kilduff et al. [10] suggested that lower molecular weight fraction of the humic acid more favorably adsorbed to activated carbon than the higher molecular weight fraction. Summers and Roberts [6] examined activated carbon adsorption of Aldrich humic acid fractionated by molecular weight and observed greater adsorption of the low molecular weight fraction. The apparent preferential adsorption of the low molecular weight fraction in the case of activated carbon would result from the size exclusion effect of pores within the activated carbon structure (*i.e.*, small adsorbates can access both small and large pores, but large adsorbates can not access small pores) [6]. However, when the adsorption was evaluated on the basis of the accessible surface area, the larger molecules were found to have greater adsorption capacity to activated carbon [5], which is consistent with findings from this study.

Effect of Water Quality Parameters. NOM adsorption to MWNT was greatly influenced by water quality parameters such as ionic strength and pH. At the same equilibrium SRNOM concentration in the liquid phase (C_e), the solid phase SRNOM concentration (q_e) was the highest in the solution containing 0.1 M NaCl and the lowest without NaCl (Figure 4.4a). The experimental data fitted well with the Freundlich isotherm model at each ionic strength. Adsorption capacity, expressed in terms of K_F, increased as ionic strength increased (K_F = 6.72 (mg C/g MWNT)$^{(1-1/n)}$ at NaCl = 0 M, 7.05 at NaCl = 0.01 M and 7.55 at NaCl = 0.1 M) presumably due to change in molecular configuration of

NOM. Gosh and Schnitzer [25] suggested that humic substances would become increasingly coiled and form more compact structures as ionic strength increased. Adsorption capacity would consequently increase as more molecules could occupy the same surface area [10]. As the NOM molecule becomes more compact, the area for NOM-MWNT interaction would be reduced and the attractive force per individual NOM molecule to MWNT surface would decrease. Consequently, 1/*n* increased (*i.e*. adsorption strength decreased) as ionic strength increased (1/*n* = 0.39 at NaCl = 0 M, 0.48 at NaCl = 0.01 M and 0.60 at NaCl = 0.1 M). This is also consistent with the observation made in Figure 4.3 that NOM with larger molecular size adsorbed to MWNT more effectively due to greater level of adsorptive interaction possible per NOM molecule with MWNT surface. At higher ionic strength, enhanced double layer compression in SRNOM-MWNT agglomerates would also enhance SRNOM adsorption onto MWNT.

Figure 4.4b shows the effect of pH on SRNOM adsorption to MWNT. The adsorption capacity decreased as pH increased (*i.e*., K_F = 8.31 (mg C/g MWNT)$^{(1-1/n)}$ at pH = 5.0, 5.10 at pH = 7.0 and 2.96 at pH = 9.0), consistent with previous observations made with NOM adsorption to various other adsorbents [18, 26, 27]. As pH increases, the NOM molecules will become less coiled and less compact due to greater charge repulsion, and the adsorption capacity might consequently decrease as discussed above. In addition, as pH increases, weakly acidic SRNOM with carboxylic and phenolic moieties becomes more negatively charged [28]. Thus, in higher pH, repulsion between SRNOM and MWNT surface coated with SRNOM would increase, hindering further

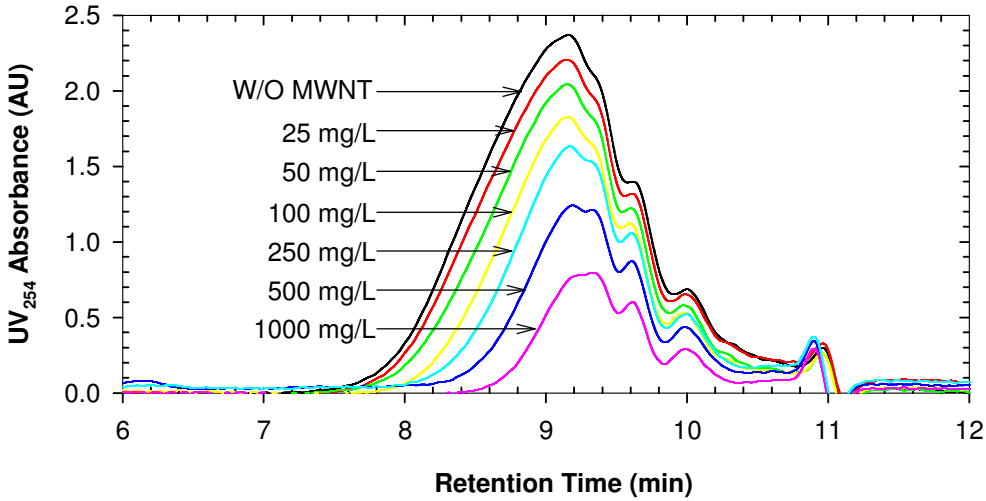

Figure 4.3. Size exclusion chromatograms of SRNOM that were not adsorbed after adding MWNT at varying doses.

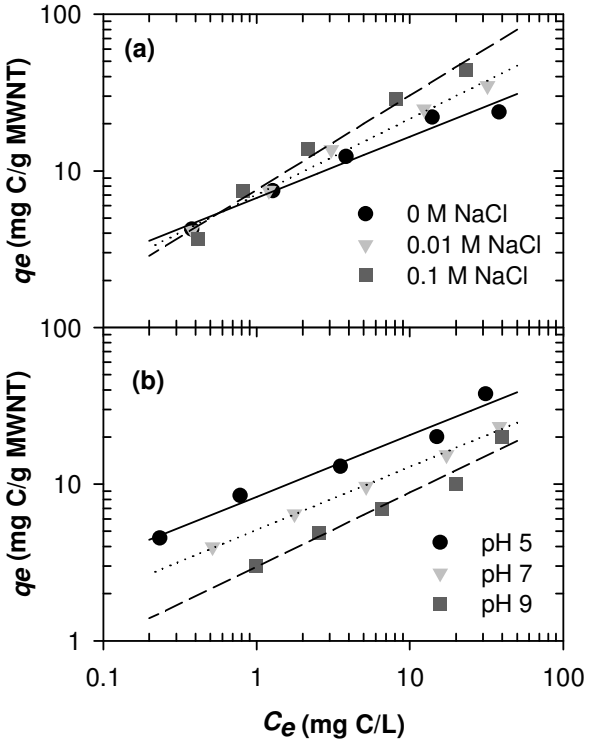

Figure 4.4. Effect of (a) ionic strength (at 22 ^{o}C, pH 7.0, [NaH_2PO_4] = 1 mM) and (b) pH (at 22 ^{o}C, [NaCl] = 5 mM, [NaH_2PO_4] = 1 mM) on SRNOM adsorption to MWNT. Lines denote Freundlich adsorption isotherm model fit.

adsorption of SRNOM. However, the strength of adsorption did not show appreciable change (*i.e.*, $1/n$ = 0.39 at pH = 5.0, 0.40 at pH = 7.0 and 0.47 at pH = 9.0).

Stability of MWNT in the Aqueous Phase. As a result of NOM adsorption to MWNT, a fraction of MWNT forms a stable suspension. TEM images of MWNT in SRNOM solutions (representative images shown in Figure 4.5) indicate that most of the MWNT were individually suspended. The amount of stable MWNT suspension in aqueous phase (C_{MWNT}) generally increased as the more SRNOM was adsorbed per MWNT (q_e) (Figure 4.6). Suspension of MWNT is facilitated by the shielding of extremely hydrophobic MWNT surface with NOM which provides thermodynamically more favorable surface. Adsorbed NOM is also expected to contribute to steric and electrostatic stabilization. Therefore, for the same type of NOM, the amount of NOM adsorbed onto MWNT would determine the extent of MWNT stability in water, *i.e.*, C_{MWNT} increased as q_e increased. C_{MWNT} seemed to be also influenced by the type of NOM. For example, at the same q_e, C_{MWNT} with SRHA was higher than that with SRNOM, implying that SRHA might have greater MWNT stabilization capacity than SRNOM (Figure 4.6). However, no obvious relationship was found between C_{MWNT} and NOM properties such as carbon functional groups, elemental composition, and distribution of acidic functional group. This is probably because other NOM properties such as electrostatic and configurational characteristics could collectively contribute to MWNT stability. For the same q_e, more MWNTs were suspended when more MWNTs were initially added to the solution (*i.e.*, higher D).

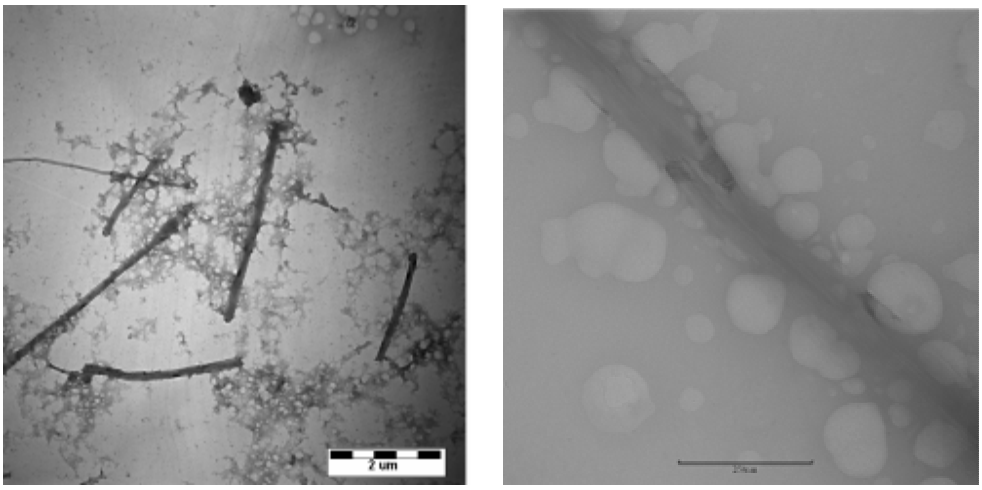

(a) (b)

Figure 4.5. TEM images of MWNT stabilized in SR NOM shown at different magnifications. The bars represent 2 μm and 25 nm for (a) and (b), respectively. Evolution of bubble-like structures adjacent to MWNT surfaces, which formed as organic matter sublimed by high energy electron beam irradiation, was visible during the first a few seconds of TEM analysis (Figure 5b).

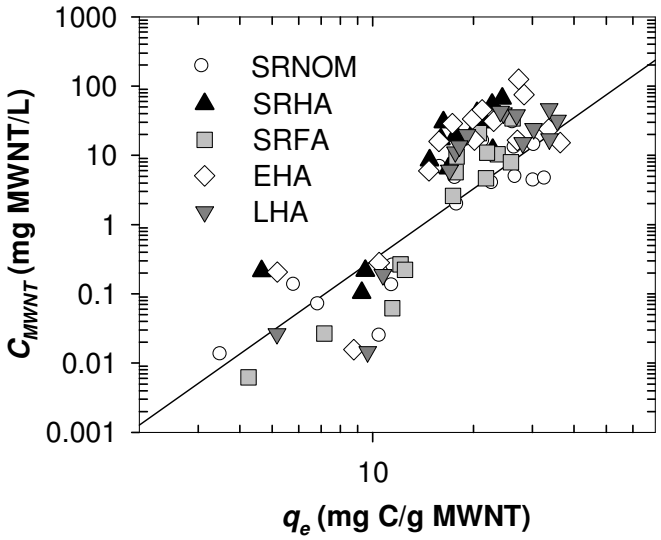

Figure 4.6. Dependency of the amount of MWNT suspended in water (C_{MWNT}) on the amount of various NOMs adsorbed onto MWNT (q_e).

The amount of MWNT suspended in water also strongly depended on solution ionic strength. The amount of MWNT suspended in water (C_{MWNT}) was plotted versus q_e at different ionic strengths in Figure 4.S4. Experimental results scattered at lower C_{MWNT} due to analytical limitations. At higher ionic strength, much less MWNT was suspended despite the similar amount of SRNOM was adsorbed. For instance, even at high q_e (> 10 mg C/g MWNT), MWNTs were only slightly suspended (*i.e.*, less than 1 mg/L) in the SRNOM solution with 0.1 M NaCl. This might be due to greater double layer compression in the high ionic strength solution. However, as MWNT used in this study has a very high aspect ratio (diameter ranges from *ca.* 10 to 20 nm and length ranges from *ca.* 10 to 30 μm) it is difficult to quantitatively analyze the zeta potential of MWNT. The effect of pH was less obvious than that of ionic strength, although electrostatic stabilization of NOM-MWNT agglomerates would be more efficient due to the deprotonation of NOM at higher pH and experimental data showed slight increase in C_{MWNT} at higher pH for the same q_e.

Environmental Significance. The results of this study suggested that the environmental fate of MWNT will be largely influenced by the amount and the type of NOM as well as solution chemistry such as ionic strength and pH. Other water quality parameters such as divalent ions and inorganic composition, which were not examined in this study, might play a critical role in determining the degree of NOM-MWNT interaction. For natural waters from different sources with different characteristics, the aromatic content and molecular weight distribution of NOM might be useful parameters to predict the extent of NOM adsorption and level of MWNT dispersion. Even though a wide range of NOM

concentrations (2.5 to 50 mg C/L) was investigated, it is noted that NOM concentrations in some natural surface and ground waters are lower than concentration levels used in this study. Therefore, further study with actual surface and ground waters with relatively low NOM contents might be necessary for a comprehensive understanding of interaction between NOM and MWNT.

In some aspects, NOM adsorption to MWNT was similar to that to activated carbon, *i.e.*, occurrence of preferential adsorption and fitting to the Freundlich adsorption isotherm model. However, difference in physical structure of MWNT and activated carbon led to a few key differences in adsorption behavior such as preferential adsorption of higher molecular weight NOM onto MWNT. Understanding both similarities and differences between well-characterized activated carbon adsorption and MWNT adsorption should be helpful to understand not only the fate of MWNT in natural waters but also that of other carbon based nanomaterials such as single-walled carbon nanotubes and C_{60}.

Acknowledgements

This study was supported by the United States Environmental Protection Agency (USEPA) STAR Grant #D832526. The authors thank Dr. Jim Millette and Whitney Hill at MVA Scientific Consultants (Duluth, Georgia) for their assistance on TEM analysis. Dr. Vernon Snoeyink at University of Illinois at Urbana-Champaign is also thanked for reviewing the manuscript and providing valuable comments.

Literature Cited

1. Kang, S.; Pinault, M.; Pfefferle, L. D.; Elimelech, M., Single-walled carbon nanotubes exhibit strong antimicrobial activity. *Langmuir* **2007,** *23*, 8670-8673.
2. Lam, C. W.; James, J. T.; McCluskey, R.; Hunter, R. L., Pulmonary toxicity of single-wall carbon nanotubes in mice 7 and 90 days after intratracheal instillation. *Toxicol. Sci.* **2004,** *77*, 126-134.
3. Warheit, D. B.; Laurence, B. R.; Reed, K. L.; Roach, D. H.; Reynolds, G. A.; Webb, T. R., Comparative pulmonary toxicity assessment of single-wall carbon nanotubes in rats. *Toxicol Sci* **2004,** *77*, 117-25.
4. Hyung, H.; Fortner, J. D.; Hughes, J. B.; Kim, J. H., Natural organic matter stabilizes carbon nanotubes in the aqueous phase. *Environ. Sci. & Tech.* **2007,** *41*, 179-184.
5. Summers, R. S.; Roberts, P. V., Activated carbon adsorption of humic substances .1. heterodisperse mixtures and desorption. *J. Colloid Interface Sci.* **1988,** *122*, 367-381.
6. Summers, R. S.; Roberts, P. V., Activated Carbon Adsorption of Humic Substances .2. Size Exclusion and Electrostatic Interactions. *J. Colloid Interface Sci.* **1988,** *122*, 382-397.
7. Sontheimer, H.; Crittenden, J. C.; Summers, R. S., *Activated Carbon for Water Treatment*; DVGW-Forschungsstelle: Karlsruhe, Germany, 1988.
8. McCreary, J. J.; Snoeyink, V. L., Characterization and activated carbon adsorption of several humic substances. *Wat. Res.* **1980,** *14*, 151-160.

9. Randtke, S. J.; Jepsen, C. P., Effects of salts on activated carbon adsorption of fulvic acids. *J. Am. Water Works Assoc.* **1982,** *74*, 84-93.

10. Kilduff, J. E.; Karanfil, T.; Weber, W. J., Competitive interactions among components of humic acids in granular activated carbon adsorption systems: Effects of solution chemistry. *Environ. Sci. & Tech.* **1996,** *30*, 1344-1351.

11. American Water Works Association, *Water quality and treatment*; McGraw Hill: New York, 1999.

12. Yang, K.; Xing, B. S., Desorption of polycyclic aromatic hydrocarbons from carbon nanomaterials in water. *Environ. Pollut.* **2007,** *145*, 529-537.

13. Kilduff, J. E.; Karanfil, T.; Chin, Y. P.; Weber, W. J., Adsorption of natural organic polyelectrolytes by activated carbon: A size-exclusion chromatography study. *Environ. Sci. & Tech.* **1996,** *30*, 1336-1343.

14. Li, Q. L.; Snoeyink, V. L.; Mariaas, B. J.; Campos, C., Elucidating competitive adsorption mechanisms of atrazine and NOM using model compounds. *Wat. Res.* **2003,** *37*, 773-784.

15. Her, N.; Amy, G.; Foss, D.; Cho, J.; Yoon, Y.; Kosenka, P., Optimization of method for detecting and characterizing NOM by HPLC-size exclusion chromatography with UV and on-line DOC detection. *Environ. Sci. & Tech.* **2002,** *36*, 1069-1076.

16. Stuart, M. A. C.; Scheutjens, J.; Fleer, G. J., Polydispersity effects and the interpretation of polymer adsorption-isotherms. *J. Polym. Sci. B* **1980,** *18*, 559-573.

17. Koopal, L. K., The effect of polymer polydispersity on the adsorption-isotherm. *J. Colloid Interface Sci.* **1981,** *83*, 116-129.

18. Li, F. S.; Yuasa, A.; Ebie, K.; Azuma, Y.; Hagishita, T.; Matsui, Y., Factors affecting the adsorption capacity of dissolved organic matter onto activated carbon: modified isotherm analysis. *Wat. Res.* **2002,** *36*, 4592-4604.

19. Karanfil, T.; Kitis, M.; Kilduff, J. E.; Wigton, A., Role of granular activated carbon surface chemistry on the adsorption of organic compounds. 2. Natural organic matter. *Environ. Sci. & Tech.* **1999,** *33*, 3225-3233.

20. Harrington, G. W.; Digiano, F. A., Adsorption equilibria of natural organic-matter after ozonation. *J. Am. Water Works Assoc.* **1989,** *81*, (6), 93-101.

21. Thorn, T. A.; Folan, D. W.; MacCarthy, P. *Characterization of the International Humic Substances Society Standard and Reference Fulvic Acids by Solid State Carbon-13 and Hydrogen-1 Nuclear Magnetic Resonance Spectrometry*; Water-Resources Investigation Report 89-4196; U.S. Geological Survey: Denver, CO, 1989.

22. Islam, M. F.; Rojas, E.; Bergey, D. M.; Johnson, A. T.; Yodh, A. G., High weight fraction surfactant solubilization of single-wall carbon nanotubes in water. *Nano Lett.* **2003,** *3*, 269-273.

23. Tan, Y.; Resasco, D. E., Dispersion of single-walled carbon nanotubes of narrow diameter distribution. *J. phys. Chem. B* **2005,** *109*, 14454-14460.

24. Gotovac, S.; Honda, H.; Hattori, Y.; Takahashi, K.; Kanoh, H.; Kaneko, K., Effect of nanoscale curvature of single-walled carbon nanotubes on adsorption of polycyclic aromatic hydrocarbons. *Nano Lett.* **2007,** *7*, 583-587.

25. Ghosh, K.; Schnitzer, M., Macromolecular structures of humic substances. *Soil Sci.* **1980,** *129*, 266-276.

26. Vermeer, A. W. P.; van Riemsdijk, W. H.; Koopal, L. K., Adsorption of humic acid to mineral particles. 1. Specific and electrostatic interactions. *Langmuir* **1998,** *14*, 2810-2819.

27. Schlautman, M. A.; Morgan, J. J., Adsorption of aquatic humic substances on colloidal-size aluminum-oxide particles - influence of solution chemistry. *Geochim. Cosmochim. Acta* **1994,** *58*, 4293-4303.

28. Ritchie, J. D.; Perdue, E. M., Proton-binding study of standard and reference fulvic acids, humic acids, and natural organic matter. *Geochim. Cosmochim. Acta* **2003,** *67*, 85-96.

Supporting Information

Natural Organic Matter (NOM) Adsorption to Multi-Walled Carbon Nanotubes: Effect of NOM Characteristics and Water Quality Parameters

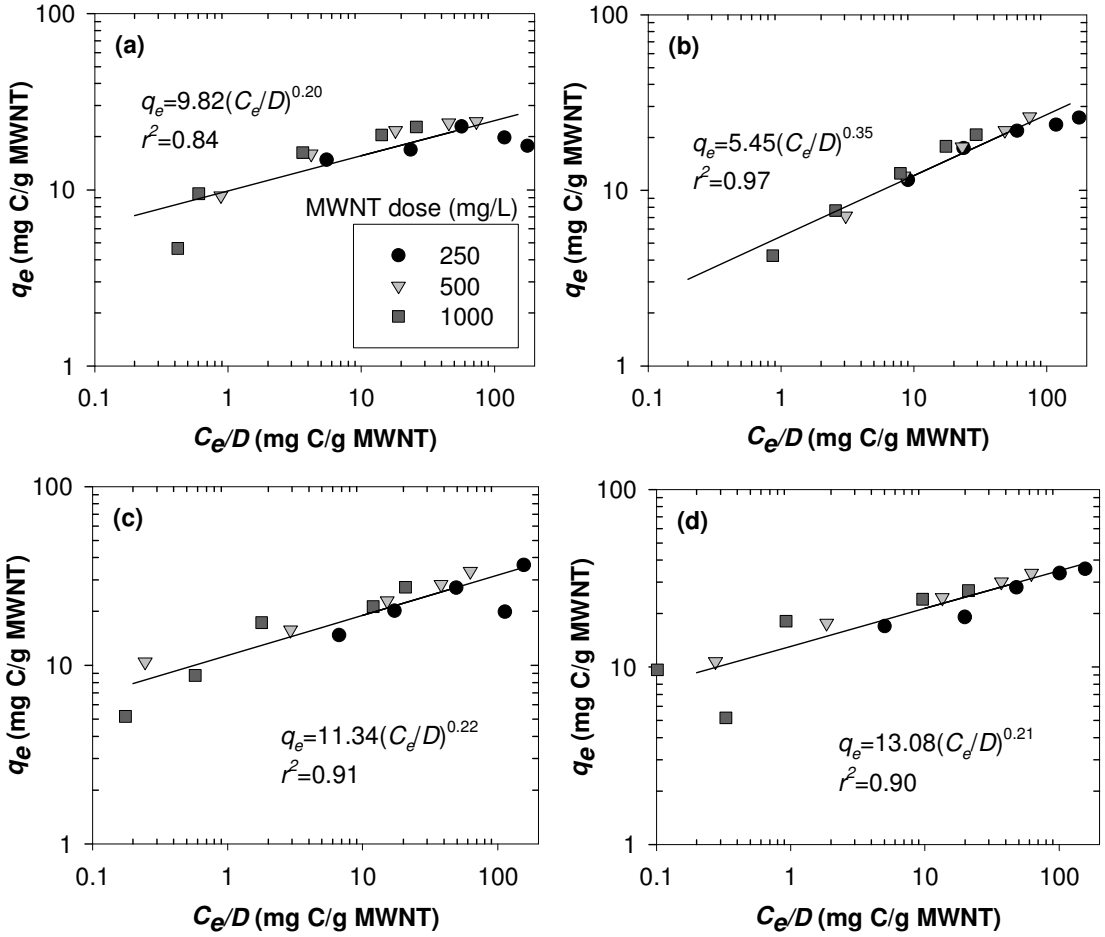

Figure 4.S1. Isotherm experimental result and Freundlich adsorption model fit for (a) SRHA, (b) SRFA, (c) ESHA, (d) LHA, (e) NLHA, (f) NLFA, (g) WPHA, and (h) WPFA. (Isotherm experimental condition: pH 7, 5 mM NaCl, and 1 mM NaH_2PO_4)

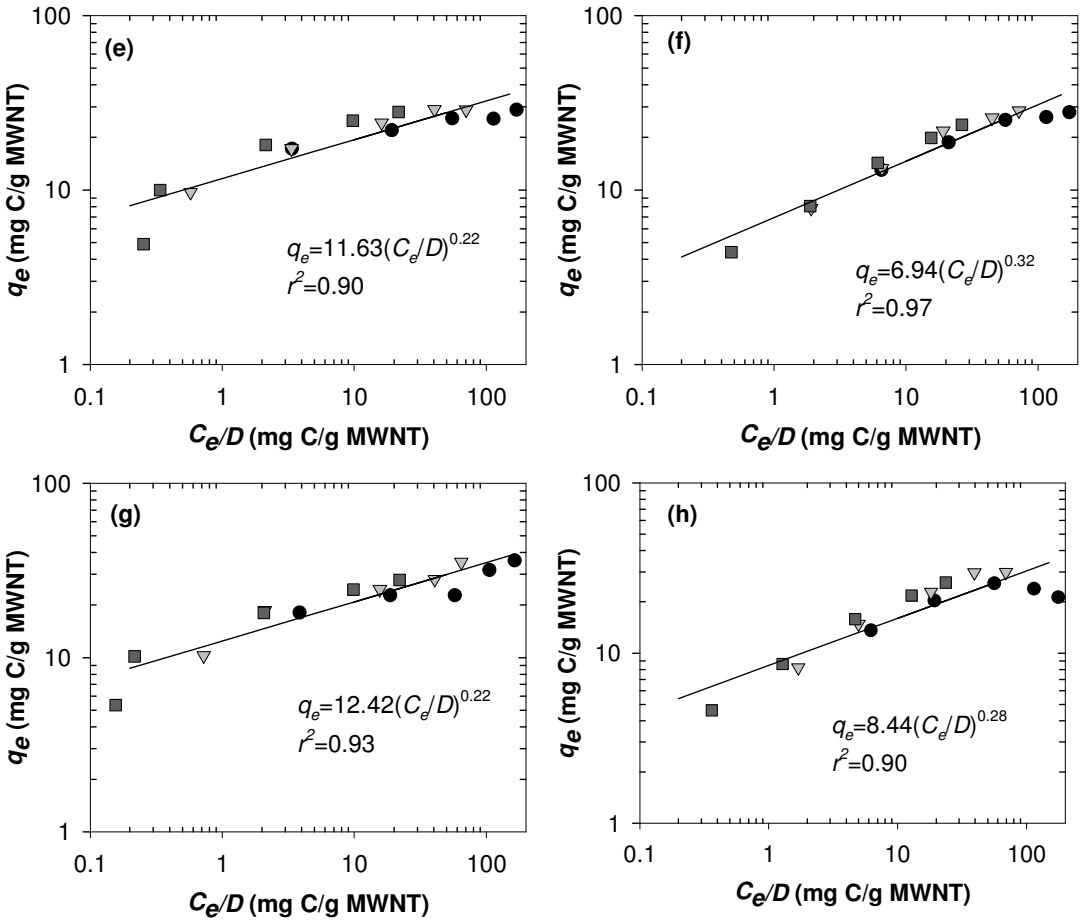

Figure 4.S1 continued.

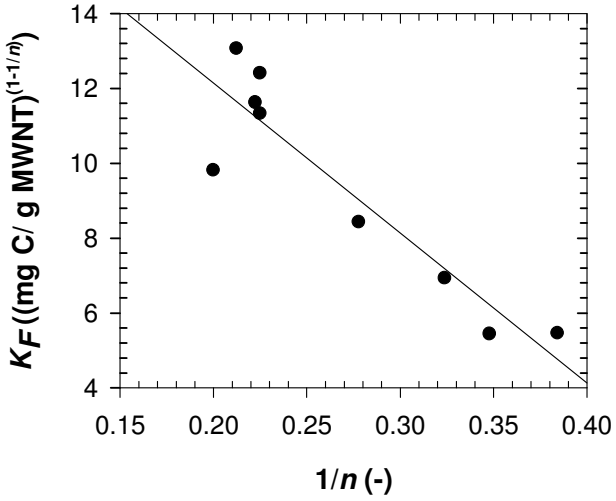

Figure 4.S2. Correlation between K_F and 1/n for various NOMs.

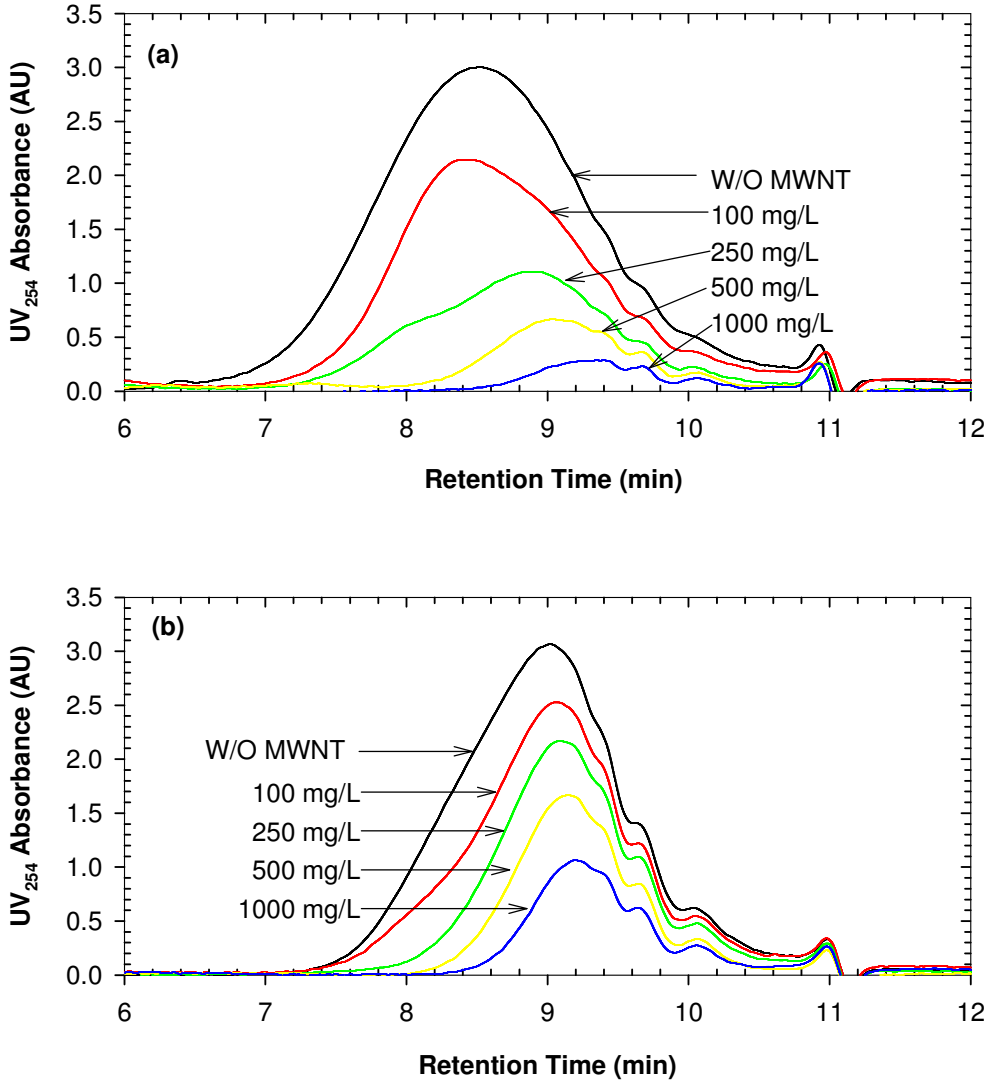

Figure 4.S3. Change of molecular weight distribution by MWNT dose for (a) SRHA and (b) SRFA.

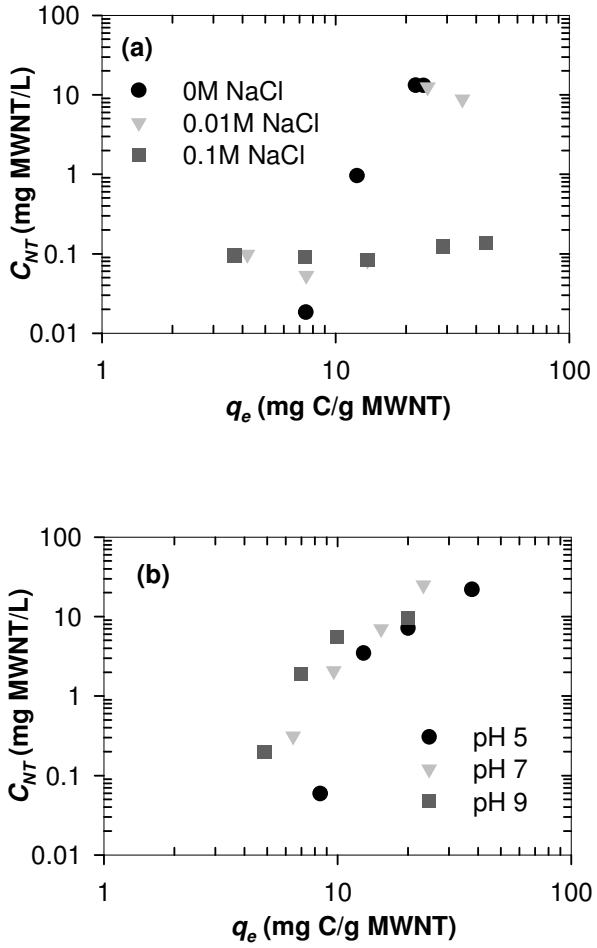

Figure 4.S4. Effect of (a) ionic strength (at 22 ^{o}C, pH 7.0, [NaH_2PO_4] = 1 mM) and (b) pH (at 22 ^{o}C, [NaCl] = 5 mM, [NaH_2PO_4] = 1 mM) on the amount of MWNT suspended in water.

Table 4.S1. Carbon Distribution and Elemental Composition of NOMs Investigated in This Study. Data Are Excerpted from International Humic Substances Society (IHSS) webpage (www.ihss.gatech.edu).

	Carbon Distribution						Elemental Composition						
	Carbonyl	Carboxyl	Aromatic	Acetal	Heteroaliphatic	Aliphatic	H_2O	Ash	C	H	O	N	S
SRHA	6	15	31	7	13	29	20.4	1.04	52.63	4.28	42.04	1.17	0.54
ESHA	6	18	50	4	6	16	8.2	0.88	58.13	3.68	34.08	4.14	0.44
LHA	8	15	58	4	1	14	7.2	2.58	63.81	3.7	31.27	1.23	0.76
SRFA	5	17	22	6	16	35	16.9	0.58	52.34	4.36	42.98	0.67	0.46
NLHA	10	19	38	7	11	15	9.1	0.31	53.33	3.97	43.09	1.16	0.58
WPHA	8	18	42	6	8	18	6.93	1.6	54.72	4.04	38.54	1.47	0.36
NLFA	10	24	31	7	12	18	9.2	0.45	52.31	3.98	45.12	0.68	0.46
WPFA	7	19	36	6	12	20	8.29	0.16	53.63	4.24	41.81	1.07	0.29
SRNOM	8	20	23	7	15	27	8.15	7	52.47	4.19	42.69	1.1	0.65

Table 4.S2. Conditions for Adsorption Experiments.

Effect of NOM Type
C_0: 2.5, 5, 10, 25, 50 mg/L
D: 250, 500, 1000 mg/L
22 ^{o}C, pH=7.0, [NaCl] = 5 mM, [NaH_2PO_4] = 1 mM
Effect of Water Quality (Ionic Strength)
C_0: 2.5, 5, 10, 25, 50 mg/L
D: 500 mg/L
22 ^{o}C, pH 7.0, [NaH_2PO_4] = 1 mM
Effect of Water Quality (pH)
C_0: 2.5, 5, 10, 25, 50 mg/L
D: 500 mg/L
22 ^{o}C, [NaCl] = 5 mM, [NaH_2PO_4] = 1 mM

CHAPTER 5

COMPARATIVE STUDY ON THE DISPERSION OF FULLERENES IN THE AQUEOUS PHASE

Abstract

Dispersivity of representative fullerenes such as C_{60}, single-walled carbon nanotube (SWNT), and multi-walled carbon nanotube (MWNT) in the aqueous phase containing model natural organic matter (NOM) was investigated. Four dispersion methods were tested (*i.e.*, mechanical mixing or sonication after either adding solid phase fullerenes into the aqueous phase or contacting organic phase containing fullerenes with the aqueous phase) to simulate possible spillage scenarios to the aqueous environment. The experimental results showed that MWNTs formed water stable suspensions by the mechanical mixing and sonication and SWNTs by the sonication, only when they were added as solids directly to water containing NOM. C_{60} formed water stable colloidal suspensions in all cases except when solids were added to water and ultrasound was applied. In most cases, the presence of NOM facilitated the fullerene dispersion in the aqueous phase. However, when C_{60} entered the aqueous phase via organic solvent, NOM appeared to retard the interphase transport. The results suggest that the fate of carbon nanomaterials in the aqueous environment would be greatly affected by the types of fullerenes and the characteristics of natural water as well as the routes of introduction to the natural waterways.

Introduction

Carbon fullerenes such as C_{60} and carbon nanotubes (CNTs) have been at the center of recent prosperity in nanoscale science and engineering. C_{60} consists of 60 carbon atoms arranged in 20 hexagons and 12 pentagons that form a perfectly symmetrical cage structure with a dimension of a soccer ball of size *ca*. 1 nm. Similarly arranged, other carbon cage structures such as $C_{70,}$ $C_{76,}$ C_{78}, C_{84}, and C_{90} have been also identified. CNTs, on the other hand, consist of sheets of carbon atoms covalently bonded in hexagonal arrays that are seamlessly rolled into a hollow, cylindrical shape with both ends rounded through pentagon ring inclusions. They present a highly flexible thread-like structure having an extremely high aspect ratio with the diameter ranging from 1 to 200 nm and length from 0.1 to 100 μm. The CNTs are categorized into two main species; single-walled carbon nanotube (SWNT) and multi-walled carbon nanotube (MWNT). The latter results from co-axial assembly of multiple SWNTs. In contrast to C_{60}, CNTs represent a mixture of molecules with different lengths and carbon arrays. With increasing commercial interest in unique chemical and physical properties, manufacture and use of fullerenes are expected to grow rapidly over the next decade [1-3].

However, information to assess the effects of these materials on natural environment and human health is scarce, like many other engineered nanomaterials. Concerns have intensified due to the findings that fullerenes can interact with living organisms and cause toxic effects that are unique to this class of materials [4-7]. For instance, SWNT showed higher pulmonary toxicity than quartz, a well known industrial

hazards [4, 5], and C_{60} showed cytotoxicity inhibiting cell growth [6, 8, 9]. Such findings carry an additional significance as fullerenes have been found in particulate matter emitted from coal-fueled power plants [10], common fuel-gas combustion source [11, 12], and even in nature, although sporadically in small masses [13, 14]. Many studies are currently being conducted to evaluate toxicological effects of fullerenes as well as other nano-scale engineered materials.

An equally important environmentally relevant issue as the toxicological effect is the fate and transport of the fullerenes in natural environment and potential exposure pathways. As the fullerenes are extremely hydrophobic and virtually non-wettable, they have not been generally considered as potential contaminants in the aqueous environment. However, a recent discovery that C_{60} forms stable, nano-scale colloidal aggregates (commonly referred to as nano-C_{60} or nC_{60}) upon release to water has redefined our view on its impact on the aqueous environment [8, 15]. It was suggested that the stability of these colloids might be even enhanced in natural water due to the steric stabilization by natural organic matter (NOM) that interacts with these colloids [16]. Furthermore, our recent study [17] suggested that MWNTs could be readily stabilized and suspended in natural water due to their association with NOM.

In this study, we performed a systematic, comparative investigation on the dispersion of representative fullerenes, C_{60}, SWNTs and MWNTs, in model natural waters. Specific objectives of this study include evaluating the dispersivity of the fullerenes under different spillage scenarios to water body, (*i.e.* the spillage of solid phase

fullerenes or fullerenes dissolved in common organic solvents) and understanding the role of NOM on fullerene dispersion under these scenarios. Different spillage scenarios were simulated by 1) applying either mechanical mixing or sonication after directly adding solid phase fullerenes into the aqueous phase and 2) applying either mechanical mixing or sonication after contacting organic solvent containing fullerenes with the aqueous phase. Ultrasound, while unlikely in natural environment, was applied to evaluate ultimate dispersion potential of the fullerenes under the extreme conditions. Suwannee River natural organic matter (SR-NOM) was used as a model NOM and sodium dodecylsulfate (SDS), an anionic surfactant commonly used for the fullerene dispersion, was used for a comparison purpose.

Experimental

Materials. C_{60} with over 99% purity and MWNTs (140 ± 30 nm diameter and 7 ± 2 μm length) with over 90% purity were obtained from MER Corporation (Tucson, AZ). Purified SWNTs (0.8-1.2 nm diameter and 0.1-1 μm length) with less than 15% ash contents were purchased from CNI (Houston, TX). ACS grade (>99% purity) SDS ($CH_3(CH_2)_{11}OSO_3Na$) was obtained from Aldrich Chemical Company (Milwaukee, WI). SR-NOM stock solution was prepared by mixing a known amount of SR-NOM (International Humic Substances Society, St. Paul, MN) with ultrapure water for 24 hours. Dissolution of SR-NOM was facilitated by adding 1 N potassium hydroxide (KOH) to increase the solution pH to 7. After dissolution, the solution pH was lowered to the original value by adding 1 N nitric acid (HNO_3). The concentration was measured using total organic carbon (TOC) analyzer (TOC-Vw, Shimadzu, Columbia, MD). This stock solution was diluted to prepare solutions of target carbon concentrations (5 mg C/L and 50 mg C/L). Ultrapure water produced by a Milli-Q water filtration system (Millipore, Billerica, MA) was used for the preparation of all the solutions.

1-Phase Mixing (1-M). 5 mg of solid MWNTs were added to 100 mL of ultrapure water, 5 mg C/L SR-NOM solution, 50 mg C/L SR-NOM solution, and 1% SDS solution (*i.e.* 50 mg MWNT/L in each solution), respectively, and the suspensions were vigorously mixed for 1 day. After 4 days of quiescent settling, the supernatant (*ca.* 60% of total volume) was filtered with a Whatman 541 filter (20-25 μm nominal pore size, Florham Park, NJ) and further analyses were performed with the filterate. SWNTs and C_{60}

samples were prepared by the same procedure except 50 mg/L of solid SWNTs and C_{60} were mixed for 4 weeks and the supernatants were filtered by a VWR 453 filter (10 μm nominal pore size, Suwannee, GA). This preparation procedure is referred to as 1-M in this study.

1-Phase Sonication (1-S). 5 mg of solid phase fullerenes (*i.e.*, $C_{60,}$ SWNTs, and MWNTs) were added to 50 mL of ultrapure water, 5 mg C/L SR-NOM solution, 50 mg C/L SR-NOM solution, and 1% SDS solution (*i.e*. 100 mg/L of fullerenes in each solution), respectively, and the mixture was sonicated at 400 W for 10 minutes using a Misonix XL2020 cuphorn sonicator (Farmingdale, NY). After 4 days of quiescent settling, the supernatant of MWNT suspension was filtered with a Whatman 541 filter for further analyses. Supernatants of SWNT and C_{60} suspensions were filtered with a VWR 453 filter. This preparation procedure is referred to as 1-S in this study.

2-Phase Mixing (2-M). MWNTs and SWNTs were dissolved in 1,3-dichlorobenzene (DCB) (Aldrich Chemical Company, Milwaukee, WI), a commonly used solvent for the nanotubes [18] by sonicating 50 mg of each nanotube in 100 mL DCB for 10 minutes and filtering the solutions using a 10 μm VWR 453 filter. A solution of 500 mg/L C_{60} in toluene (Aldrich Chemical Company, Milwaukee, WI) was prepared by mixing dry C_{60} in toluene for 6 hrs. An aliquot (20 mL) of each fullerene solution in the organic solvent was added to an 125 mL Erlenmeyer flask containing 100 mL of various aqueous solutions (*i.e.*, ultrapure water, 5 mg C/L SR-NOM solution, 50 mg C/L SR-NOM solution, and 1 % SDS solution) and agitated for 1 week. After 3 days of quiescent

settling and phase separation, aqueous phase was carefully taken and purged with 99.999% purity N_2 (NI UHP300, Airgas Inc., Randor, PA) for 3 hours to remove residual organic solvents (DCB or toluene). This preparation procedure involving mixing of two solvent phases is referred to as 2-M in this study.

2-Phase Sonication (2-S). The same procedure as 2-M was followed except 10 minutes of sonication was applied instead of 1 week of mixing. This preparation procedure involving sonication of two solvent phases is referred to as 2-S in this study.

Analysis. Concentrations of nanotubes suspended in the aqueous phases were determined using a thermal optical transmittance (TOT) analyzer (Sunset Laboratory, Tigard, OR). The TOT measures the concentration of nanotubes in a solution containing both nanotubes and NOM based on difference in the thermal stability of elemental carbons (*i.e.*, nanotubes) and organic carbons (*i.e.*, NOM). Details of the analytical principle and experimental protocols are described in our previous work [17]. Briefly, an MWNT specimen for the TOT analysis was prepared by retrieving the MWNTs from a known volume of an aqueous phase using a 0.3 μm Pallflex 2500 quartz filter (Pall Corporation, Ann Arbor, MI). In contrast to the MWNTs, SWNTs in aqueous phase could not be entirely retained by the filtration since some of the SWNTs might be smaller than pore size of the Pallflex 2500 quartz filter. Hence, an SWNT specimen for the TOT analysis was prepared by dropping a small amount of an SWNT suspension on a rectangular-shaped 1.45 cm^2 quartz filter and drying in a 90 ^oC oven for several hours and repeating the procedure until the sufficient amount of the SWNT solution was dried upon the filter

surface. A C_{60} specimen for the TOT analysis was prepared by the same procedure with the SWNTs. The particle size of C_{60} aggregates dispersed in the aqueous phase was analyzed using a Zetasizer ZS90 (Malvern Instruments, Worcestershire, UK) with the dynamic light scattering (DLS) method. Electron microscopic images were analyzed by a Philips 120 transmission electron microscope (TEM) (New York, NY). A TEM specimen was prepared by placing a droplet of fullerene suspension on a copper carbon grid (Electron Microscopy Science, Hatfield, PA) and drying overnight at room temperature. UV-Vis absorbance of the fullerene suspension was measured by an Agilent 8453 UV-Vis Spectroscopy System (Palo Alto, CA).

Results and Discussions

Solid MWNTs were readily dispersed in SR-NOM and SDS solutions by mechanical mixing (*i.e*. 1-M) or sonication (*i.e*. 1-S) (Figure 5.1). The resulting suspensions were stable for more than a month. In contrast, the MWNTs in ultrapure water settled down quickly regardless of preparation methods. MWNT suspensions with 5 mg C/L or 50 mg C/L SR-NOM appeared darker and looked more turbid than 1% SDS solution, implying that higher concentration of MWNTs might be suspended in the SR-NOM solutions. These findings from 1-M were consistent with our previous study [17]. However, the MWNTs were not dispersed in the aqueous phase when they were introduced via the organic solvent (*i.e*. 2-M or 2-S) (results not shown). The MWNTs are expected to have very high affinity with the organic solvent compared to water due to their extremely hydrophobic nature. This might hinder partitioning of the MWNTs from the organic phase to the aqueous phase and result in negligible dispersion of the MWNTs in aqueous phase by the phase exchange methods (2-M or 2-S).

The TEM images of MWNTs in SR-NOM solutions (Figures 5.2a and 5.2b) clearly indicate that most of the MWNTs were individually dispersed. In contrast to the MWNTs in the aqueous suspension prepared by 1-M (Figure 5.2a), most MWNTs by 1-S appeared shorter than manufacturer's specifications (Figure 5.2b). It has been reported that sonication produces shorter and more stable nanotubes by the fragmentation of the nanotubes in the organic solvents or aqueous solutions [19-21]. This was also consistent with the result that the concentration of the MWNTs suspended in water was higher when

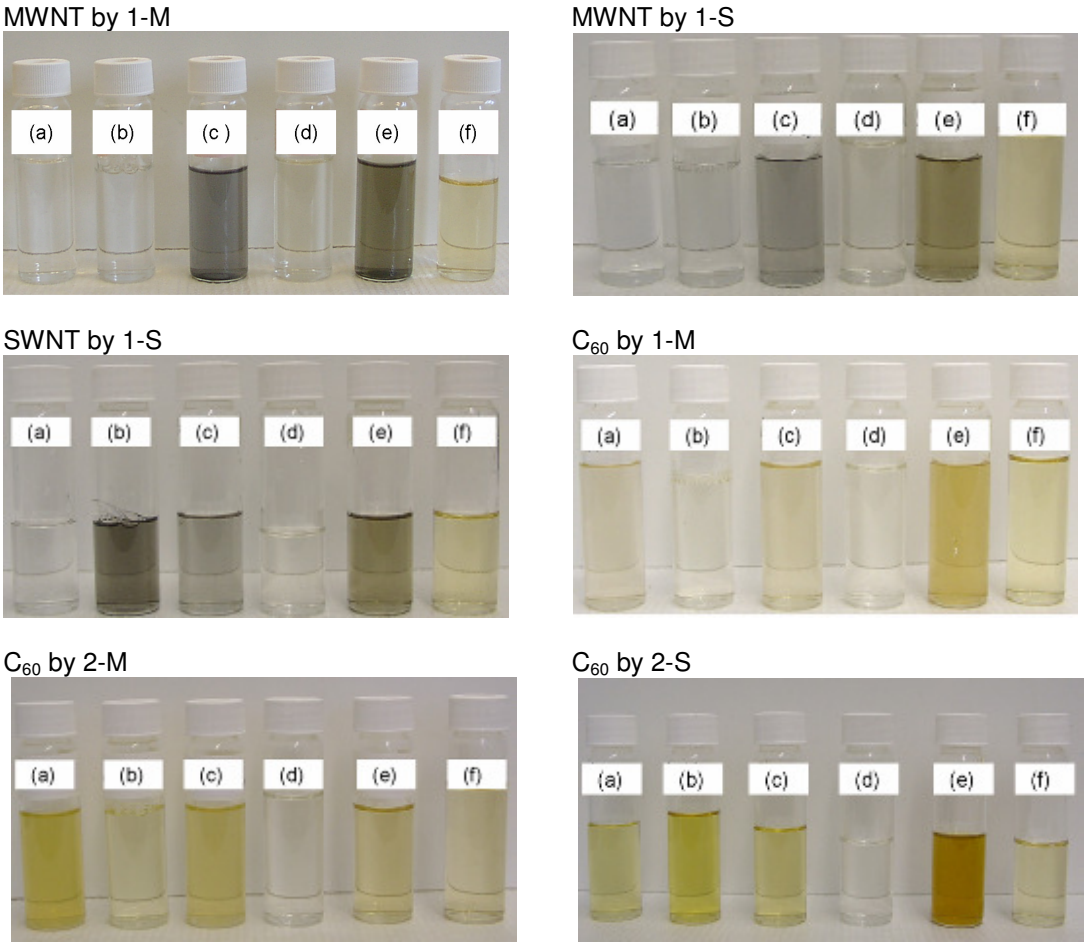

Figure 5.1. Visual examination of fullerenes in (a) Milli-Q water, (b) 1% SDS solution, (c) 5 mg C/L SR-NOM solution, and (e) 50 mg C/L SR-NOM solution prepared by various preparation methods. 5 mg C/L and 50 mg C/L SR-NOM solutions without fullerenes are also shown in (d) and (f).

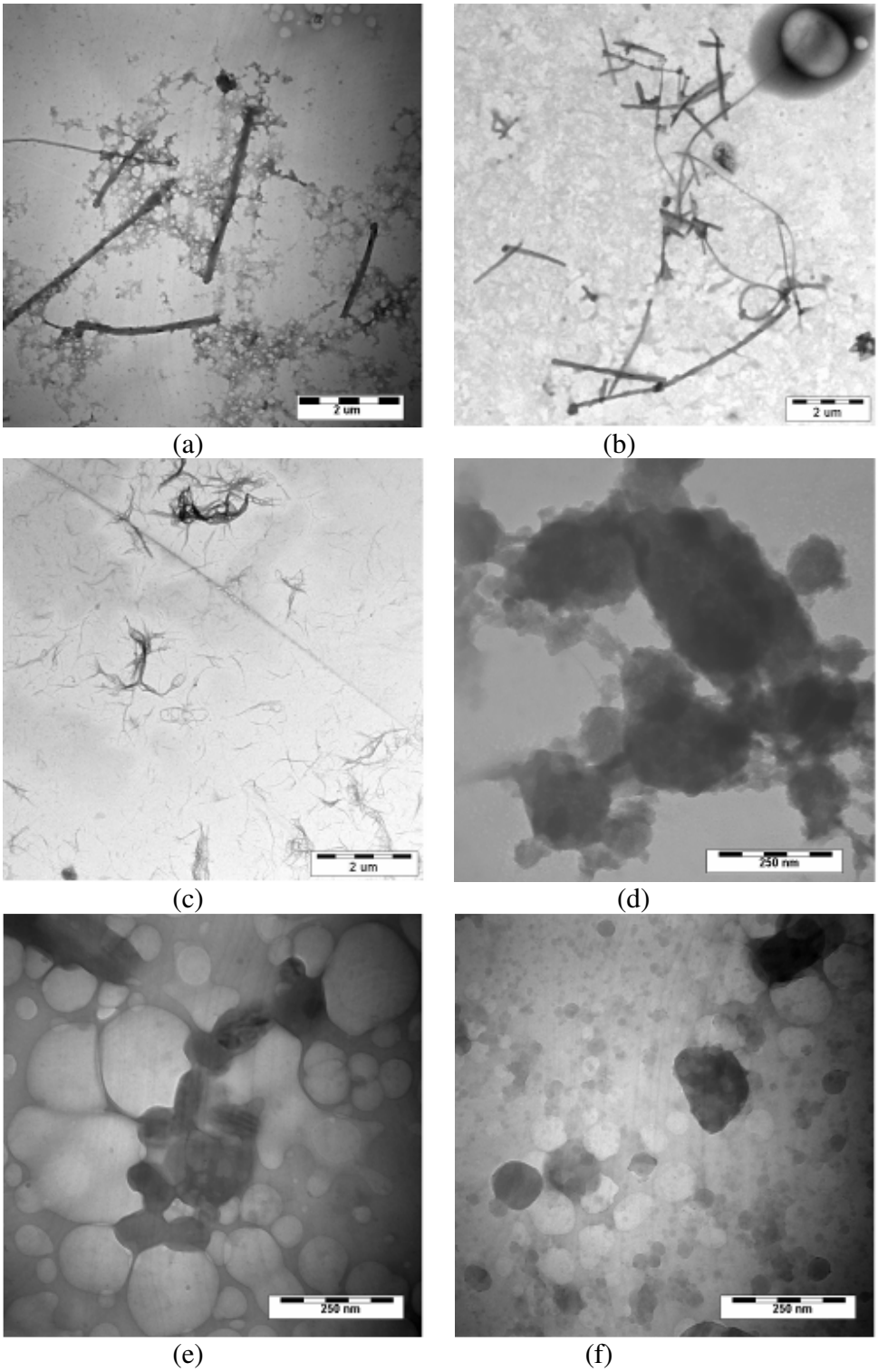

Figure 5.2. Transmission electron microscopy images of fullerenes stabilized in SR-NOM solutions produced by various preparation methods. (a) MWNT by 1-M, (b) MWNT by 1-S, (c) SWNT by 1-S, (d) C_{60} by 1-M, (e) C_{60} by 2-M, and (f) C_{60} by 2-S.

sonication was applied. The TOT measurement showed that, 3.3 mg/L and 5.3 mg/L of the MWNTs were suspended in 5 mg C/L and 50 mg C/L SR-NOM solution, respectively, by 1-M. In contrast, 7.3 mg/L and 9.1 mg/L of the MWNTs were suspended in 5 mg C/L and 50 mg C/L SR-NOM solutions, respectively, by 1-S. It was also noteworthy that, for both preparation methods, the concentrations of the MWNTs suspended in the SR-NOM solutions increased as the SR-NOM concentration increased. Increase in UV-Vis absorbance over entire wavelength (*i.e.* baseline increase) suggested light scattering by the stabilized MWNTs in the SR-NOM solutions (Figure 5.3) and appeared to be proportional to the concentration of the MWNTs measured by the TOT. SWNTs were not dispersed in the aqueous phase by simple mixing (1-M) under the experimental conditions investigated in this study. Phase exchange methods (2-M or 2-S) also did not produce aqueous suspensions of the SWNTs. However, significant amount of the SWNTs were dispersed in the SR-NOM or SDS solutions when sonication was applied to mixture of dry phase SWNT and water (1-S) (Figure 5.1). The SWNT suspension in the SR-NOM solution exhibited a transparent dark brown color. Even though a small portion of the SWNTs gradually precipitated as time elapsed, most of them remained suspended for several months. The TEM analysis showed randomly dispersed hairy images of the SWNTs (Figure 5.2c). The TOT analysis suggested that the concentrations of SWNTs suspended in the SR-NOM solution increased as the SR-NOM concentration increased, *i.e.* 2.19 mg/L and 9.10 mg/L of the SWNTs were stabilized in 5 mg C/L and 50 mg C/L solutions, respectively. However, the SWNTs in SDS solution could not be measured by TOT due to a large difference between SWNT

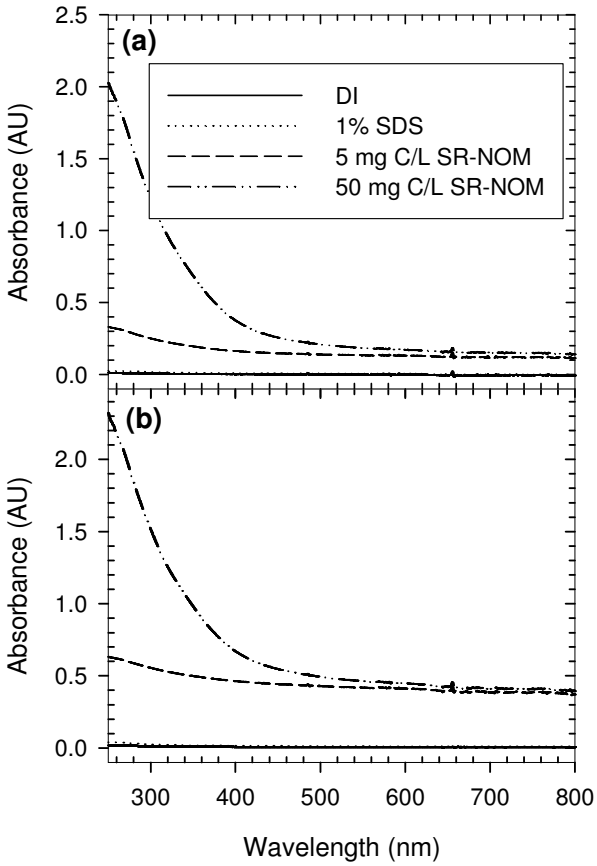

Figure 5.3. UV-Vis spectra of MWNT suspensions in various aqueous phases prepared by (a) 1-M and (b) 1-S.

and SDS concentrations. In each specimen, there existed more than three orders of magnitude difference in the SDS and SWNT concentrations (based on carbon content) such that the concentration of SDS exceeded the upper detection limit of the TOT before the SWNTs reached measurable concentration However, comparison of the solution darkness (Figure 5.1) and increase in the UV-Vis spectrum baseline (Figure 5.4) indicated that more SWNTs might have been suspended in the 1% SDS solution than in the 50 mg C/L SR-NOM solution.

The above findings suggest a distinct difference between MWNTs and SWNTs when they are introduced to the aqueous phase. Only when both MWNTs and the SWNTs were introduced into water as a solid form, the MWNTs were dispersed in the aqueous phase by mixing and sonication and SWNTs by sonication. This difference in solubility might originate from the difference in the strength of intermolecular attractive forces among the nanotubes. Both MWNT and SWNT are extremely hydrophobic and prone to aggregate as a result of strong van der Waals force between molecules, which increases as surface area increases [22, 23]. However, the SWNTs have higher specific surface area per unit volume than MWNTs due to their much smaller diameter (generally, the diameters of the MWNTs range from *ca.* 10 to 100 nm, while the diameters of SWNTs are less than a few nanometers) and, therefore, would be subject to higher attractive forces among individual tubes. The higher intermolecular attractive forces might prevent individual SWNT from being separated and dispersed by the simple mechanical mixing. In contrast, the sonication appeared to provide sufficient energy to overcome the molecular interaction among SWNT. It is noteworthy that sonication alone

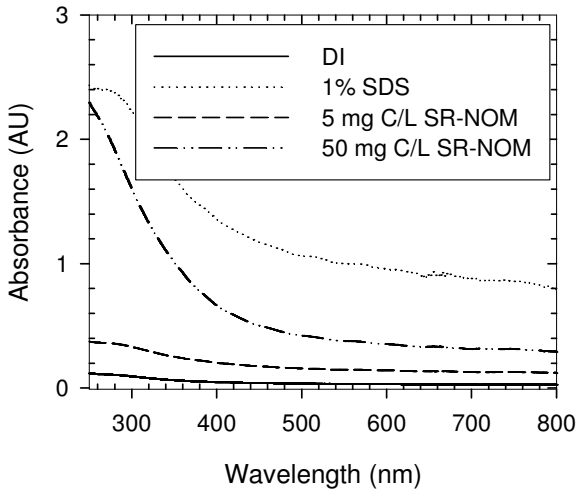

Figure 5.4. UV-Vis spectra of SWNT suspensions in various aqueous phases prepared by 1-S.

did not disperse SWNTs nor MWNTs in the absence of SR-NOM or SDS. The SWNTs are known to be dispersed by the sonication in the presence of various surfactants such as sodium dodecylsulfate (SDS) [23-27], sodium dodecylbenzene sulfonate (SDBS) [20, 26], and Triton X [26, 27]. These surfactants adsorb onto the surface of the nanotubes and stabilize them by inducing electrostatic and steric stabilization [20, 24] and providing thermodynamically more favorable surfaces. The similar mechanism is expected for the dispersion of the SWNT by SR-NOM from sonication.

In contrast to the CNTs, C_{60} formed stable suspensions by mixing solid C_{60} with all the aqueous phases (*i.e.*, ultrapure water, 5 mg C/L SR-NOM solution, 50 mg C/L SR-NOM solution, and 1% SDS solution) (Figure 5.1), consistent with the previous findings [9, 28, 29]. However, solid C_{60} were not dispersed in any aqueous solutions by sonication (1-S). Characteristics of the C_{60} suspension produced by 1-M were consistent with those of the nC_{60} reported in the literature [8, 9, 15]. All aqueous suspensions prepared by 1-M showed characteristic orange-yellow color of the nC_{60} suspension [8, 30], while the intensity of the color varied depending on the aqueous phase. The TEM analysis suggests that most C_{60} aggregates existed as oval or circular shapes in cross section and were surrounded by SR-NOM (Figure 5.2d), while the possibility that the agglomerates of SR-NOM and the C_{60} aggregates were formed during the drying process could not be ruled out. Average diameters of the C_{60} aggregates prepared by 1-M and measured by the DLS (Figure 5.6a) ranged from *ca.* 380 nm (C_{60} in 50 mg C/L SR-NOM solution) to 580 nm (C_{60} in 5 mg C/L SR-NOM solution) and matched well with the observations by the TEM analysis.

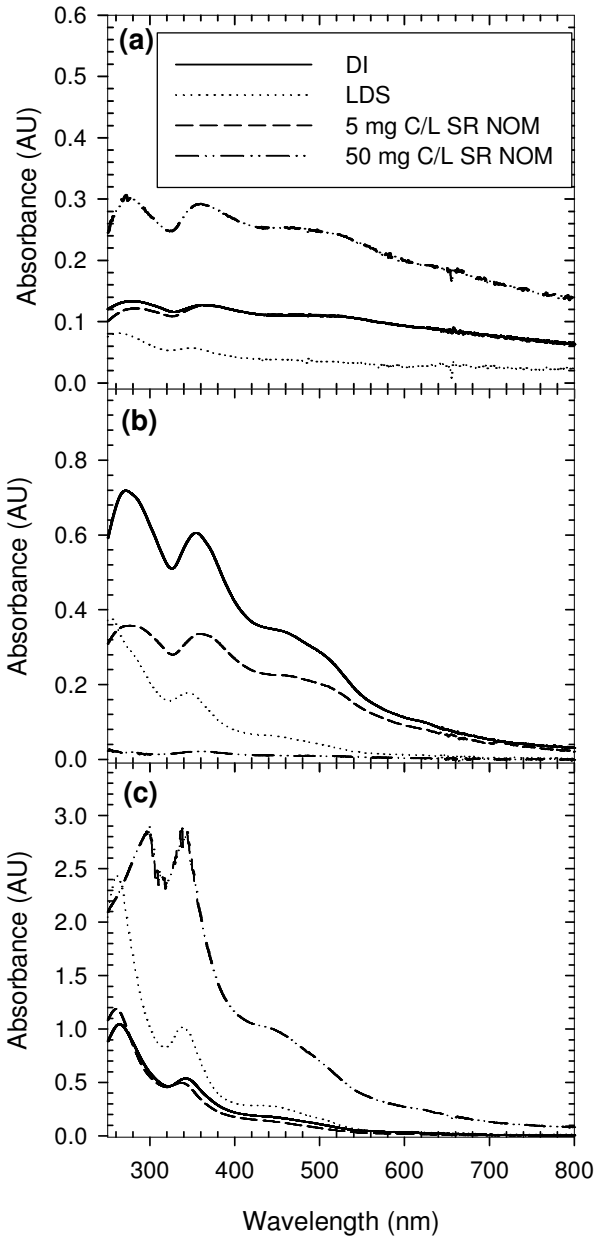

Figure 5.5. UV-Vis spectra of C_{60} suspensions prepared by (a) 1-M, (b) 2-M, and (c) 2-S. These spectra were obtained after subtracting the spectra of SR-NOM only solution from the original spectra.

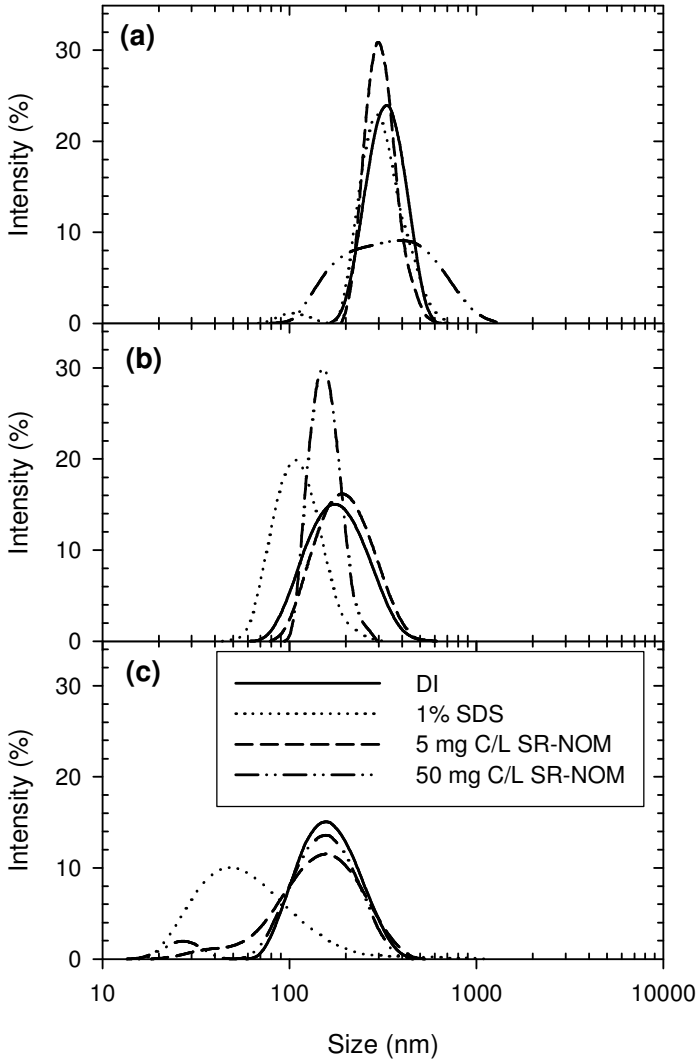

Average diameter (nm)	DI	1% SDS	5 mg C/L SR-NOM	50 mg C/L SR-NOM
1-M	473.54	524.91	581.93	378.45
2-M	168.54	123.14	188.61	249.62
2-S	154.14	53.13	125.03	128.32

Figure 5.6. Size distribution and average diameter of nC_{60} prepared by (a) 1-M, (b) 2-M, and (c) 2-S.

Figure 5.5a shows UV-Vis spectra of C_{60} suspensions prepared by 1-M. Spectra of the C_{60} suspensions in the SR-NOM solutions were presented after subtracting the spectra of SR-NOM only solutions from the original spectra. UV-Vis absorbance of all C_{60} suspensions showed characteristic absorption peaks of solvated C_{60}, which generally located between 330 and 360 nm [8, 9] (Figure 5.5a). Peaks were red-shifted, which appears to be due to the existence of aggregate forms of C_{60} [8]. Broad band absorption at 400 to 500 nm also indicates the presence of aggregate forms of C_{60}. However, these spectra were considered inappropriate for quantification of C_{60} in the aqueous solutions, since a portion of SR-NOM which adsorbed onto nC_{60} might contribute to the overall absorbance differently from SR-NOM freely solubilized in the aqueous phase. In addition, baseline increase over entire wavelength, which was not related to the light absorption by C_{60}, was apparent in these spectra. During nC_{60} preparation by 1-M, portions of black C_{60} powders did not rearrange into crystalline nC_{60} and remained suspended in the solution. They were presumably further stabilized through the interaction with SR-NOM, and passed through the 10 μm filters. These black carbon powders might have scattered incident light and resulted in transmittance loss over entire wavelength, similar to the CNTs. Rough estimation of absorption intensity at 360 nm by subtracting this baseline (*i.e.*, absorbance at 800nm) from the original spectrum showed that the absorption intensity at 360 nm of the C_{60} suspensions in the 50 mg C/L SR-NOM solution (*ca.* 0.156) was higher than that in the ultrapure water (*ca.* 0.064). This suggests that SR-NOM might enhance the dispersion of C_{60} in the aqueous phase, probably following the similar mechanism for the nanotube stabilization by the NOM

discussed previously (*i.e.*, enhanced steric stabilization and charge repulsion provided by the adsorbed SR-NOM).

Stable C_{60} suspensions were readily obtained by both phase exchange methods (*i.e.* 2-M and 2-S). During these processes, the aqueous phases gradually acquired characteristic orange-yellow color of the nC_{60} suspension (Figure 5.1), as C_{60} transferred from the organic phase into the aqueous phase. C_{60} suspensions in the aqueous phase were stable for several months. The diameters of C_{60} aggregates generated from 2-M and 2-S were much smaller than those produced by the 1-M according to the DLS analysis (Figure 5.6b and 5.6c). The average diameters of the C_{60} aggregates generated by 2-M ranged from *ca.* 120 to 250 nm and those by 2-S from *ca.* 50 to 150 nm. In general, average particle sizes of the C_{60} suspensions produced by 2-M were slightly larger than those generated by 2-S. TEM images (Figure 5.2e and 5.2f) showed circular or oval shaped C_{60} aggregates surrounded or connected by NOM. The diameters of C_{60} aggregates measured by the DLS matched well with the size of C_{60} aggregates observed in the TEM images.

All the C_{60} suspensions prepared from the both methods (2-M and 2-S) showed UV-Vis absorption peaks at 360 nm as well as broad band absorption between 400 to 500 nm (Figures 5.5b and 5.5c), confirming the existence of nC_{60}. For the C_{60} suspensions produced by 2-M, it was notable that the intensity of UV-Vis absorbance at 360 nm (after subtracting the absorbance of the background SR-NOM solution) decreased significantly as the SR-NOM concentration increased. This result was contrary to other cases in this

study in which SR-NOM enhanced the dispersion of carbon nanomaterials (SWNT, MWNT, and C_{60} by other preparation methods). In case of 2-M, the SR-NOM at the interface of the organic solvent and the aqueous phase might hinder the interphase transport of C_{60}. SDS also appeared to retard the transport of C_{60} from the organic phase to the aqueous phase (*i.e.* compared to DI), but to a much less extent than SR-NOM, when compared under the same carbon concentration basis (50 mg C/L SR-NOM versus *ca.* 5,000 mg C/L SDS). In contrast, for C_{60} suspensions prepared by 2-S, UV-Vis absorbance at 360 nm increased as the SR-NOM concentration increased suggesting the enhanced dispersion of C_{60} in presence of SR-NOM. For 2-S, SR-NOM also showed better C_{60} stabilization capability than SDS, when compared under the same carbon concentration basis. This suggests that the hindrance of interphase transport by SR-NOM and SDS at the organic solvent-water interface is eliminated by ultrasound application.

As UV absorbance was not appropriate to accurately quantify the amount of C_{60} dispersed in the aqueous phase due to the presence of NOM and C_{60} powders, the TOT analysis was attempted. Even though the TOT was proven effective to measure SWNT and MWNT concentrations in SR-NOM solutions, C_{60} (elemental carbon) could not be differentially measured from SR-NOM (organic carbon) by the TOT, *i.e.* the elemental carbon peak was not detected in the samples containing both C_{60} and SR-NOM. This was attributed to a relatively low sublimation temperature of C_{60} [31, 32]. The TOT analysis proceeds in two distinct stages [33]. In the first stage, temperature increases up to 820 ^{o}C in He atmosphere to volatilize organic carbon (OC) which is then oxidized to CO_2 via granular MnO_2 at 900 °C. CO_2 is subsequently reduced to CH_4 by a Ni/firebrick

methanator at 450 °C and quantified by a flame ionization detector (FID). In the second stage, temperature is again raised stepwise in O_2 (10%) and He (90%) mixed atmosphere to oxidize elemental carbon (EC) and EC concentration is measured with FID after reduction to CH_4. However, it has been reported that C_{60} sublimes under Ar and N_2 atmospheres at 400 [31] and 550 ^oC [32], respectively. Similarly, C_{60} (EC) sublimed in the first stage of the TOT analysis along with organic carbon making differential combustion impossible.

The role of NOM on the stability of various fullerenes is summarized in Table 5.1. Only in the presence of NOM, the MWNTs were relatively easily stabilized in water when it was introduced as solid phase (1-M and 1-S). The solid phase SWNTs could be stabilized in the presence of the NOM but requires a relatively high energy (sonication) for dispersion (1-S). For both nanotubes, transport from the organic solvent to the aqueous phase did not occur. Compared to the nanotubes, C_{60} was readily dispersed in the aqueous phase whether the NOM was present or not. However, the role of the NOM varied, as the NOM appeared to enhance the dispersion of C_{60} for 1-M and 1-S, while the NOM hindered the transport of C_{60} across the organic solvent-water interface in case of 2-M.

The above findings collectively suggest that fullerene dispersion in the aqueous phase would be greatly influenced by the types of fullerenes and the spillage scenarios and NOM could play a varying role in their ultimate fate The experimental results also

Table 5.1. Role of NOM on the Dispersion of Fullerenes in the Aqueous Phase.

	1-M	1-S	2-M	2-S
MWNTs	+	+	O	O
SWNTs	O	+	O	O
C_{60}	+	O	–	+

\+ NOM enhances fullerene dispersivity
– NOM reduces fullerene dispersivity
O Fullerenes are not dispersed under this condition

suggest that findings from a selected model fullerene (*e.g.*, MWNT or C_{60}) should not be extrapolated to predict the behavior of other compounds in this general class of materials (*i.e.*, carbon nanomaterials). In addition, varying water quality parameters such as types and quantity of NOM, pH, ionic strength, and ionic composition might make laboratory findings oversimplified to represent complex environmental disposal scenarios. Finally, the fullerenes might enter the natural environment as derivatized products (*e.g.*, chemically modified or as composite materials) and their behaviors might be different from the parent materials. Therefore, the further study with different types of fullerenes under various water quality parameters would be necessary to better understand the fate and transport of the carbon nanomaterials.

Acknowledgements

This study was supported by the United States Environmental Protection Agency (USEPA) STAR Grant #D832526. The authors thank Dr. John Fortner at School of Civil and Environmental Engineering, Georgia Institute of Technology, for his assistance on DLS analysis and Dr. Jim Millette and Whitney Hill at MVA Scientific Consultants (Duluth, Georgia) for their assistance on TEM analysis.

Literature Cited

1. Ball, P. Roll up for the revolution. *Nature* **2001,** *414*, 142-144.
2. Colvin, V. L. The potential environmental impact of engineered nanomaterials. *Nat. Biotechnol.* **2003,** *21*, 1166-1170.
3. Wiesner, M. R.; Lowry, G. V.; Alvarez, P.; Dionysiou, D.; Biswas, P. Assessing the risks of manufactured nanomaterials. *Environ. Sci. Technol.* **2006,** *40*, 4336-4345.
4. Warheit, D. B.; Laurence, B. R.; Reed, K. L.; Roach, D. H.; Reynolds, G. A.; Webb, T. R. Comparative pulmonary toxicity assessment of single-wall carbon nanotubes in rats. *Toxicol. Sci.* **2004,** *77*, 117-25.
5. Lam, C. W.; James, J. T.; McCluskey, R.; Hunter, R. L. Pulmonary toxicity of single-wall carbon nanotubes in mice 7 and 90 days after intratracheal instillation. *Toxicol. Sci.* **2004,** *77*, 126-134.
6. Sayes, C. M.; Fortner, J. D.; Guo, W.; Lyon, D.; Boyd, A. M.; Ausman, K. D.; Tao, Y. J.; Sitharaman, B.; Wilson, L. J.; Hughes, J. B.; West, J. L.; Colvin, V. L. The differential cytotoxicity of water-soluble fullerenes. *Nano Lett.* **2004,** *4*, 1881-1887.
7. Cui, D. X.; Tian, F. R.; Ozkan, C. S.; Wang, M.; Gao, H. J. Effect of single wall carbon nanotubes on human HEK293 cells. *Toxicol. Lett.* **2005,** *155*, 73-85.
8. Fortner, J. D.; Lyon, D. Y.; Sayes, C. M.; Boyd, A. M.; Falkner, J. C.; Hotze, E. M.; Alemany, L. B.; Tao, Y. J.; Guo, W.; Ausman, K. D.; Colvin, V. L.; Hughes, J. B. C-60 in water: Nanocrystal formation and microbial response. *Environ. Sci. Technol.* **2005,** *39*, 4307-4316.

9. Lyon, D. Y.; Adams, L. K.; Falkner, J. C.; Alvarez, P. J. J. Antibacterial activity of fullerene water suspensions: Effects of preparation method and particle size. *Environ. Sci. Technol.* **2006,** *40*, 4360-4366.

10. Utsunomiya, S.; Jensen, K. A.; Keeler, G. J.; Ewing, R. C. Uraninite and fullerene in atmospheric particulates. *Environ. Sci. Technol.* **2002,** *36*, 4943-4947.

11. Murr, L. E.; Bang, J. J.; Esquivel, E. V.; Guerrero, P. A.; Lopez, A. Carbon nanotubes, nanocrystal forms, and complex nanoparticle aggregates in common fuel-gas combustion sources and the ambient air. *J. Nanoparticle Res.* **2004,** *6*, 241-251.

12. Bang, J. J.; Guerrero, P. A.; Lopez, D. A.; Murr, L. E.; Esquivel, E. V. Carbon nanotubes and other fullerene nanocrystals in domestic propane and natural gas combustion streams. *J. Nanosci. Nanotechnol.* **2004,** *4*, 716-718.

13. Chijiwa, T.; Arai, T.; Sugai, T.; Shinohara, H.; Kumazawa, M.; Takano, M.; Kawakami, S. Fullerenes found in the Permo-Triassic mass extinction period. *Geophys. Res. Lett.* **1999,** *26*, 767-770.

14. Heymann, D.; Chibante, L. P. F.; Brooks, R. R.; Wolbach, W. S.; Smalley, R. E. Fullerenes in the Cretaceous-Tertiary boundary layer. *Science* **1994,** *265*, 645-647.

15. Deguchi, S.; Alargova, R. G.; Tsujii, K. Stable dispersions of fullerenes, C-60 and C-70, in water. Preparation and characterization. *Langmuir* **2001,** *17*, 6013-6017.

16. Chen, K. L.; Elimelech, M. Influence of humic acid on the aggregation kinetics of fullerene (C60) nanoparticles in monovalent and divalent electrolyte solutions. *J. Colloid Interface Sci.* **2007,** *309*, 126-134.

17. Hyung, H.; Fortner, J. D.; Hughes, J. B.; Kim, J. H. Natural organic matter stabilizes carbon nanotubes in the aqueous phase. *Environ. Sci. Technol.* **2007,** *41*, 179-184.

18. Bahr, J. L.; Mickelson, E. T.; Bronikowski, M. J.; Smalley, R. E.; Tour, J. M. Dissolution of small diameter single-wall carbon nanotubes in organic solvents? *Chem. Commun.* **2001**, 193-194.

19. Huang, W. J.; Lin, Y.; Taylor, S.; Gaillard, J.; Rao, A. M.; Sun, Y. P. Sonication-assisted functionalization and solubilization of carbon nanotubes. *Nan. Lett.* **2002,** *2*, 231-234.

20. Matarredona, O.; Rhoads, H.; Li, Z. R.; Harwell, J. H.; Balzano, L.; Resasco, D. E. Dispersion of single-walled carbon nanotubes in aqueous solutions of the anionic surfactant NaDDBS. *J. Phys. Chem. B* **2003,** *107*, 13357-13367.

21. Hilding, J.; Grulke, E. A.; Zhang, Z. G.; Lockwood, F. Dispersion of carbon nanotubes in liquids. *J. Disper. Sci. Technol.* **2003,** *24*, 1-41.

22. Girifalco, L. A.; Hodak, M.; Lee, R. S. Carbon nanotubes, buckyballs, ropes, and a universal graphitic potential. *Phys. Rev. B* **2000,** *62*, 13104-13110.

23. Shen, K.; Curran, S.; Xu, H. F.; Rogelj, S.; Jiang, Y. B.; Dewald, J.; Pietrass, T. Single-walled carbon nanotube purification, pelletization, and surfactant-assisted dispersion: A combined TEM and resonant micro-Raman spectroscopy study. *J. Phys. Chem. B* **2005,** *109*, 4455-4463.

24. O'Connell, M. J.; Bachilo, S. M.; Huffman, C. B.; Moore, V. C.; Strano, M. S.; Haroz, E. H.; Rialon, K. L.; Boul, P. J.; Noon, W. H.; Kittrell, C.; Ma, J. P.; Hauge, R. H.; Weisman, R. B.; Smalley, R. E. Band gap fluorescence from individual single-walled carbon nanotubes. *Science* **2002,** *297*, 593-596.

25. Jiang, L. Q.; Gao, L.; Sun, J. Production of aqueous colloidal dispersions of carbon nanotubes. *J. Colloid Interface Sci* **2003,** *260*, 89-94.

26. Islam, M. F.; Rojas, E.; Bergey, D. M.; Johnson, A. T.; Yodh, A. G. High weight fraction surfactant solubilization of single-wall carbon nanotubes in water. *Nano Lett.* **2003,** *3*, 269-273.

27. Moore, V. C.; Strano, M. S.; Haroz, E. H.; Hauge, R. H.; Smalley, R. E.; Schmidt, J.; Talmon, Y. Individually suspended single-walled carbon nanotubes in various surfactants. *Nano Lett.* **2003,** *3*, 1379-1382.

28. Lecoanet, H. F.; Wiesner, M. R. Velocity effects on fullerene and oxide nanoparticle deposition in porous media. *Environ. Sci. Technol.* **2004,** *38*, 4377-4382.

29. Brant, J. A.; Labille, J.; Bottero, J. Y.; Wiesner, M. R. Characterizing the impact of preparation method on fullerene cluster structure and chemistry. *Langmuir* **2006,** *22*, 3878-3885.

30. Scrivens, W. A.; Tour, J. M.; Creek, K. E.; Pirisi, L. Synthesis of C-14-labeled C-60, its suspension in water, and its uptake by human Keratinocytes. *J. Am. Chem. Soc.* **1994,** *116*, 4517-4518.

31. Cataldo, F. A study on the thermal stability to 1000 degrees C of various carbon allotropes and carbonaceous matter both under nitrogen and in air. *Fullerenes Nanotubes Carbon Nanostruct.* **2002,** *10*, 293-311.

32. Ismail, I. M. K.; Rodgers, S. L. Comparisons between Fullerene and forms of well-known carbons. *Carbon* **1992,** *30*, 229-239.

33. Birch, M. E.; Cary, R. A. Elemental carbon-based method for monitoring occupational exposures to particulate diesel exhaust. *Aerosol Sci. Technol.* **1996,** *25*, 221-241.

CHAPTER 6
REMOVAL OF FULLERENES IN CONVENTIONAL WATER TREATMENT PROCESS

Abstract

Removal of water dispersed multi-walled carbon nanotubes (MWNT), C_{60} and hydroxylated C_{60} (fullerol) in conventional water treatment process was investigated from the jar test. Effect of water quality parameters such as NOM concentration and alkalinity as well as operational parameters such as pH and coagulant dose was evaluated. Experimental results suggested that these carbon nanomaterials would be generally well removed by conventional water treatment processes under typical operating conditions. Sweep floc appears to be dominant mechanism for fullerenes removal and feed alkalinity and coagulation pH were important factors to determine the removal efficiency. MWNT removal was found to be hindered by the presence of NOM, presumably due to the preferential interaction of metal coagulants with NOM and the enhanced stability of the fullerenes due to NOM adsorption.

Introduction

Fullerenes such as C_{60} and carbon nanotubes (CNT) have been at the center of recent prosperity in nanoscience and engineering. C_{60} consists of 60 carbon atoms arranged in 20 hexagons and 12 pentagons that form a perfectly symmetrical cage structure with ca. 1 nm in size [1]. CNT, on the other hand, consist of sheets of carbon atoms covalently bonded in hexagonal arrays that are seamlessly rolled into a hollow, cylindrical shape with both ends rounded through pentagon ring inclusions [2]. CNT present a highly flexible thread-like structure having an extremely high aspect ratio with the diameter ranging from 1 to 200 nm and length from 0.1 to 100 μm. CNT are categorized into two main species; single-walled carbon nanotube (SWNT) and multi-walled carbon nanotube (MWNT). The latter result from co-axial assembly of multiple SWNT. With increasing commercial interest due to their unique chemical and physical properties, production and use of fullerenes are expected to grow rapidly over the next decades [3-6].

However, concerns have risen due to recent findings that fullerenes can interact with living organisms causing toxic effects [4, 7-9]. For instance, SWNT showed higher pulmonary toxicity than quartz [10, 11], a well known industrial hazards, and C_{60} exhibited cytotoxicity inhibiting humane and microbial cell growth [7, 12]. Considering recent studies that they might form water-stable suspension upon release to aquatic environment [13, 14], human exposure to these materials via water consumption will be strongly influenced by the behavior of these carbon based nanomaterials in drinking water treatment systems, the first line of defense against human exposure from the drinking water pathways.

The conventional water treatment process consists of a series of physicochemical processes, *i.e.*, coagulation, flocculation, sedimentation, filtration and disinfection, to remove contaminants and inactivate pathogens in the source water. Coagulation and flocculation processes destabilize particulate matter to form flocs that can settle in the subsequent sedimentation process. Several mechanisms for the destabilization of the particles during the coagulation process have been suggested including electrical double layer (EDL) compression, charge neutralization, interparticle bridging, and sweep floc [15]. Among these, charge neutralization and sweep floc mechanisms are known to be the most relevant mechanisms of the particle destabilization during drinking water treatment [15]. Colloidal particles in the natural water are stabilized mainly due to the repulsion between their negatively charged surfaces. However, upon the addition of the positively charged coagulants, the particles are destabilized due to the neutralization of the surface charge and subsequent reduction of the charge repulsion. When a sufficient amount of metal salts, which would exceed the solubility of metal ions, are added into the water, amorphous metal hydroxides would form. These metal hydroxide precipitates can destabilize the particles in the water by the entrapment (*i.e.* sweep floc). The sweep floc is the dominant mechanism in most of the coagulation process utilizing aluminum sulfate and ferric chloride. The dosage of aluminum salt or iron salt required for sweep floc typically does not depend on the types of particulates, but largely depends on the water quality parameters such as pH and alkalinity [16]. In the United States, aluminum sulfate (alum) is the most widely used coagulant [16]. For the alum coagulation, charge neutralization is dominant coagulation mechanism at low pH values and low alum

dosages, while the sweep floc dominates at high pH values and high alum dosages [17]. In the current water treatment practice, alum dosages and pH generally range from 10 to 150 mg/L and 5 to 8, respectively, depending on raw water quality [16].

In this study, jar tests were performed using MWNT, C_{60} and hydroxylated C_{60} (fullerol) as model fullerene compounds to investigate the behavior of water-stable fullerene suspensions in conventional drinking water treatment process. Specifically, the effects of water quality parameters such as natural organic matter (NOM) concentration and alkalinity of feed solution as well as operation parameters such as pH and coagulant dose on the removal of these carbon nanomaterials were investigated.

Experimental

Materials. MWNT (10-20 nm diameter × 10-30 μm length) with over 95% purity was obtained from the Cheap Tubes Inc. (Brattleboro, VT). C_{60} (99.9%) and fullerol ($C_{60}(OH)_{22\text{-}24}$, polyhydroxyfullerene, 99%) were purchased from MER corporation (Phoenix, AZ). Suwannee River natural organic matter (SRNOM) was obtained from the International Humic Substances Society (IHSS) (St. Paul, MN).

Solution Preparation. SRNOM stock solution was prepared by mixing a known amount of SRNOM with deionized (DI) water for 24 hours. Dissolution of SRNOM was facilitated by increasing solution pH to 7 using NaOH. Aggregate forms of C_{60} which are stable in the aqueous phase (termed as nC_{60}) were prepared by the modification of solvent exchange protocol by Lyon et al. [8]. Firstly, powdered C_{60} was dissolved in toluene at

concentration of 200 mg/L. After adding 200 mL of DI water into 50 mL of pink hued C_{60} in toluene solution, the two phase solution was mildly sonicated using a Bransonic 5510R ultrasonicator (Danbury, CT) at output power of 135 W. After overnight sonication, the aqueous phase changed to yellow color due to the interphase transport of C_{60} from toluene and subsequent formation of nC_{60}. The aqueous nC_{60} suspension was separated from toluene phase using a separation funnel and purged with high purity nitrogen gas (99.999% purity, NI UHP300, Airgas Inc., Randor, PA) for 3 hours to remove residual toluene. MWNT stock was produced by adding 10 mg of dry phase MWNT in 100 mL of 50 mg C/L SRNOM solution and sonicating the solution with a Bransonic 5510R ultrasonicator at 135 W for 30 min. After 2 days of quiescent settling, the solution was filtered with a Whatman 541 filter (20-25 μm nominal pore size, Florham Park, NJ) to remove MWNT not dispersed in SRNOM solution (*i.e.* MWNT aggregates). 50 mg/L of fullerol stock solution was produced by simple mixing with DI for 24 hours. These nC_{60}, MWNT, and fullerol stock solutions were diluted with DI and/or mixed with SRNOM stock solution for the further experiments.

Jar Test. Jar tests were performed Phipps and Bird Model 7790-400 Jar Tester using 250 mL beakers containing 150 mL of test solutions (Richmond, VA). Alkalinity and pH of each solution was adjusted using 0.1 M $NaHCO_3$ and 0.1 N NaOH and 0.1 N H_2SO_4. After adding an aliquot of 10 g/L alum ($Al_2(SO_4)_3 \cdot 18\ H_2O$) (Aldrich, Milwaukee, WI) stock solution, the mixture was agitated at a paddle speed of 200 rpm for 2 min, followed by 30 min of slow mixing at 25 rpm. After 1 hr of quiescent settling, the supernatant was carefully taken at the depth of approximately 10 cm from the surface using syringe for

further analyses. After the sampling, pH was measured and recorded for the analysis of experimental results. Filterability of flocs formed from the jar test was estimated by filtering the supernatant with a Whatman Grade No. 40 Quantitative Filter (Florham, NJ).

Analysis. Concentration of MWNT suspended in the aqueous phase was determined by a visible light absorbance at 800 nm (VIS_{800}) (8453 UV-Vis Spectroscopy System, Agilent, Palo Alto, CA) after calibration using a Thermal Optical Transmittance (TOT) Analyzer (Sunset Laboratory, Tigard, OR). In our previous study, the TOT analysis was proven to be accurate to measure the MWNT concentration in an NOM background solution [13]. Concentrations of NOM and fullerol (in DI water) were measured by a Total Organic Carbon Analyzer (TOC-Vw, Shimadzu, Columbia, MD). Concentration of C_{60} in DI was determined by an Agilent 8453 UV-vis Spectroscopy System (Palo Alto, CA) at characteristic absorption at 346 nm. The concentration of C_{60} in toluene was analyzed using a 1100 series HPLC system (Agilent) equipped with a Zorbax 4.6×150 mm XDB-C8 column (Agilent) and a Diode-Array Detector (DAD) at 333 nm wavelength. The HPLC was operated using 40% acetonitrile and 60% toluene as an eluent at the flow rate of 1 mL/min and the injection volume of 0.1 mL. The retention time of C_{60} was 3.15 min in this analytical condition. The method detection limit of HPLC analysis was 0.15 mg/L and all the extraction experiments were duplicated. Zeta potential of nC_{60} in aqueous suspension was analyzed by a Zeta Plus Zeta Potential Analyzer (Brookhaven Instruments Co., Holtsville, NY).

Results and Discussion

MWNT Removal. Experimental results shown in Figure 6.1(a) suggest that MWNT would be removed very well by coagulation/flocculation/sedimentation processes. At the MWNT concentration of 1 mg/L in the feed solution with alkalinity of 100 mg/L as $CaCO_3$ and SRNOM concentration of 2.5 mg C/L, up to 99.9 % removal of MWNT was obtained. At the lowest coagulant dosage of 10 mg/L, only *ca*. 60 % removal of MWNT was obtained around pH 6. However, when the coagulant dosage is higher than 25 mg/L, the removal of MWNT increases and, especially in the pH range of 6 to 7.5, it reaches more than 90% regardless of the coagulant dosage. When the coagulant dosage was 100 mg/L, the MWNT removal was more than 90% in the entire pH range of the investigation and was more than 99.9% in the pH range of 6 to 8. Amirtharajah and Mills [18] developed coagulation diagram (pC-pH diagram) from the experimental results of the previous studies. The removal of MWNT assessed in our study appears to match well with sweep coagulation zone of the coagulation diagram, suggesting the sweep coagulation might be the dominant mechanism of MWNT removal. Considering this experimental result and the fact that a typical dosage of alum in practice ranges from 10 to 150 mg/L [16], MWNT are expected to be effectively removed by the conventional water treatment process.

The filterability of MWNT flocs in the supernatant was estimated by filtering the supernatant with a Whatman Grade 40 Quantitative Filter. Whatman Grade 40 filter has been used for the simulation of a rapid granular media filtration in the conventional water

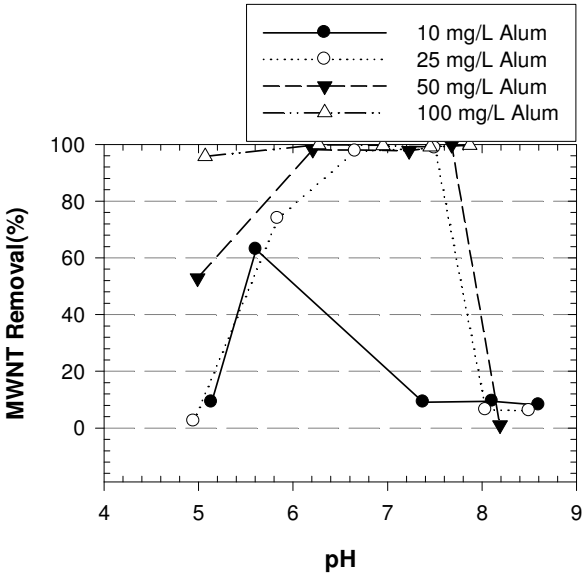

(a)

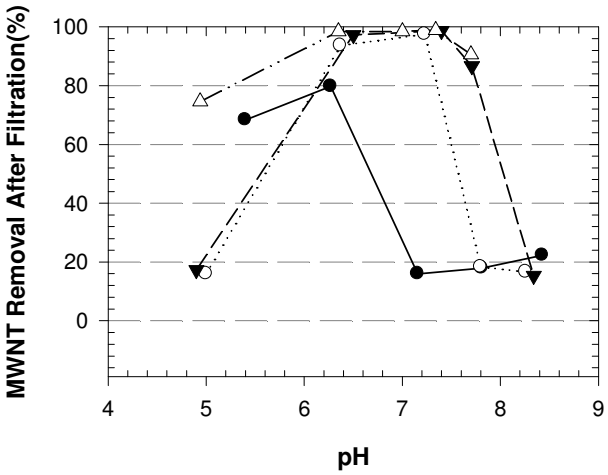

(b)

Figure 6.1. Jar test result with MWNT: (a) Removal of MWNT by coagulation, (b) Removal of MWNT coagulation/sedimentation/filtration, and (c) Removal of NOM (Initial MWNT concentration = 1 mg/L, Alkalinity = 100 mg/L as $CaCO_3$, SRNOM concentration = 2.5 mg/L).

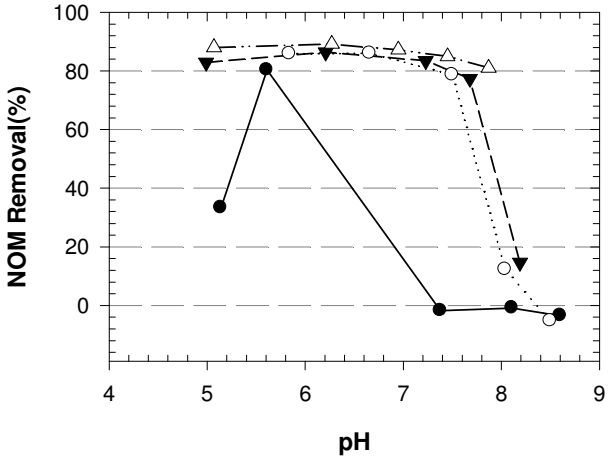

(c)

Figure 6.1 continued.

treatment process [16]. It evaluates the filterability of the flocs suspended in the effluent from sedimentation process. The comparison of Figure 6.1(a) and Figure 6.1(b) revealed that, when the MWNT removal in the coagulation step was less than 60%, MWNT removal further increased up to *ca*. 20% by filtration. However, when the removal in the coagulation step was higher than 80%, additional removal from the filtration was minimal. This result suggests when MWNT removal is low during the coagulation process additional removal might be achievable by the rapid filtration. During the coagulation of MWNT, SRNOM in the solution was removed as well (Figure 6.1(c)). When alum dosages were higher than 25 mg/L, more than 80% removal of SRNOM was obtained in the pH range of 5 to 8. This level of dissolved organic carbon (DOC) removal in the presence of MWNT is considerably higher compared to DOC removal by coagulation reported in the literature. For example, with 16 different source waters with wide range of NOM and alkalinity, Bell-Ajy et al. [19] reported less than 60% of DOC removal from the enhanced coagulation. White et al. [20] reported that, among 31 natural waters from a variety of sources, most of the waters showed less than 60% of NOM (DOC) removal from the enhanced coagulation. It is possible that MWNT might participate in the coagulation process as an adsorbent and assist further removal of NOM. It is also known that SRNOM has higher molecular weight compare to NOM from typical natural water and therefore it might yield a better removal by coagulation. However, the exact mechanism for the enhanced removal of NOM in the presence of MWNT is not clear and further investigation might be necessary.

The removal of MWNT was also affected by the alkalinity of feed water. From the discussion in the previous paragraph, it is suggested that sweep floc would be a dominant mechanism for MWNT removal. In the sweep floc mechanism, the formation of insoluble amorphous alum hydroxide, which would entrap and/or adsorb particles and settle down, is a key step to obtain high coagulation efficiency. Alkalinity plays an important role on the formation of aluminum hydroxide precipitates and, if sufficient alkalinity does not exist, soluble aluminum can be formed which would reduce the efficiency of the particle removal [16]. Experimental results from this study are consistent with this argument and, for all pH and alum dosages, removal of MWNT generally increases, as the alkalinity of feed water increases (Figure 6.1(a) and 6.2).

NOM dramatically changed the removal of MWNT during the coagulation process. As the NOM concentration in the solution increased, less MWNT was removed by the coagulation/flocculation/sedimentation processes (Figure 6.3). For example, at the SRNOM concentration of 2.5 mg C/L and the alum dosage of 25 mg/L, more than 80% removal of MWNT is achieved in the pH range of 6 to 7.5. However, as the SRNOM concentration increased, the removal of MWNT decreased for all pH ranges. When the SRNOM concentration in the solution was as high as 10 mg C/L, virtually no MWNT was removed. This result might be due to the preferential interaction between NOM and the coagulant. For instance, O'Melia et al. [21] suggested that metal coagulants preferentially bound with NOM and the coagulant dosage would be mostly determined by the NOM-metal ion interaction rather than particles (latex)-metal ions interaction. Hence, NOM that is not bound to MWNT could dominantly consume metal ions upon the

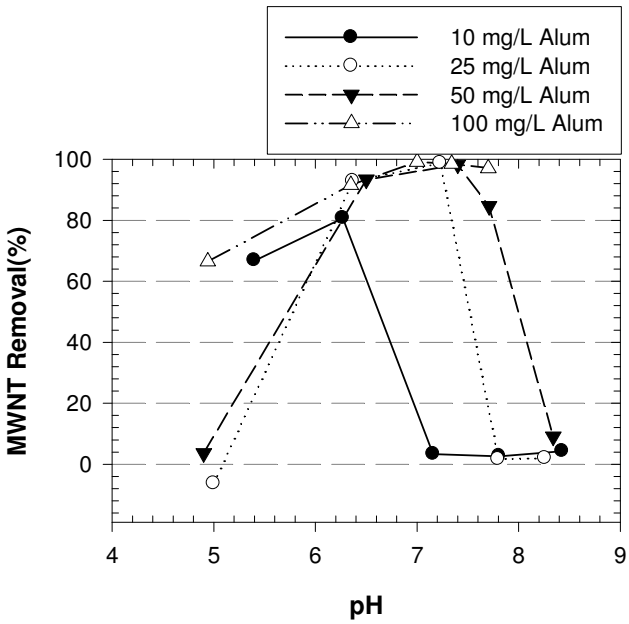

Figure 6.2. Removal of MWNT by coagulation at 50 mg/L as $CaCO_3$ alkalinity (Initial MWNT concentration = 1 mg/L, SRNOM concentration = 2.5 mg/L).

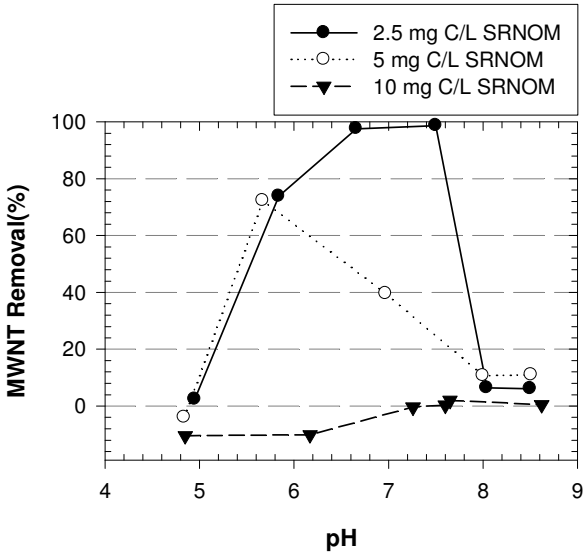

Figure 6.3. Effect of NOM concentration on MWNT removal (Initial MWNT concentration = 1 mg/L, Alkalinity = 100 mg/L as CaCO3, Alum dose = 25 mg/L).

addition of the coagulants, limiting the opportunity to destabilize MWNT-NOM complexes. Furthermore, our previous study [22] shows that the adsorption of NOM provides MWNT with thermodynamically more favorable surfaces as well as steric and electrostatic stabilization and NOM adsorption to MWNT would be enhanced as the concentration of NOM in the aqueous phase increases. The enhanced stability of MWNT due to the NOM adsorption might hinder the removal of MWNT by the coagulation.

Measurement of C_{60} Concentration in NOM Background Solution. nC_{60}, stable aggregates of C_{60} in aqueous phase, exhibits characteristic peaks from UV-vis spectroscopy and concentration of C_{60} in DI can be measured by UV absorbance at 346 nm [23]. However, the presence of NOM in the aqueous phase interferes with the measurement of C_{60} concentration by UV absorbance and a method to measure C_{60} concentration in the NOM background need to be developed. In the previous studies [24-26], it was shown that the addition of salts, acids, and/or oxidants could destabilize aqueous nC_{60} suspension and C_{60} could be efficiently extracted to a toluene phase by vigorous mixing. The extraction kinetics of C_{60} in the presence of NOM with three representative extraction agents (*i.e.*, salt (KCl), mild oxidant ($Mg(ClO_4)$), and acid (glacial acetic acid (GAA) (CH_3COOH))) are shown in Figure 6.4. In these experiments, the aqueous phase was prepared by spiking 5 mg/L of nC_{60} in 5 mg C/L SRNOM solution and adding 10 mM of each extraction agent. An aliquot of 2.5 mL aqueous phase and 2.5 mL toluene were added to a 12 mL test tube. The tube was agitated for various hours in a rotary shaker at 200 rpm after capping the test tube. After providing 1 hr for the separation of two layers, 0.5 mL of toluene phase was carefully taken for the HPLC

analysis. At 10 mM of extraction agent concentration, $Mg(ClO_4)_2$ showed the fastest extraction kinetics with recovery reaching 100% in less than two hours. KCl also exhibited relatively rapid extraction kinetics, but showed lower recovery (*ca.* 10%). GAA showed the slowest extraction kinetics among three extraction agents. Effect of the concentration of the extraction agents on C_{60} recovery after 6 hr of agitation is shown in Figure 6.5. At low concentration, $Mg(ClO_4)_2$ showed *ca.* 100% of C_{60} recovery, but the C_{60} recovery gradually decreased to less than 30% as the concentration of $Mg(ClO_4)_2$ increased to 100 mM. At high concentration of $Mg(ClO_4)_2$, the formation of emulsion, which is known to form from the presence of large amount of proteins, lipids, and surfactants found in the natural samples [25], at the interface was visually observed. The emulsion might hinder the transport of C_{60} from the aqueous phase to the toluene phase. In contrast to $Mg(ClO_4)_2$, C_{60} recovery increased as concentrations of KCl and GAA increased and almost 100% recovery could be obtained when KCl and GAA concentrations are more than 50 mM. For KCl and GAA, no emulsion formation was observed. The presence of coagulant further aggravated the emulsion formation for $Mg(ClO_4)_2$. When 25 mg/L alum was added to the solution, the C_{60} recovery decreased to 20% even with a low concentration of $Mg(ClO_4)_2$ (10 mM) (Figure 6.6). However, the recovery by GAA was not influenced by the presence of alum, although a slight decrease was observed for the highest GAA dose. In the previous study, GAA could suppress emulsion formation from the usage of $Mg(ClO_4)_2$ during C_{60} extraction [25]. However, the mixture of GAA and $Mg(ClO_4)_2$ still shows the reduced recovery suggesting limited role of GAA for enhancing the extraction efficiency in the presence of NOM and alum. The experimental result suggests that in the presence of NOM and/or coagulant, acids or

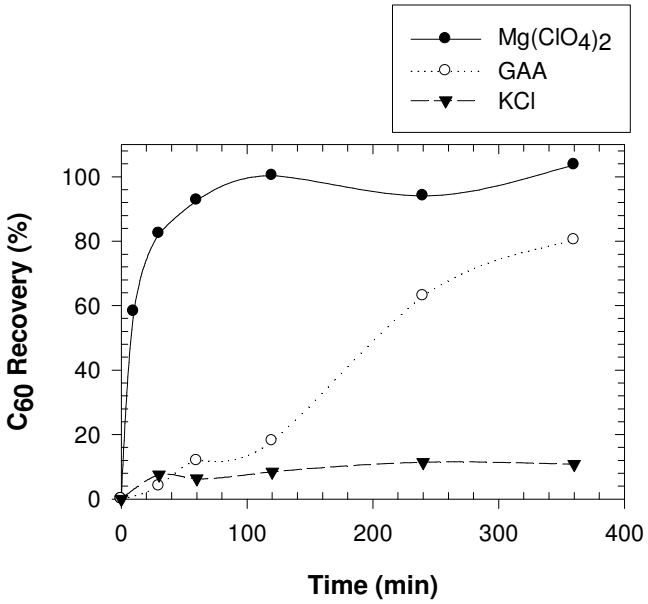

Figure 6.4. Extraction kinetics of C_{60} from different extraction agents (Extraction agent concentration = 10 mM, Initial C60 concentration = 5 mg/L, NOM concentration = 5 mg C/L).

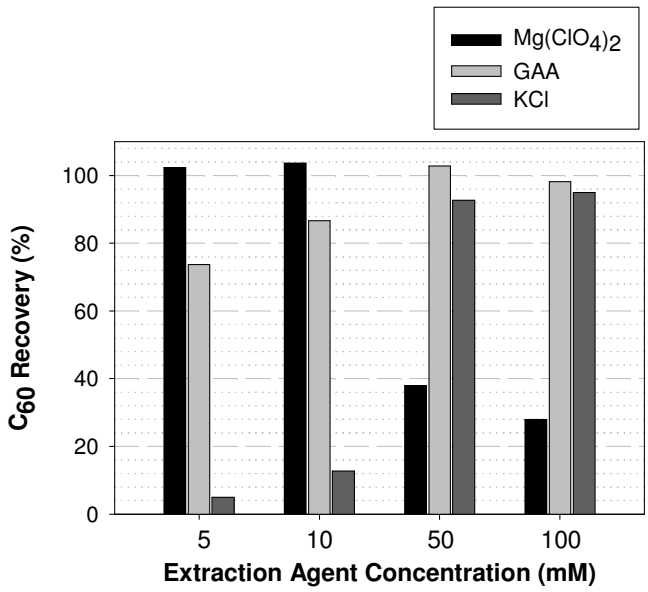

Figure 6.5. Effect of the extraction agent concentration on the C_{60} recovery (without alum) (Extraction time = 6 hr, Initial C_{60} concentration = 5 mg/L, NOM concentration = 5 mg C/L).

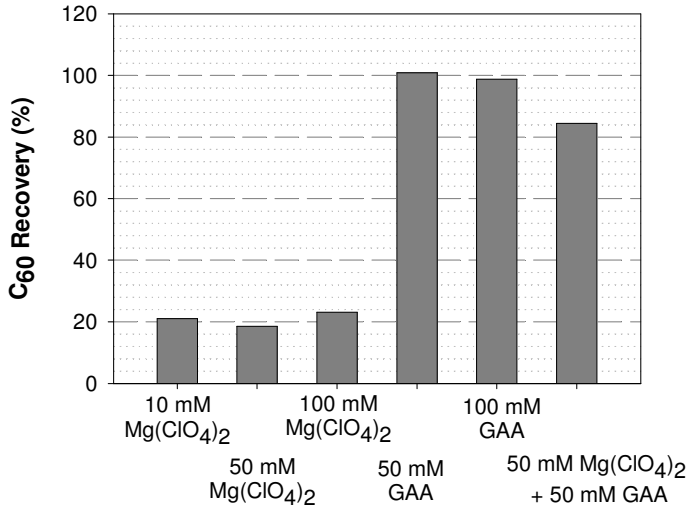

Figure 6.6. Effect of the extraction agent concentration on the C_{60} recovery (with alum) (Extraction time = 6 hr, Initial C_{60} concentration = 5 mg/L, NOM concentration = 5 mg C/L, Alum concentration = 25 mg/L).

ionic salts might be a better choice for the extraction of C_{60}, while mild oxidants such as $Mg(ClO_4)_2$, which has been used to destabilize nC_{60} in organic free water [23], might not be a good extraction agent due to the formation of emulsion.

C_{60} *Removal.* Jar test results with 1 mg/L C_{60} solution suggested that the removal of C_{60} was largely dependent on water quality parameters and operating conditions. When the alkalinity of feed water was 100 mg/L as $CaCO_3$, C_{60} was removed relatively well at all pH and alum dosages. More than 60% of C_{60} removal was achieved for all coagulant dosages when pH ranged 6 to 8 (Figure 6.7(a)). In particular, when the alum dosage was 100 mg/L, more than 60% of the C_{60} removal was achieved at all pH ranges and the removal reached up to 97% at pH between 7 and 8. However, at lower alkalinity of feed water (50 mg/L as $CaCO_3$), C_{60} was removed in the limited range of pH (pH 7 to 8) when alum dose was less than 75 mg/L (Figure 6.7(b)). When alum dose was 100 mg/L, more efficient C_{60} removal was observed even at low alkalinity and especially more than 60 % removal was obtained in the pH range of 6 to 8. The removal of C_{60} assessed in our study matched well with sweep coagulation zone of the coagulation diagram developed by Amirtharajah and Mills [18] and the sweep coagulation is also considered to be the dominant mechanism of C_{60} removal.

The filterability of C_{60} flocs suspended in the supernatant after sedimentation is presented in Figure 6.7(c). Generally *ca*. 20% increase in C_{60} removal was observed after filtration when C_{60} removal by coagulation was less than 20%. However, when C_{60}

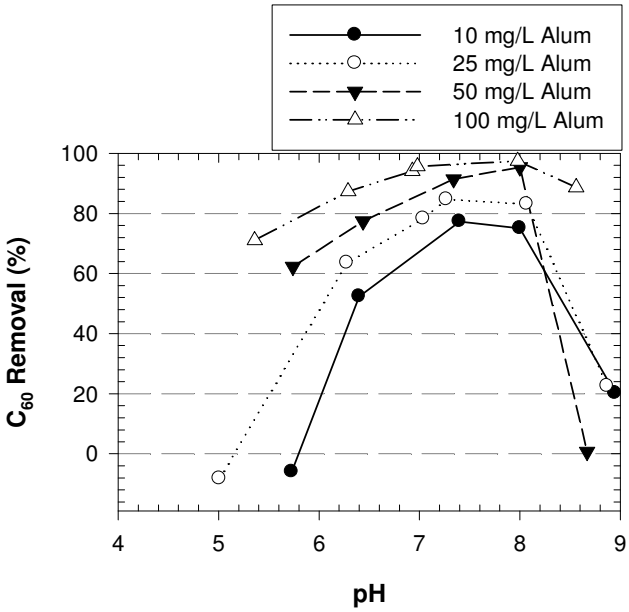

(a)

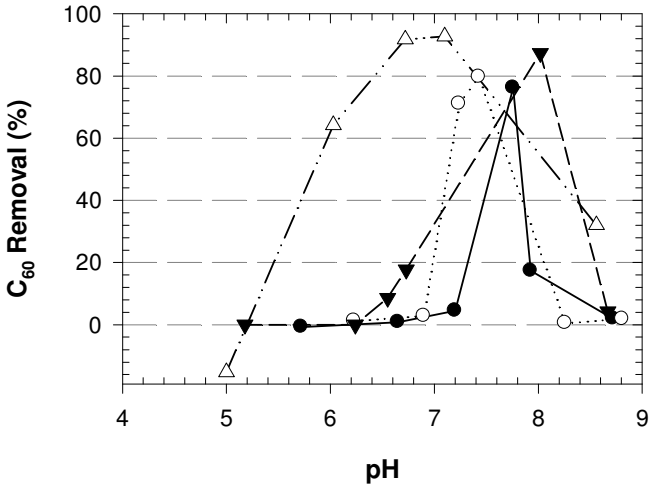

(b)

Figure 6.7. Jar test result with 1 mg/L C_{60}: (a) Removal of C_{60} at alkalinity of 100 mg/L as $CaCO_3$, (b) Removal of C_{60} at alkalinity of 50 mg/L as $CaCO_3$, and (c) Removal of C_{60} after coagulation/sedimentation/filtration at alkalinity of 50 mg/L as $CaCO_3$.

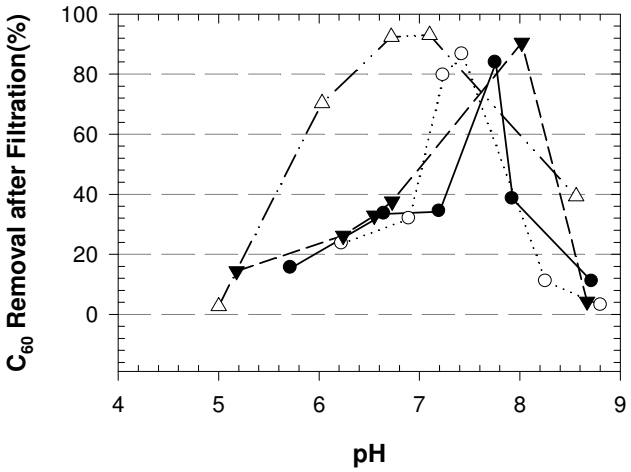

(c)

Figure 6.7 continued.

removal by coagulation was already high (more that 60%), additional removal from the filtration was minimal.

NOM appeared to hinder the removal of C_{60} during the coagulation. In the absence of NOM, C_{60} removal was more than 60% at pH 5 to 8 (alkalinity = 100 mg/L as $CaCO_3$ and alum dose = 25 mg/L) (Figure 6.8). However, as SRNOM concentration increased, the range of pH for more than 80% of C_{60} removal became narrower. When SRNOM concentration was 10 mg C/L, C_{60} removal higher than 80% was obtained only when pH ranges 5 to 6. This result (*i.e.*, decreased removal of C_{60} with increased NOM concentration) was similar to the experimental result from MWNT and the same explanation would be applicab

le; preferential binding between NOM and metal coagulants and enhanced stability of C_{60} in the presence of NOM. The enhanced stability of C_{60} in the presence of NOM is further investigated with zeta potential measurement of C_{60} suspension under different NOM concentrations. Figure 6.9 shows zeta potential of C_{60} suspension at different pH and SRNOM concentration. As the SRNOM concentration increased, the zeta potential of C_{60} shifted toward more negative values implying the enhanced stability of nC_{60} particles.

The removal of representative fullerol species ($C_{60}(OH)_{24}$), derivatized and molecularly soluble form of C_{60}, is investigated for the comparison purpose. The fullerol is also known to be formed from the ozonation of C_{60} during the water treatment process [14]. Compared to C_{60}, C_{60} derivatized with hydroxyl groups was more difficult to

remove by the coagulation (Figure 6.10) at the same water quality condition. When the alum dosage was less than 25 mg/L, more than 80% of fullerol was removed only in a very narrow pH range of 7 to 8. When alum dose was 100 mg/L and pH 5, the fullerol removal is *ca*. 45% and increases up to 98% (pH 7.5) as pH increased. Even though C_{60} and fullerol presented similar maximum removal by the jar test (*ca*. 97%), fullerol was removed in a much narrower pH range and the removal of fullerol was consistently lower than that of C_{60} at the same pH and alum dosage. In contrast to C_{60} which exist as aggregates (nC_{60}) in water, fullerol will suspend as molecular form. In addition, the derivatization of hydroxyl groups on C_{60} might provide more hydrophilic surface which does not aggregate easily during the coagulation process. This result implies that derivatization of fullerenes which has been applied to enhance dispersion of fullerenes in aqueous phase might reduce removal efficiency of fullerenes in water treatment process. The maximum removal of C_{60} and fullerol is relatively lower than that of MWNT (99.9%). Better removal of MWNT might be originated from the larger particle size and uncharged surface of MWNT, which make MWNT favorable for aggregation during the coagulation.

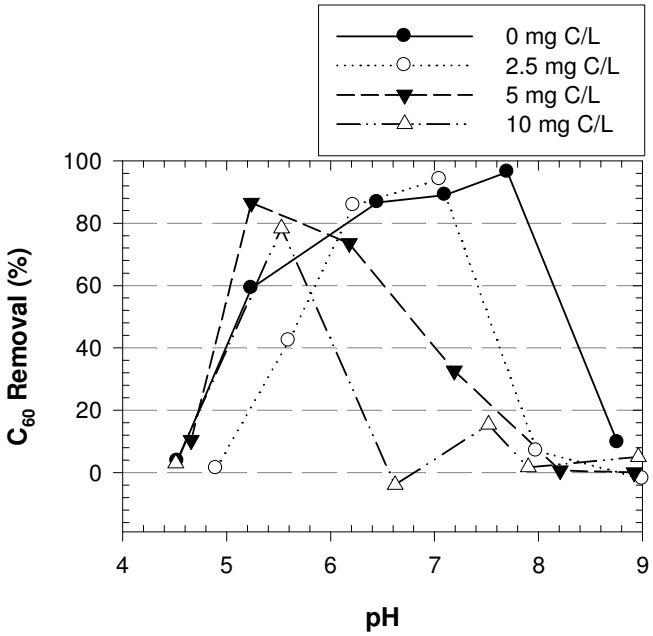

Figure 6.8. Effect of NOM concentration on C_{60} removal (Initial C_{60} concentration = 5 mg/L, Alkalinity = 100 mg/L as $CaCO_3$, Alum dose = 25 mg/L).

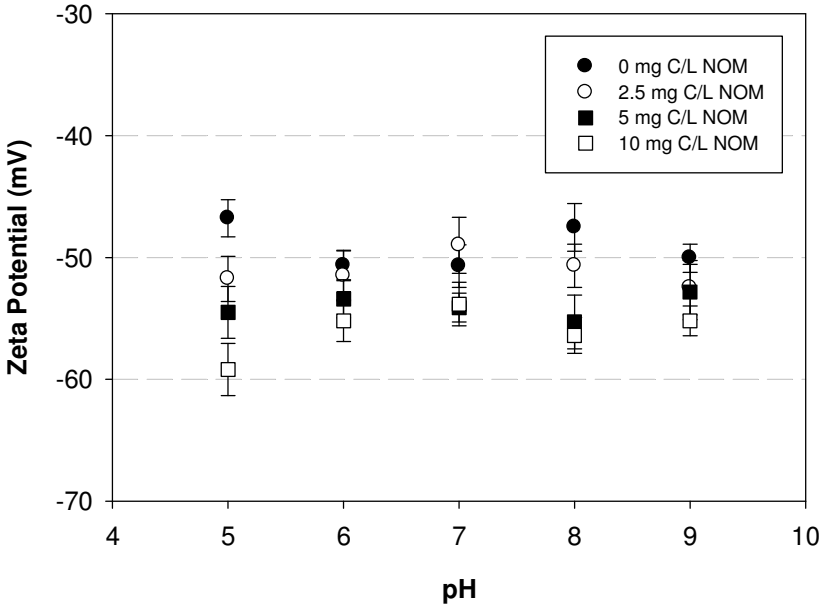

Figure 6.9. Zeta potential of C_{60} with different background SRNOM concentrations.

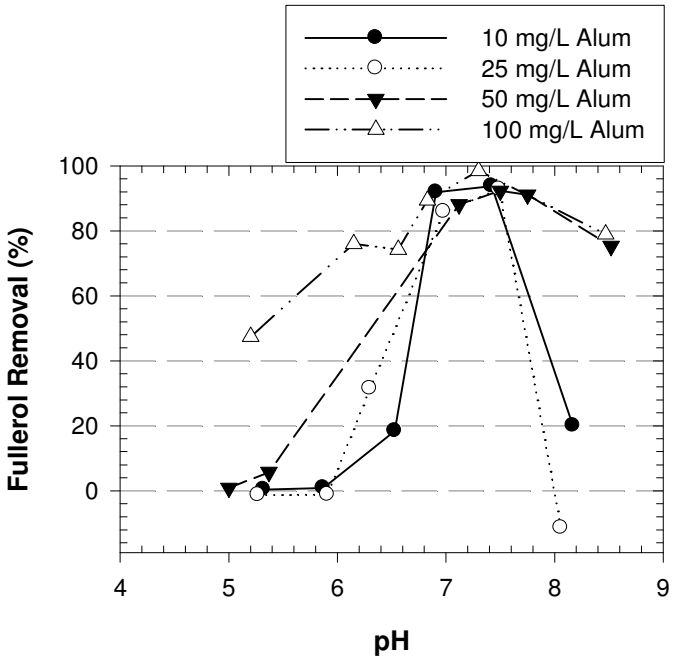

Figure 6.10. Removal of fullerol by coagulation (Initial fullerol concentration = 1 mg/L, Alkalinity = 100 mg/L as $CaCO_3$).

The experimental results showed that, in the scenario of the fullerene spillage, the fullerenes would be well removed by the conventional water treatment process (coagulation – flocculation – sedimentation – filtration) in the general operation ranges of pH and alum dosage (pH 5.5 to 7.7 and alum dosage of 10 to 150 mg/L [16]). However, the removal of these carbon nanomaterials is hindered by the presence of NOM presumably due to the preferential interaction between NOM and metal coagulants and the enhanced stability of the fullerenes from the NOM adsorption. Water quality parameters such as pH and alkalinity are also important factors for the removal of fullerenes and, by adjusting those parameters, higher removal of the novel carbon nanomaterials might be achievable. The removal efficiency of fullerenes would be also affected by other water quality parameters not investigated in this study such as particulate matters and ionic contents. For instance, the existence of particulate matters can affect the removal of fullerenes. The removal of fullerenes in the coagulation process follows the sweep floc mechanism, in which particle removal efficiency does not depend on the types of the particles, but the total amount of the particulate matters [16]. Hence, when the same amount of fullerenes is present, the existence of additional particulate matters would reduce the removal efficiency of fullerenes.

Acknowledgements

This study was supported by the United States Environmental Protection Agency (USEPA) STAR Grant #D832526.

Literature Cited

1. Kroto, H. W.; Heath, J. R.; Obrien, S. C.; Curl, R. F.; Smalley, R. E., C-60 - Buckminsterfullerene. *Nature* **1985,** *318*, (6042), 162-163.
2. Iijima, S., Helical Microtubules of Graphitic Carbon. *Nature* **1991,** *354*, (6348), 56-58.
3. Ball, P., Roll up for the revolution. *Nature* **2001,** *414*, (6860), 142-144.
4. Colvin, V. L., The potential environmental impact of engineered nanomaterials *Nature Biotechnology* **2004,** *22*, (6), 760-760.
5. Wiesner, M. R.; Lowry, G. V.; Alvarez, P.; Dionysiou, D.; Biswas, P., Assessing the risks of manufactured nanomaterials. *Environmental Science & Technology* **2006,** *40*, (14), 4336-4345.
6. Tremblay, J. F., Mitsubishi chemical aims at breakthrough. *Chemical & Engineering News* **2002,** *80*, (49), 16-17.
7. Cui, D. X.; Tian, F. R.; Ozkan, C. S.; Wang, M.; Gao, H. J., Effect of single wall carbon nanotubes on human HEK293 cells. *Toxicology Letters* **2005,** *155*, (1), 73-85.
8. Lyon, D. Y.; Adams, L. K.; Falkner, J. C.; Alvarez, P. J. J., Antibacterial activity of fullerene water suspensions: Effects of preparation method and particle size. *Environmental Science & Technology* **2006,** *40*, (14), 4360-4366.
9. Porter, A. E.; Gass, M.; Muller, K.; Skepper, J. N.; Midgley, P. A.; Welland, M., Direct imaging of single-walled carbon nanotubes in cells. *Nature Nanotechnology* **2007,** *2*, (11), 713-717.

10. Lam, C. W.; James, J. T.; McCluskey, R.; Hunter, R. L., Pulmonary toxicity of single-wall carbon nanotubes in mice 7 and 90 days after intratracheal instillation. *Toxicological Sciences* **2004,** *77*, (1), 126-134.

11. Warheit, D. B.; Laurence, B. R.; Reed, K. L.; Roach, D. H.; Reynolds, G. A.; Webb, T. R., Comparative pulmonary toxicity assessment of single-wall carbon nanotubes in rats. *Toxicological Sciences* **2004,** *77*, (1), 117-25.

12. Sayes, C. M.; Fortner, J. D.; Guo, W.; Lyon, D.; Boyd, A. M.; Ausman, K. D.; Tao, Y. J.; Sitharaman, B.; Wilson, L. J.; Hughes, J. B.; West, J. L.; Colvin, V. L., The differential cytotoxicity of water-soluble fullerenes. *Nano Letters* **2004,** *4*, (10), 1881-1887.

13. Hyung, H.; Fortner, J. D.; Hughes, J. B.; Kim, J. H., Natural organic matter stabilizes carbon nanotubes in the aqueous phase. *Environmental Science & Technology* **2007,** *41*, (1), 179-184.

14. Fortner, J. D.; Kim, D. I.; Boyd, A. M.; Falkner, J. C.; Moran, S.; Colvin, V. L.; Hughes, J. B.; Kim, J. H., Reaction of water stable C60 aggregates with ozone. *Environmental Science & Technology* **2007,** *41*, (21), 7497-7502.

15. Letterman, R. D., *Water quality and treatment: a handbook of community water supplies* McGraw Hill: New York, 1999.

16. Crittenden, J. C., *Water Treatment Principles and Design*. John Wiley and Sons: New Jersey, 2005.

17. Edwards, G. A.; Amirtharajah, A., Removing color caused by humic acids. *Journal American Water Works Association* **1985,** *77*, (3), 50-57.

18. Amirtharajah, A.; Mills, K. M., Rapid-mix design for mechanisms of alum coagulation. *Journal American Water Works Association* **1982,** *74*, (4), 210-216.

19. Bell-Ajy, K.; Abbaszadegan, M.; Ibrahim, E.; Verges, D.; LeChevallier, M., Conventional and optimized coagulation for NOM removal. *Journal American Water Works Association* **2000,** *92*, (10), 44-58.

20. White, M. C.; Thompson, J. D.; Harrington, G. W.; Singer, P. C., Evaluating criteria for enhanced coagulation compliance. *Journal American Water Works Association* **1997,** *89*, (5), 64-77.

21. O'Melia, C. R.; Becker, W. C.; Au, K. K., Removal of humic substances by coagulation. *Water Science and Technology* **1999,** *40*, (9), 47-54.

22. Hyung, H.; Kim, J. H., Natural organic matter (NOM) adsorption to multi-walled carbon nanotubes: Effect of NOM characteristics and water quality parameters. *Environmental Science & Technology* **2008,** *in press*.

23. Fortner, J. D.; Lyon, D. Y.; Sayes, C. M.; Boyd, A. M.; Falkner, J. C.; Hotze, E. M.; Alemany, L. B.; Tao, Y. J.; Guo, W.; Ausman, K. D.; Colvin, V. L.; Hughes, J. B., C-60 in water: Nanocrystal formation and microbial response. *Environmental Science & Technology* **2005,** *39*, (11), 4307-4316.

24. Santa, T.; Yoshioka, D.; Homma, H.; Imai, K.; Satoh, M.; Takayanagi, I., High-performance liquid-chromatography of fullerene (C60) in plasma using ultraviolet and mass spectrometric detection. *Biological & Pharmaceutical Bulletin* **1995,** *18*, (9), 1171-1174.

25. Xia, X.-R.; Monteiro-Riviere, N. A.; Riviere, J. E., Trace analysis of fullerenes in biological samples by simplified liquid-liquid extraction and high-performance liquid chromatography. *Journal of Chromatography A* **2006,** *1129*, (2), 216-222.

26. Isaacson, C. W.; Usenko, C. Y.; Tanguay, R. L.; Field, J. A., Quantification of fullerenes by LC/ESI-MS and its application to in vivo toxicity assays. *Analytical Chemistry* **2007,** *79*, (23), 9091-9097.

27. Chen, K. L.; Elimelech, M., Influence of humic acid on the aggregation kinetics of fullerene (C60) nanoparticles in monovalent and divalent electrolyte solutions. *Journal of Colloid and Interface Science* **2007,** *309*, (1), 126-134.

CHAPTER 7

CONCLUSION

The following are the primary conclusions that are drawn from this dissertation:

The stability of fullerenes in natural environments would be largely affected by their interaction with natural organic matter (NOM). NOM adsorbed onto multi-walled carbon nanotubes (MWNT) can produce a stable and individual dispersion of MWNT in the aqueous phase. Thermal optical transmittance (TOT) analysis was proven to be an effective method to measure MWNT concentration from an NOM background.

NOM adsorption to MWNT was largely influenced by NOM characteristics. NOM adsorption to MWNT could be reasonably well represented by the adsorbent dose normalized Freundlich isotherm model, which has frequently used to describe aqueous phase adsorption phenomena. Among various carbon groups in NOM, the aromatic group content exhibits a reasonable relationship with the adsorption capacity. This result suggests the importance of π-π interactions during NOM adsorption to MWNT. Water quality parameters such as pH and ionic strength also play an important role to NOM adsorption to MWNT.

The amount of MWNT stabilized in the aqueous phase was dependent on the amount of NOM adsorbed onto MWNT as well as water quality parameters such as pH and ionic strength. This result implies that the dispersion of MWNT into the natural

environment would be largely affected by the characteristics of NOM and the water quality parameters.

Experimental results with representative fullerenes, C_{60}, SWNT and MWNT, in model natural water suggested that dispersion of the carbon nanomaterials in the aqueous phase would be greatly influenced by the type of fullerenes and the spillage scenario. Specifically, MWNT formed water stable suspensions by the mechanical mixing and sonication, and SWNT formed water stable suspensions by the sonication, only when they were added as solids directly to water containing NOM. C_{60} formed water stable colloidal suspensions in all cases. In most cases, the presence of NOM facilitated fullerene dispersion in the aqueous phase.

Coagulation experiments suggested that in the scenario of fullerenes release in water environments, fullerenes would be generally well removed by the conventional water treatment process. The removal of these carbon nanomaterials was hindered by the presence of NOM presumably due to the preferential interaction of NOM with metal coagulants and the enhanced stability of the fullerenes from the NOM adsorption. Water quality parameters such as pH and alkalinity were also important factors for the removal of fullerenes by the water treatment process and, by adjusting those parameters, higher removal of the novel carbon nanomaterials might be achievable.

The experimental result in this study implies that the dispersion of fullerenes in aquatic environment can occur beyond the level predicted only based on its

hydrophobicity and NOM can play a critical role on the ultimate fate of these carbon based nanomaterials. However, in the scenario of the fullerene spillage, it is expected that the fullerenes can be generally well removed by the conventional water treatment process. The experimental result of this research is considered to provide useful insight on the fate of carbon nanomaterials in natural and engineered water environments.

CHAPTER 8

FUTURE WORK

The stability of derivatized fullerenes and their fate in water environments need to be investigated. Fullerenes have been chemically modified to enhance their stability in the aqueous phase. Thus induced functional groups include carbonyl, carboxylic and hydroxyl functional groups. However, due to the derivaization, the characteristics of fullerenes can be altered. Therefore the behavior of derivatized fullerenes in the water environments would be much different from that of fullerenes and their stability needs to be estimated under different water quality conditions. In addition, their interaction with NOM needs to be assessed for the better understanding of their fate in the natural environment.

Chapter 5 provides interesting observations regarding the removal of fullerenes in conventional water treatment processes. However, the experiment was performed with model NOM compounds and the removal of fullerene species in actual river water needs to be investigated. From the experiments with model NOM compound (SRNOM), this study suggests that fullerenes are expected to be relatively well removed by conventional water treatment processes. However, the behavior of fullerenes in actual river water may be different from that in model NOM compound due to the presence of other colloidal species, different ion contents, and lower solubility of fullerenes. Due to the limitation of laboratory scale experiment, pilot tests should be performed for an in-depth understanding of their removal in actual water treatment plants.

The removal of fullerenes derivatized with various functional groups in conventional water treatment processes also needs to be investigated. As observed in the coagulation experiment result, derivatized fullerenes appear to exhibit different removal efficiencies compared to underivatized counterparts. Further investigation on the behavior of C_{60} and derivatized CNT should be assessed for an in-depth understanding of removal in conventional water treatment processes.

VITA

HOON HYUNG

Hoon Hyung was born in Keo-Chang, South Korea. He received a B.S. and a M.S. in Chemical Engineering from Seoul National University, Seoul, South Korea in 1997 and 1999, respectively. He worked for Saehan Industries Inc., Seoul, South Korea as a research engineer before coming to Georgia Tech to pursue a doctorate in Environmental Engineering.